THEOPHYLLINE-DERIVED N-HETEROCYCLIC CARBENES AND THEIR METAL COMPLEXES

Exploring Ligand Design and Coordination Chemistry of Theophylline-based-N-Heterocyclic Carbenes

Masoomeh Fereidoonzadeh

Nothing in life is to be feared; it is only to be understood.

Now is the time to understand more, so that we may fear less.

Marie Curie.

Theophylline-derived *N*-heterocyclic carbenes and their metal complexes

A Dissertation submitted to

The University of Wuppertal

For the degree of

Doctor of Science

In the Faculty of

Mathematics and Natural Sciences

By

Masoomeh Fereidoonzadeh

“This research was conducted between October 2021 and March 2025 at the Faculty of Mathematics and Natural Sciences at the University of Wuppertal, under the supervision and guidance of Prof. Dr. Fabian Mohr.”

Acknowledgment

I sincerely thank **Prof. Dr. Fabian Mohr** for giving me the invaluable opportunity to join his research group and for fostering such a friendly and supportive environment. I am deeply grateful for his patience and understanding throughout this journey and his thoughtful guidance whenever I faced challenges. His encouragement and expertise have been crucial in helping me grow both academically and personally, and I feel truly privileged to have worked under his supervision.

“To the soul of my Dad, who was a dedicated Chemistry Teacher…”

Table of Contents

Figures:

Schemes:

Tables:

Abstract

In this project, a series of *N*-heterocyclic carbene (NHC) precursors was synthesized, starting from theophylline as the base structure. Novel alkylating agents, such as dialkyl sulfates and alkyl sulfonates, were utilized to alkylate NHC precursors, leading to the successful synthesis of xanthinium salts with halide and PF_6^- counterions. The structures of all synthesized compounds were thoroughly analyzed using NMR spectroscopy and mass spectrometry techniques.

Given the extensive applications of metal-NHC complexes, particularly silver-NHC complexes in medicinal chemistry, the study proceeded to prepare Ag(NHC) complexes. These were further utilized to synthesize gold, rhodium, and palladium complexes via transmetalation or weak base reaction pathways. All synthesized metal-NHC complexes were comprehensively characterized by NMR spectroscopy, Electrospray Ionization mass spectrometry (ESI-MS), and, in selected cases, single-crystal X-ray diffraction to confirm their structural integrity.

Moreover, we optimized certain synthetic protocols, such as preparing [NHCH]I and $[Au(NHC)_2]PF_6$. While these reactions were traditionally carried out under harsh conditions (60–80 °C), we successfully conducted them at room temperature, demonstrating a significant improvement in reaction efficiency and conditions.

Finally, two novel silver-NHC complexes were synthesized, incorporating sulfur and tosylate in their structure, which imparts an additional nucleophilic center. These precursors show promising potential for future exploration in the synthesis of silver and other metal-NHC complexes, opening avenues for further investigations and applications in coordination chemistry.

Chapter 1

Introduction

1.1. Carbenes

Carbon in its divalent state, with two bonds and a lone pair, is known as a "carbene". [1] It is a well-known transient species among the most studied reactive species in organic chemistry [2,3] since the first definitive evidence of its existence. [4] These compounds consist of two nonbonding electrons that can have either parallel or anti-parallel spins (singlet or triplet states)[5] (Figure 1.1). As a result, the typical carbon atom in a carbene may simultaneously exhibit an electron deficiency or an electrophilic nature. [6,7] The spin state significantly dictates their reactivity in the solution. [8]

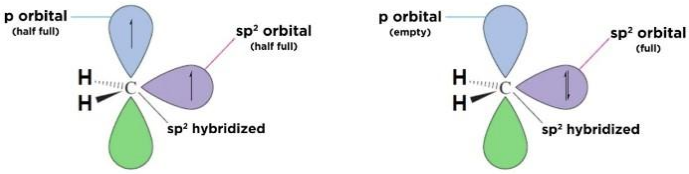

a) Triplet Carbene b) Singlet Carbene

Figure 1.1. Types of Carbenes. [8]

Anyway, for a long time, these species were perceived as excessively reactive to isolation. [9] So, numerous chemists hesitated to employ them, especially as passive ligands in transition metal chemistry. However, it's important to note that while most carbenes are fleeting reactive intermediates, this perception doesn't hold true for *N*-heterocyclic carbenes. [10]

1.2. *N*-Heterocyclic Carbenes

N-heterocyclic carbenes (NHCs) are a particular type of carbenes in which the carbene is situated on an *N*-heterocyclic scaffold [5,7] defined

as heterocyclic species containing at least one nitrogen atom within the ring structure. [11,12]

The lone pair of electrons on nitrogen contributes to the vacant *p*-orbital of the carbene, positioned perpendicular to the ring plane, resulting in aromatic stability. However, the increase in *σ*-electron density around the carbene is mitigated by the backflow of *σ*-electrons to the nitrogen atom, thereby enhancing the thermodynamic stability of the carbene (Figure 1.2). [13] Additionally, substituents attached to the nitrogen atom possess both steric and electronic properties that play a crucial role in stabilizing and isolating stable carbenes. [14] This observation was first noted by Pauling in 1980, who proposed that well-chosen substituents could stabilize singlet carbenes by maintaining electro-neutrality around the carbene center. [15]

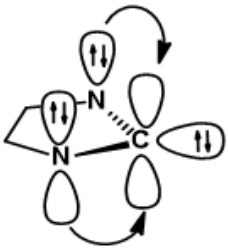

Figure 1.2. Stabilization of Carbene carbon in a five-membered heterocycle. [16]

Despite being identified and isolated more than thirty years ago, NHCs continue to pique scientists' curiosity as adaptable, modular, and powerfully coordinating moieties. [17] They have since found applications across a diverse array of fields, including organocatalysis [2] and organometallic chemistry [18] as adaptable organo-catalysts in a range of processes involving the formation of heteroatom bonds between carbon and carbon. [19,20]

Initial applications of NHCs in organometallic chemistry involved their use as ligands for transition metal complexes, replacing traditional

ligands such as phosphines because of their superior performance and reduced toxicity. [21–23] This led to the discovery of novel catalytic systems with improved activity and selectivity in various transformations. [10] Throughout the 2000s, researchers explored the catalytic potential of NHC-metal complexes in a wide range of transformations, including cross-coupling reactions, C-H activation, olefin metathesis, and various asymmetric processes. [5] The use of NHCs as ancillary ligands in transition metal-catalyzed reactions became more widespread, with numerous studies demonstrating their versatility and efficiency in catalysis. [24]

1.2.1. History

N-heterocyclic carbenes (NHCs) have a fascinating history dating back over a century. In 1895, **Nef** declared that isolating methylene would be his next endeavor. [25] However, despite his efforts and those of many others, no one believed any longer that carbenes would ever be isolated after numerous unsuccessful attempts. In the early 1920s, Russian chemist **Tschugajeff** and his colleagues conducted an interesting experiment. They treated potassium tetrachloroplatinate with methyl isocyanide and then added hydrazine. [26] Contrary to their expectations, this reaction did not yield a dimeric species as anticipated. Instead, it led to a compound that is likely the first diamino carbene complex isolated in pure form. The structure of this salt **1**, known as Tschugajeff's carbene complex (Figure 1.3) and its bis-carbene derivative **2**, was only fully understood decades later [27–31], Fritz *et al*. demonstrated that this technology may be utilized to synthesize NHC complexes using functionalized isocyanides. [32]

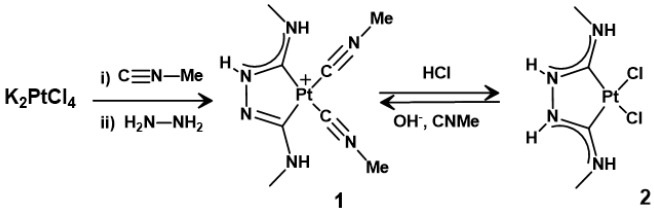

Figure 1.3. Tschugajeff's (Chugaev) carbene complexes. [26,32]

In 1958, **Skell** and **Sandler** identified normal carbenes while exploring a synthetic pathway to extend the carbon chain by inserting carbon atoms between double-bonded atoms. [33] Subsequently, **Fischer** and **Maasbol** conducted research on tungsten carbonyl complexes containing reactive carbon centers, providing valuable insights into the nature of carbenes. [34] In the early 1960s, **Wanzlick** and colleagues noted that aromatic resonance structures in unsaturated *N*-heterocyclic five-membered rings play a role in stabilizing carbenes. Free carbenes, like 1,3,4,5-tetraphenyl-2,3-dihydro-1H-imidazole-2-ylidene **3**, were produced by deprotonating imidazolium salts with KOtBu (Figure 1.4), and subsequently, they were reacted with isothiocyanates or metal-containing precursors. [35] Despite being so close to carbenes, Wanzlick *et al*. were unable to separate them. [36]

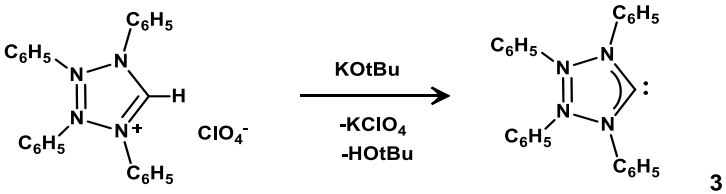

Figure 1.4. Attempted synthesis of carbene 3 from tetraphenyl imidazolium perchlorate. [16]

It is worth noting that the exploration of *N*-heterocyclic carbene chemistry had primarily focused on metal coordination complexes originating from azolium precursors, a progression initiated by Wanzlick [37] and Öfele [38] in 1968. Wanzlick and colleagues identified NHCs while synthesizing mercury-NHC complexes **4** from imidazolium chlorates (Figure 1.5). They underscored the significance of nucleophilic saturated and unsaturated carbenes as active intermediates. [37]

Following this, **Öfele** produced mercury and chromium pentacarbonyl imidazolium NHC complexes **5** from the corresponding chlorate salt (Figure 1.6), setting a standard for the synthesis of Cr-NHCs. [38]

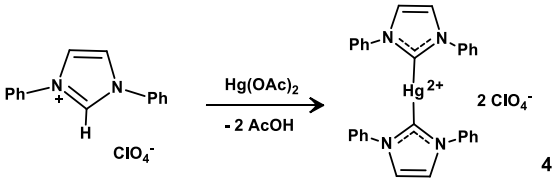

Figure 1.5. Wanzlick's NHC complex. [33,37]

However, it remains valid to note that, in many instances, the structures of carbenes are uncertain due to the lack of compelling evidence for the formation of NHCs. [39]

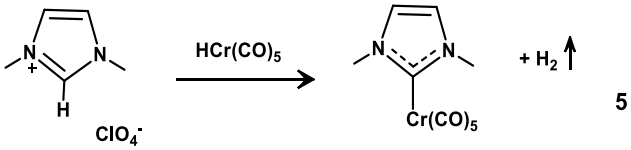

Figure 1.6. Öfele's Carbene. [39]

In 1988, **Bertrand** and colleagues achieved a milestone by synthesizing the first stable carbene, supported by advantageous interactions with neighboring phosphorus and silicon substituents **6**, which did not act as a ligand. [40] Subsequently, in 1991**, Arduengo's** breakthrough paved the way for accessible, isolable *N*-heterocyclic carbenes by deprotonation of the corresponding imidazolium salt **7** (Figure 1.7). [41]

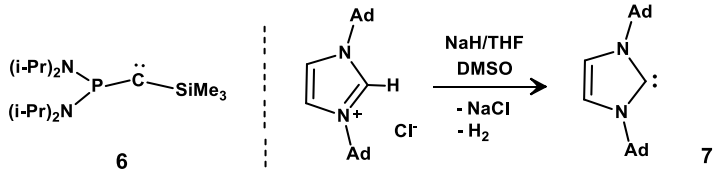

Figure 1.7. Bertrand and Arduengo carbenes. [40,41]

Since Arduengo's original isolation of the stable, “bottleable” *N*-heterocyclic carbene (NHC), this chemical class has received a lot of interest and has grown quickly. [42] **Kuhn,** later in 1993, improved on this deprotonation approach by introducing reductive desulfurization of thiones to produce stable imidazol-2-ylidenes. [43] In 1997, Bertrand and colleagues introduced silver acetate as a foundational material to interact with dicationic 1,2,4-trisubstituted triazolium salts, resulting in the synthesis of unstable polymeric Ag(I)-NHCs in THF under reflux conditions. [44] In the next year, **Lin's** team reported the straightforward creation of Ag(I)-NHCs using Ag_2O to react with benzimidazolium salt in CH_2Cl_2 at room temperature, stumbled upon as a fortunate discovery. [45] These reports sparked researchers' interest in the potential use of NHCs as ligands, which has resulted in an extraordinary amount of research activity. [46]

The majority of stable heterocyclic carbenes originate from five-membered heterocycles that contain heteroatoms such as nitrogen, sulfur, or phosphorus. [16] The unsaturated imidazolin-2-ylidene from this group likely represents the most extensive collection of stable heterocyclic carbenes. The first stable *N*-heterocyclic carbene, identified **7**, is also a member of this category. Currently, a vast array of imidazolin-2-ylidenes type **9** with various substitutions has been documented. [41] Typically, these are produced through the deprotonation of imidazolium salts **8** (Figure 1.8). [16] NHCs **9** are typically obtained as colorless, diamagnetic crystalline solids, characterized by remarkably high melting points. [47]

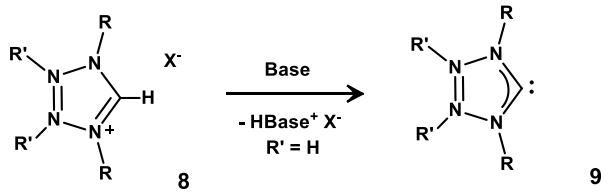

Figure 1.8. Synthesis of imidazolin-2-ylidene of type 9. [47]

Today, *N*-heterocyclic carbenes (NHCs) are regarded as favored ligands in transition metal complex chemistry (Figure 1.9). [45] The potent *σ*-donating capabilities of NHCs play a vital role in defining their interaction with metal centers, which, together with their steric characteristics, significantly affect the selectivity and reactivity in transition-metal catalysis. [48]

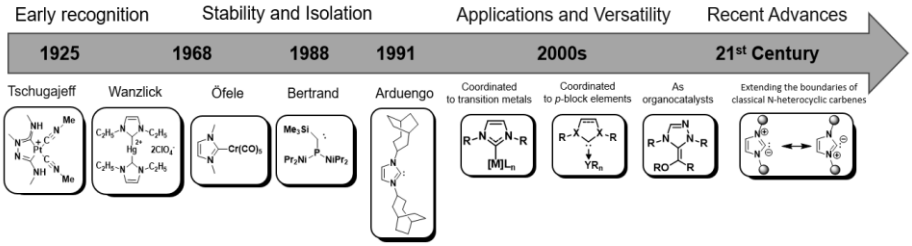

Figure 1.9. The historical timeline of NHCs (*N*-Heterocyclic Carbenes) from early recognition to recent advances.

1.2.2. Importance

In recent years, there has been increased focus on improving the value and impact of heterocycles in drug discovery and medicinal chemistry. [49] NHCs have emerged as the favored ligands in multiple domains, such as main-group chemistry [50–53], transition-metal chemistry [54–57] and organometallic catalysis [58–61], as well as in medicine [62,63], materials science [64–67] and organocatalysis. [68–71]

As the rich chemistry of these compounds was increasingly revealed [72], numerous studies documenting the applications of *N*-heterocyclic carbenes in organocatalysis have been reported. [73–77] *N*-heterocyclic carbenes (NHCs) exhibit distinct steric and electronic properties, which make them efficient ligands in coordination chemistry for the construction of stable metal-ligand frameworks involving main group metals and transition metals. [78]

Eduardo Peris describes NHCs as smart ligands in his review article [79], which is also referred to by terms like noninnocent [80,81], cooperative [82–84], switchable [85,86], and multifunctional [87,88], serving roles beyond merely furnishing an electronic context and a spatially precise cavity for the metal fragment in catalysis. The widespread utility of NHC ligands is mainly due to their facile synthesis [89], which permits the generation of diverse structural geometries and electron-donating characteristics. [16,90] Additionally, NHCs can include an endless array of extra functions, providing these distinct ligands with clear benefits for the customized synthesis of homogeneous catalysts on demand. [79]

1.2.3. Structure and properties

The successful isolation of stable NHCs **7** by Arduengo *et al*. marked a pivotal moment that enabled the thorough characterization of this important class of compounds. Initially, there was uncertainty regarding whether steric or electronic effects contributed to the stability of these species. Subsequently, it was proposed that the stability of NHCs originated from electronic factors rather than steric effects alone or possibly from a combination of both factors. [91] It was later discovered that one of the key characteristics of this class of small molecules, which contributes to their high affinity for both metal and non-metallic species, is the ability to adjust both electronic and steric properties. [17] Steric and electronic effects are closely linked and hard to separate from one another. [92]

In general, the appeal of *N*-heterocyclic carbenes as ligands in transition metal catalysis stems from the following characteristics: [93]

i) electronic character:

The electronic stabilization is influenced by the σ-withdrawing properties of the nitrogen atoms and also depends on π-donation into the carbene p_π orbital from the π-system, which involves the nitrogen atoms' p_π orbitals.[41] Overall, *N*-Heterocyclic Carbenes function as σ-

basic/π-acid ligands [94–97], with their electronic behavior explained through the Molecular Orbitals diagram shown in Figure 1.10. This diagram outlines how the basic imidazolidinydene structure interacts with a transition metal.

NHCs possess a lone electron pair in a high-energy σ orbital (Figure 1.10a), giving them a σ-donicity (basicity) that exceeds that of even basic phosphines like PCy_3. [10,98] They also have a low-energy empty π^* orbital (Figure 1.10b), allowing them to accept electron density from the metal's filled *d* orbitals through a classical $\sigma \rightarrow \pi^*$ back-donation process. [99,100] Additionally, with electron-deficient metals, NHCs can engage in $\pi \rightarrow d$ donation, where the electron density is transferred from the NHC's combined filled and empty π orbitals (Figure 1.10c) to the metal's empty *d* orbitals, demonstrating π-basicity. [101]

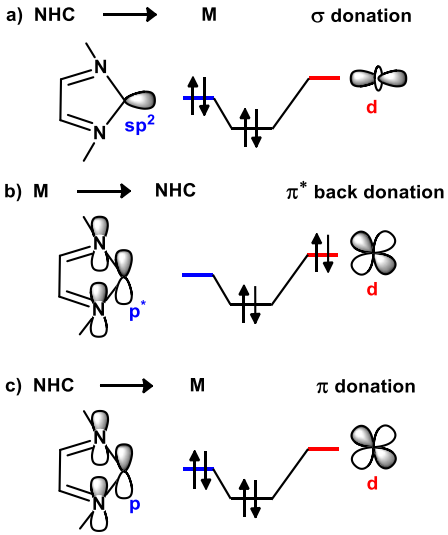

Figure 1.10. Diagram illustrating (a) the NHC → M, σ-donation, (b) the M → NHC, π^*-back donation, and (c) the NHC → M, π-donation bonding modes occurring between NHCs and transition metals. [106]

This understanding of M–NHC bonding has developed over years of research since NHC ligands were initially perceived as merely σ-donors with negligible π-acidity. Almost ten years later, key studies [99,100,102,103]

showed NHCs can accept electron density into their π^* orbitals from metals, highlighting this significant aspect of their bonding properties. More recently, the π-donor ability of NHC ligands towards electron-poor metals has been acknowledged [95,96,101,104], completing the understanding of their electronic characteristics. However, it is now widely accepted that some NHCs can also function as significant π-acceptors. [99,102,103] In their study, Meyer and colleagues showed that NHCs can exhibit significant π^*-back donation. [99]

The structure of *N*-heterocyclic carbenes can significantly influence their behavior as ligands. [105] The 4 primary structural parameters that can be adjusted to modify the electronic properties of five-membered NHCs, as illustrated in Figure 1.11, are: a) The type and placement of heteroatoms (like nitrogen and others); b) Substituents at proximal positions; c) The structure of the backbone (e.g., level of unsaturation) and its substituents; d) The size of the ring. [13,17,46,72,91]

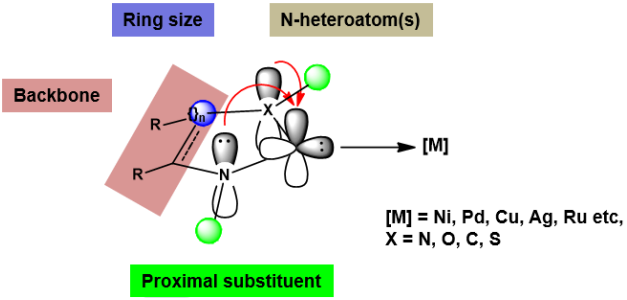

Figure 1.11. Schematic illustration of the structural elements that can be modified to adjust the electronic properties of NHC ligands. [105]

a) The effect of heteroatom (Nitrogen)

Adjacent nitrogen atoms, due to their high electronegativity, withdraw electron density from the non-bonding lone pair at the carbenic carbon (HOMO, σ-electron withdrawing). Meanwhile, their available lone pairs

can overlap with the empty *p*-orbital (LUMO, π-electron donating). [105] NHCs are bent carbenes with sp^2-hybridized (σ) and orthogonal p_π orbitals. They have four possible electronic configurations (Figure 1.12), predominantly presenting a singlet $^1A_1$ ground state with a σ^2 configuration. Competing states include the triplet $^3B_1$ and singlet $^1B_1$, which have occupied σ and p_π orbitals. The stability of NHCs is influenced by the singlet-triplet σ-p_π gap (E_{S-T})[106], with a gap greater than 40 kcal/mol favoring the singlet state. [36] This stabilization is mainly attributed to the inductive effect of the amine group substituents, which stabilize the carbene's σ orbital and increase the singlet-triplet energy gap, favoring the singlet state. [11]

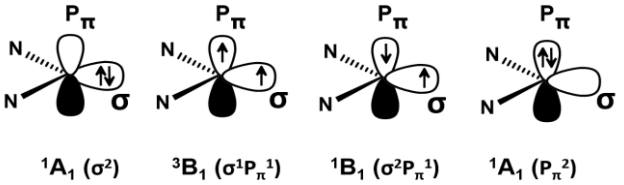

Figure 1.12. Electronic configurations of NHC carbenes. [97]

Figure 1.13 also illustrates that the two nitrogen atoms adjacent to the carbene center create significant mesomeric effects, destabilizing the π orbital and resulting in a large σ–π gap. [11] Consequently, NHCs are strong nucleophiles rather than electrophiles. [107]

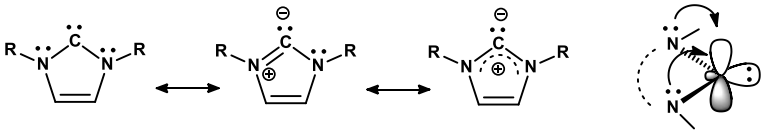

Figure 1.13. Mesomeric structures of NHCs and mesomeric stabilization of the singlet ground state. [68]

b) Proximal Substituents

Bulky substituents on nitrogen atoms can positively affect the stability of monomeric NHCs by protecting the reactive center from kinetic dimerization and decomposition while modifying the electronic properties of the ring system. [4,105,108,109] Because the tendency of a given NHC to dimerize is connected to its steric and electronic properties [106,110–112], Alder *et al*. conducted a comprehensive study using B3LYP DFT, examining NHCs of different ring sizes (5-, 6-, and 7-membered) with various alkyl substitutions. They found that bulkier alkyl groups increase monomeric NHC stability, particularly in larger ring systems where the *N*-substituents are less constrained by the N–C–N angle. [110]

Additionally, functional groups may have inductive (I) and mesomeric (M) effects. Electron-withdrawing groups exert a negative inductive effect (−I), while electron-releasing groups show a positive inductive effect (+I). The relative inductive impacts of some common functional groups, ranked from strongest −I to strongest +I, are essential to consider:

$$NH_3^+ > NO_2 > SO_2R > CN > SO_3H > CHO > COR > COOH > COCl > CONH_2 > F > Cl > Br > I > OR > OH > NH_2 > C_6H_5 > CH{=}CH_2 > H > CH_3 > CH_2CH_3 > CH(CH_3)_2$$

Mesomeric effects involve lone-pair donation (+M) or withdrawal (−M) [113], also referred to as resonance effects (+R/−R). [114]

Decreasing +M effect:

$$O^- > NH_2 > NHR > OR > NHCOR > OCOR > Ph > F > Cl > Br > I$$

Decreasing -M effect:

$$NO_2 > CN > CHO > COR > CO_2COR > CO_2R > CO_2H > CONH_2 > CO_2^-$$

Substituents with +I and +M effects increase NHC electron density, enhancing donor properties, while those with −I and −M effects

decrease it. Some substituents, like halo groups (F, Cl, Br, I), have both −I and +M effects, adding complexity to their influence. [113] More specifically, for different alkyl groups, Denk *et al*. indicated that higher alkyls have stronger electron-donating qualities, and the monomeric NHC's stability increases respectively for R = Me, Et, *i*Pr, and *t*Bu. [115]

c) Backbone structure

Backbone modifications significantly influence the electronic properties of NHC ligands. Significant efforts have been made to investigate the differences in bonding properties between saturated and unsaturated NHCs. Among the three main NHC families shown in Figure 1.14, the family of unsaturated NHCs based on **3** is the most thermodynamically stable [97] because Unsaturation enhances the ring's aromaticity. [72] On the other hand, Computational and structural investigation by Nolan and co-workers demonstrated that the bond distances between the metal and NHC are consistently slightly shorter for saturated NHCs compared to their unsaturated counterparts. [116] These findings suggest that saturated NHCs are slightly better donor ligands.

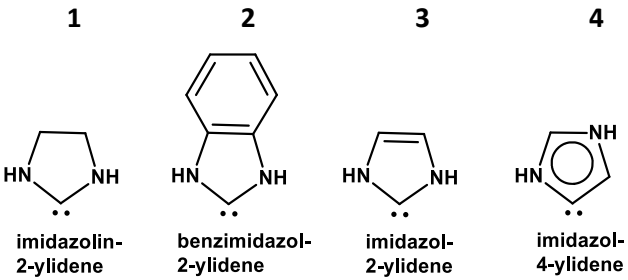

Figure 1. 14. Different NHC skeletons. [97]

The same authors recently synthesized and analyzed [(NHC)Pt^{II}] compounds. NMR results and electron density analysis confirmed that

saturated NHCs have a stronger σ-donor ability compared to unsaturated NHCs. [117] More significant insights were gained from the IR spectroscopic analysis of a series of [IrCl(CO)$_2$(NHC)] model systems, which revealed that NHCs with **alkyl** *N*-substituents are **superior electron donors** compared to those with aromatic substituents. [118,119] It has been well established that saturated NHCs based on the imidazolin-2-ylidene skeleton 1 of Figure 1.14 are more basic than NHCs with a fused aromatic ring (structure 2 of Figure 1.14), and the unsaturated NHCs (structure 3 of Figure 1.14). This variation in the NHC skeleton, along with changes in the *N*-bonded substituents, allows for the tuning of the electronic properties of specific NHC ligands. [97]

d) Ring size

The variety of NHC classes with different ring sizes highlights this feature's significant impact on both steric and electronic properties. It influences the preference for bent singlet ground states and profoundly affects the overall stability and reactivity of the compounds. [17] Increasing the NHC ring size from five- to six-membered cycles [120] and even seven [121] and eight-membered cycles [122] results in greater electron richness and significantly impacts steric demand. [123] Due to the specific electronic arrangement within the molecule, the carbenic carbon atom in NHCs exhibits significant nucleophilic character, distinguishing them from other carbenes. [90] This characteristic makes them highly prone to binding with metal centers, facilitating the broad utilization of NHC-ligated metal complexes in catalytic processes. [17]

ii) Steric characteristics

The most frequently utilized measure of steric impact is the Tolman cone angle, which is a cone that extends from the metal center of phosphanes and encloses the substituents. Tolman suggested using the

cone angle θ, which is defined by placing the atoms at the cone's perimeter and the metal at its vertex to determine the size of a ligand (Figure 1.15).

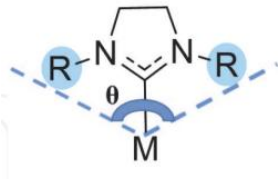

Figure 1.15. The Tolman cone angle θ. [1,48]

However, since NHCs and phosphanes usually have somewhat different shapes, NHC ligands cannot be fitted with the Tolman cone angle. [124] The fence model [125] along with other early attempts, these were soon replaced by the idea of the percent of buried volume (%V_{bur}) introduced by Nolan *et al*. [92] The %V_{bur}, as shown in Figure 1.16, is the percentage of the first coordination sphere's volume surrounding the metal that a specific ligand occupies. The area surrounding the metal atom that each ligand must share upon coordination is represented by the volume of this sphere. [126]

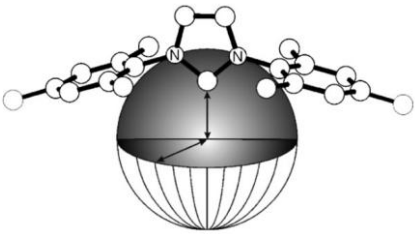

Figure 1.16. Schematic representation of the sphere used for the determination of the steric parameter %V_{bur}. [1,17,48]

The steric bulk of NHC ligands can be quantitatively compared to that of phosphine ligands or any other ligands using the percentage buried volume (%V_{bur}) measurement. [101] A straightforward web-based program created by Cavallo and colleagues makes it possible to

calculate $\%V_{bur}$ easily from crystallographic data. [126] Examining the $\%V_{bur}$ values of NHCs reveals that their steric bulkiness is one crucial factor influencing their capacity to attach to transition metal systems. [127] The larger a specific ligand, the greater the percentage of the coordination sphere ($\%V_{Bur}$) it occupies. Bayat *et al*. 2017 [128], in a theoretical study, indicated that the variations in R and R' have a negligible impact on the C→M bond lengths. Conversely, when the M atoms remain the same but R substitutions vary, the C→M bond lengths in the [NHC(R) → MR'] complexes are slightly shorter compared to those in the [{$(Ph)_3$PCHR} → MCl] complexes. [128] However, $\%V_{Bur}$ alone cannot fully describe steric effects as it does not account for the ligand's anisotropy. [93]

iii) Complex Stability

N-heterocyclic carbenes (NHCs) exhibit remarkably stable bonds with most metals. [10,129,130] While both saturated and unsaturated NHCs with similar steric demands display comparable bond dissociation energies, phosphines typically form much weaker bonds. [129] As a result, the equilibrium between the free carbene and the carbene-metal complex heavily favors the formation of the complex, much more so than for phosphines (see Figure 1.17).

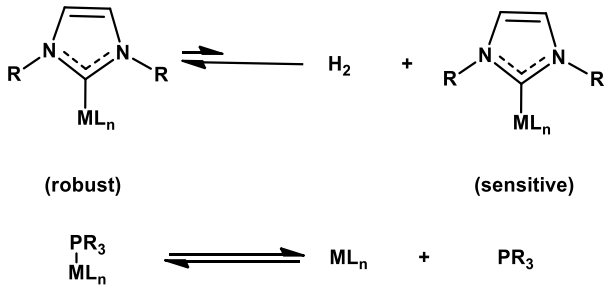

Figure 1.17. Equilibrium of complexation. [93]

This significantly reduces the free NHC in solution, enhancing the complex's lifetime and its heat, air, and moisture resistance. While *N*-heterocyclic carbenes can be isolated and stored, they remain highly sensitive and reactive to many electrophilic compounds. The remarkable stability of NHC-metal complexes has been leveraged in various demanding applications. However, an increasing number of studies indicate that the metal-carbene bond is not entirely inert. [130–138]

1.2.4. Basicity and nucleophilicity of *N*-heterocyclic carbenes

The basicity and catalytic reactivity of NHC precursors are closely linked. Therefore, studying the pK_a of NHCs is essential for understanding their properties as carbenes and their actual impact on the reaction mechanism. [1] More precisely, the reactivity of NHCs is primarily influenced by their Lewis base and/or Brønsted base characteristics. [107,139] Upon deprotonation, imidazolium salts convert into NHCs (Figure 1.18). A strong base and an aprotic solvent such as THF, Et_2O, or toluene are usually needed. [68] The pK_a values reflect the ease with which imidazolium salts form NHC precursors [72,140,141] and also provide insights into the nucleophilicity of the resulting NHCs. [1]

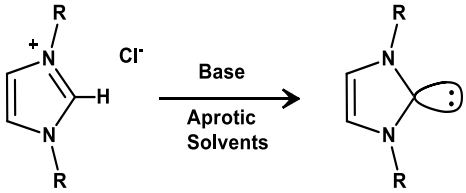

Base: NaH, *t*-BuOK, KHMDS, LDA, *n*-BuLi

Figure 1.18. Deprotonation of imidazolium salt to form *N*-heterocyclic carbenes. [68]

Breslow first proposed measuring NHCs' basicity in 1958, but couldn't isolate a stable NHC. However, he recognized the significance of the deprotonated ylide or carbene form of thiamin. [142] In 1988, **Washabaugh** and **Jencks** measured the pK_a of protonated NHCs in

aqueous solutions. [143] **Bordwell** and **Satish** later developed a technique to measure NHCs' pK_a in DMSO, identifying thiamin's pK_a as over 16.0. [144] **Alder** found 1,3-diisopropyl-4,5-dimethylimidazole-2-ylidene to be more basic than diazabicycloundecane (DBU) and diazabicyclononane (DBN) with a pK_a of 24.0. [145] **Kim** and **Streiwieser** further tested NHCs' pK_a in different solvents. [146]

In 2002, **Cheng** and colleagues studied the basic properties of 1,3-dialkyl imidazolium salts in DMSO, finding pK_a values between 19.7 and 23.4, and noted that N-substitutions influenced pK_a while counter ions do not affect the acidity [147], while Feroci *et al*. later showed that the counter-ion Y^- also plays a vital role. [148] Subsequently, Ayes *et al*. reported the pK_a values of several imidazolium salts in an aqueous medium through deuterium exchange studies. [149] In 2011, **Grishina**'s team identified a series of carbenes (*N,N'*-dialkyl-4,5-dimethylimidazol-2-ylidenes) and found that changing substituents on Nitrogen atoms (from methyl to isopropyl and isobutyl) can influence the basicity of NHCs. They also discovered that solvation effects resulted in higher pK_a values than pyridine bases. [150] The nucleophilicity and basicity of NHCs were studied experimentally by Mayr *et al.* in 2011. The study's methodology analyzed the reaction kinetics between *N*-heterocyclic carbenes and reference electrophiles. The authors established that various *N*-substitutions influence nucleophilicity. [107] One year later, O'Donoghue *et al*. conducted deuterium exchange studies on triazolium salts, which helped elucidate the relationship between the cationic structures of NHC precursor salts and their acidity. [151] In 2017, **Harper** and co-workers measured the pK_a values of various alkyl and aromatic imidazolium salts in DMSO, which exhibited a range of electronic and steric properties, finding that pK_a values were affected by variable substituents. They used the bracketing/overlapping indicator method (Figure 1.19). [152] In this process, which was first

applied by Streitwieser *et al.*, the deprotonated form of a fluorene-based indicator (with a known pK_a value) undergoes a notable change in UV-Vis absorption upon the addition of the NHC precursor salt. This change enables the monitoring of the equilibrium, allowing for the determination of the pK_a value. [146]

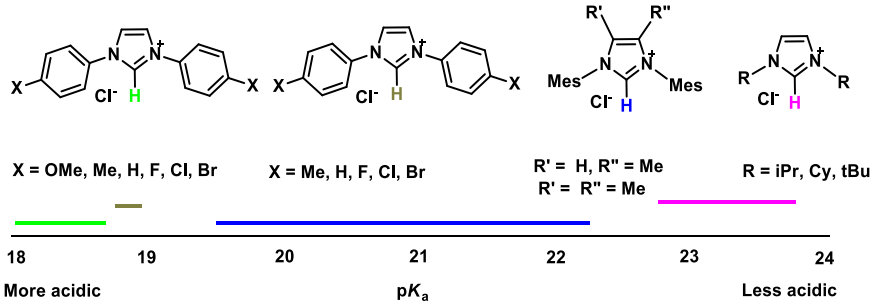

Figure 1.19. Arrangement of imidazolium salts based on their pK_a values in DMSO as determined by Harper *et al*. using the bracketing indicator method. [152]

In 2017, Dunn *et al.* updated and extended this method for various alkyl imidazolium salts. [152] They evaluated the deprotonation ability of NHCs from acidic hydrocarbons with known pK_a values. This method measures the difference in equilibrium acidity (pK_a) between an "unknown" acid and an "indicator" acid with a known pK_a (Figure 1.20).

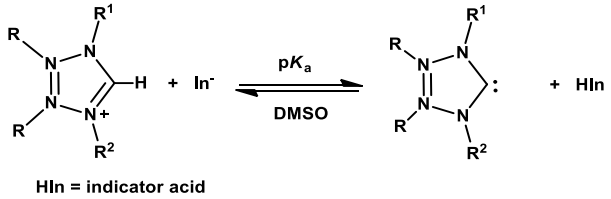

Figure 1.20. Acid-base equilibrium between NHC and the indicator acid. [147]

By observing the changes in UV/Vis absorption of either the indicator or the unknown acid during titrations of one acid with the other under standard conditions [153], the absolute equilibrium acidity of the unknown acid can be determined. The calculation is based on the following equations: [147]

$$HA + In^- \overset{K_{eq}}{\rightleftharpoons} HIn + A^- \quad (1.1)$$

$$pK_{HA} = pK_{HIn} - \log K_{eq} = pK_{HIn} - \log([HIn][A^-]/[In^-][HA]) \quad (1.2)$$

The overall trend is consistent regardless of the solvent: The pK_a values increase as the electron-donating character of the nitrogen substituents increases. Additionally, the pK_a values rise with an increase in the carbene bond angle, progressing from 5-membered to 6-membered ring NHCs. This indicates that both the electronic properties of the nitrogen substituents and the geometric structure of the NHC significantly influence the basicity of the carbenes. [68] Nonetheless, the pK_a value in DMSO is lower than in aqueous media because the neutral carbene is insensitive to solvent stabilization, while the azolium cation is more stabilized by hydrogen bonding in water than in an aprotic solvent. [140] Increasing the electron density on the carbene center significantly enhances its basicity.[154] Besides being used as Lewis base catalysts, NHCs act as nucleophiles. They typically have moderate nucleophilicity but high Lewis basicity. [155] Nucleophilicity is also important for their coordination with transition metal complexes. [156] Because of their nucleophilic nature and high Lewis basicity, NHCs readily form stable adducts with various substrates, including transition metals [145], main group elements [128,133,157] and organic molecules. [158–161]

1.3. Nature of Metal-NHC bond

To fully grasp the characteristics of metal-NHC complexes, it's essential to closely analyze the nature of the bond between the metal and the

NHC ligand. [162] Until the early 2000s, NHCs were seen exclusively as σ-donor ligands. [113] However, Meyer and others have shown that NHCs possess some π-acceptor properties (see page 7-electronic character), which vary based on the specific NHC ligand, the metal center, and the auxiliary ligands involved. [99,100] In many instances, NHCs behave similarly to the traditional dihydroxycarbene (Fischer carbene [1]), with approximately 20-30% of their bonding involving π-back bonding. [162] Therefore, the bond between an NHC carbene and a metal is a dative bond rather than a double bond (Figure 1.21). [13]

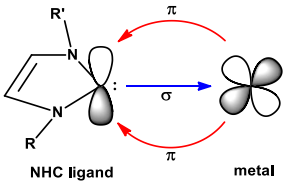

Figure 1.21. σ and π interactions of an NHC and a transition metal. [163]

Unsaturated NHCs are both weaker σ-donors and π-acceptors than their saturated congeners. [113] Nolan and his team demonstrated that the M-(NHC) bond lengths are consistently a bit shorter in saturated NHCs compared to their unsaturated analogs. [116] Comparing the two interactions, σ-donation is the primary and most significant aspect of the bonding between an NHC and a metal. [163] Over the years, several experimental methods have been developed to quantify the overall donor character of the most common NHC ligands. Notably, some of these methods have been developed to distinguish between σ-donation and π-back-bonding contributions. Huynh *et al*. uniquely

[1] **Fischer carbenes** are a class of carbenes that bind to metals, typically characterized by their strong electrophilic nature when attached to metals in low oxidation states. These carbenes are most commonly associated with mid-to-late transition metals, especially in the presence of π-accepting ligands. The carbene carbon in Fischer carbenes typically features a π-donating substituent, such as an alkoxy or alkylamino group, stabilizing the carbene's interaction with the metal.

utilized NMR to study the donor properties of NHCs. [164] This method employs the ^{13}C-NMR technique and uses a parameter known as the Huynh electronic parameter (HEP), which corresponds to the ^{13}C NMR signal (ppm) of the carbenic carbon of iPr_2-bimy (Figure 1.22).

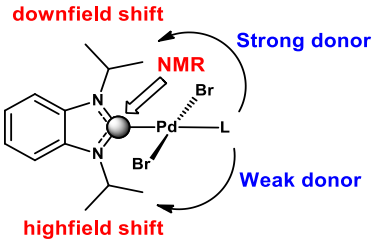

Figure 1.22. Huynh electronic parameter. [113]

The ligands L (including NHCs) with good *σ*-donor ability cause a downfield shift in the carbene carbon peak, resulting in higher HEP values (ppm). The J_{M-C} spin-spin coupling constant between the metal center and the carbene NHC atom can also be analyzed. Nolan and his team conducted this analysis on NHC-Pt(DMSO)Cl_2 complexes to measure the *σ*-donor properties of NHCs. [117] For the measurement of the *π*-acceptor character of NHCs (Figure 1.23), Nolan used platinum active nuclei to analyze the $^1J_{Pt-C}$ coupling constants in [$PtCl_2$(DMSO)(NHC)] complexes. [117] Bertrand reported determining the *π*-acceptor ability of NHC ligands using the ^{31}P NMR chemical shifts of carbene-phosphine adducts, [165] (increased electron density on phosphorous atom leads to an upfield shift in ^{31}P NMR). Much like carbene-phosphine adducts, an increase in the *π*-accepting property of NHCs is indicated by a higher chemical shift value in ^{77}Se NMR, as established by Ganter *et al*. in 2015. Besides *π*-acceptor abilities, the *σ*-donor capabilities of NHCs can also be determined using carbon-selenium coupling constant values. [166,167] High chemical shift values indicate a strong π-acceptor character of any given carbene. [162]

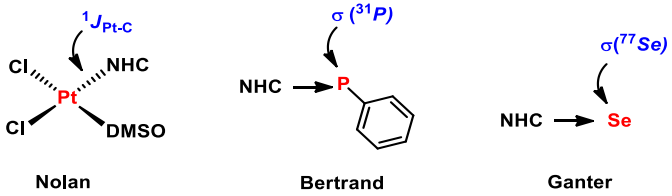

Figure 1.23. Techniques developed to quantify the π-acceptor properties of NHCs as proposed by Nolan, Bertrand, and Ganter. [117,165,167]

1.4. Synthesis of Metal-NHC complexes

Traditionally, two primary methods have been employed for the synthesis of transition metal–NHC complexes. [168] (Figure 1.24):

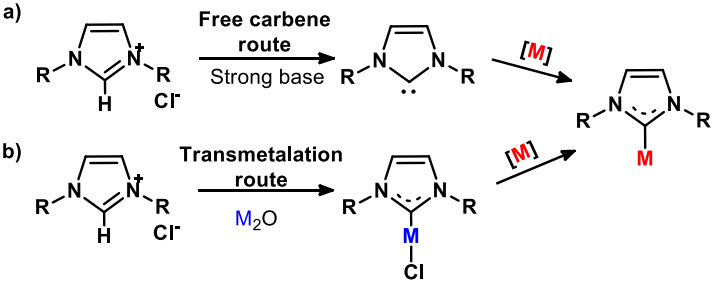

Figure 1.24. Methods for the synthesis of metal–NHC complexes. [169]

The first method (Figure 1.24a) involves generating a free carbene as the initial step. [170–174] This is typically achieved by adding a strong base to an azolium salt. The subsequent step involves adding a transition metal source to the reaction mixture containing the *in situ* generated NHC or the isolated NHC. Notably, the **free carbene route** is a two-step process that requires strictly anhydrous conditions and the use of strong bases, which are often costly and potentially hazardous. [169] The second method, known as the "**transmetallation route**," is also a two-step process. [171,175–177] (Figure 1.24b). This method involves reacting an

azolium salt with copper or silver oxides to produce the corresponding Cu- or Ag-NHC complexes. Followed by transferring the NHC to a desired second transition metal. This concept originated in 1998 when Lin and coworkers reported synthesizing an NHC-silver complex without the requirement for an external base. [178] Silver oxide served as the base and the supply of silver in their methodology. Then, in dichloromethane, the resultant silver complex was combined with a source of palladium or gold to facilitate the NHC's transport to the target metal center (Figure 1.25). Since then, various NHC-transition-metal complexes have been synthesized using this method. [176] (including earlier work done by our institute, Mokfi *et al*. [179]).

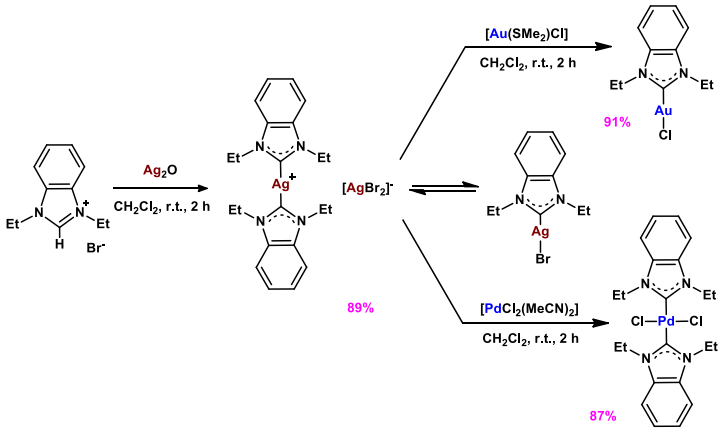

Figure 1.25. Synthesis of Au and Pd Complexes using Transmetalation from Ag Species. [162]

Although this method has advantages, like using air-stable starting materials and producing water as a by-product in the first step, it also has notable drawbacks. This method is restricted to using copper and silver oxides most of the time, and in some cases, it necessitates high temperatures or toxic solvents and produces considerable waste.

Additionally, it is challenging to use when synthesizing metal complexes with bulky NHC ligands. [169]

Weak Base Route. In the past ten years, a different way to create NHC complexes of varying transition metals has been intensively investigated. This strategy is distinct from the free carbene and transmetalation approaches. [162] Jiang [180] and Navarro [181] provided some of the earliest examples of the direct synthesis of complexes from NHC·HCl salts using weak bases. This technique (Figure 1.26) combines the azolium salt with a metal supply and a weak base, like potassium carbonate, triethylamine, or sodium acetate. Usually, the reaction is conducted under mild circumstances with green solvents and in the presence of moisture or air. [162]

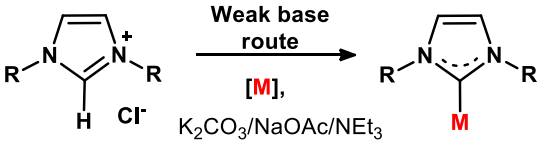

Figure 1.26. Weak base route for the synthesis of metal–NHC complexes. [169]

Chapter 2

Results and discussion

2.1. Aim and objective

Xanthine-derived-carbene-metal complexes have been synthesized in the past and have demonstrated potential as antimicrobial agents (particularly with silver) and have also exhibited promising antitumor activity with palladium, copper, and gold. [182,183] We have previously reported a facile route to access xanthinium salts and their corresponding carbene complexes. [179] In this work, we have extended this approach to include olefin- and halide-functionalities in the xanthine backbone (Scheme 1). The reaction of the xanthinium salts with Ag_2O or AgOAc [184] gave several types of carbene species. With Ag_2O and NH_3, cationic complexes of the type $[Ag(NHC)(NH_3)]^+$ or $[Ag(NHC)_2]^+$ were observed. When AgOAc was used, neutral complexes of the type [Ag(NHC)(OAc)] were formed.

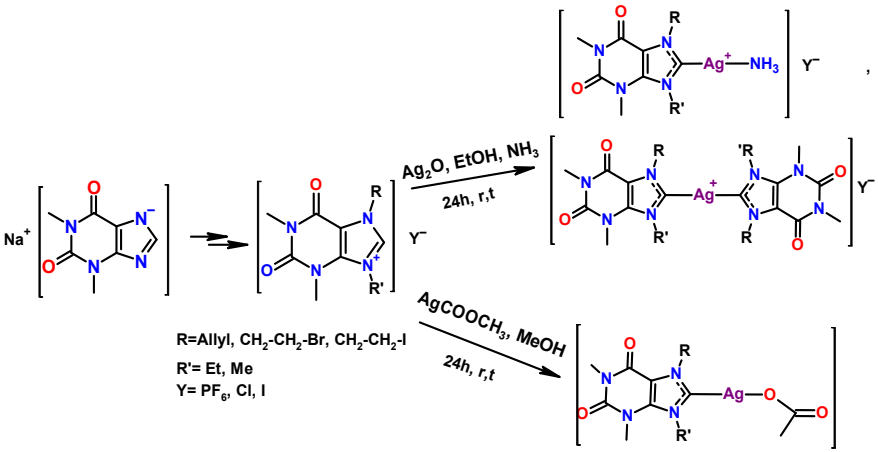

Scheme 1. Synthesis of silver-based carbene complexes of Theophylline.

Carbene can be transferred to other metals by transmetallation processes using silver molecules. In our work, we particularly concentrated on synthesizing Au, Rh, and Pd, among other transition

metals. In some cases, the corresponding metal xanthine-8-ylidene derivatives were characterized through spectroscopic techniques and X-ray diffraction studies.

2.2. Synthesis of *N*-heterocyclic carbene ligands

Xanthine, also known as 3,7-dihydropurine-2,6-dione (Figure 2.1), is a heterocycle consisting of a pyrimidine ring fused with an imidazole ring. [185] Caffeine and theophylline, which are widely available and frequently present in food [186], have become highly significant due to their extensive applications in medicinal chemistry [187–191], owing to their remarkable chemical or physical properties. [192]

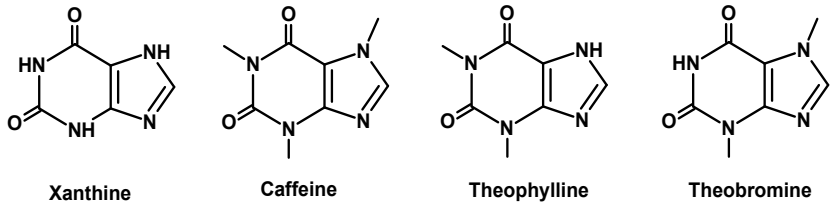

Figure 2.1. Xanthine and naturally occurring derivatives of xanthine.

The xanthinium salt, derived from xanthine or its derivatives, serves as a catalyst and a precursor for ligands in various metal complexes. These complexes involve metals such as palladium (Pd) [193], platinum (Pt) [194,195], ruthenium (Ru) [196], silver (Ag) [184], gold (Au) [197], iridium (Ir) and rhodium (Rh) [198]. In keeping with our curiosity about NHC ligand development, [179] in this work, we reported metal-*N*-heterocyclic carbene derived from xanthines. For this aim, we initially sought *N*-functionalized theophylline derivatives, which are described as follows:

2.2.1. Synthesis of mono-substituted theophylline

In this project, theophylline was employed as the precursor, followed by functionalization on the N7 position with allyl bromide or 1,2-dibromoethane [199] (Scheme 2) which gave N7-allyl theophylline **(1a)** and N7-bromoethyl theophylline **(1b)** in good yield. No N9 alkylated product was visible, and the reaction proceeded regio-selectively at the N7 position. [200]

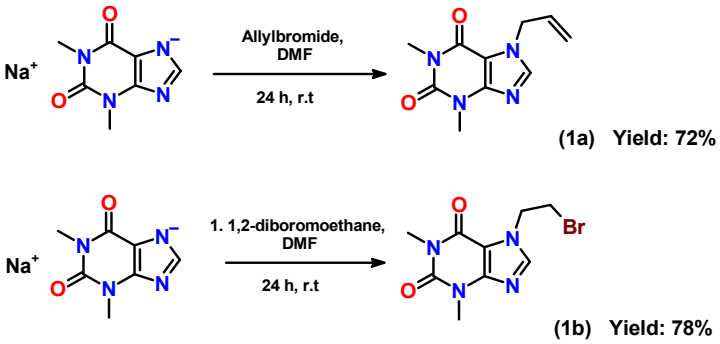

Scheme 2. Functionalization of Theophylline at N7 position.

It should be noted that the reactivity of theophylline with 1,2-diboromethane is much greater than that of allyl bromide. Proligands **1a** and **1b** were characterized by NMR spectroscopy, ESI-MS, and single-crystal X-ray diffraction. The ^{1}H-NMR spectrum of **1a** (in DMSO-d6) features the resonances for the allyl group around 5-6 ppm. For compound **1b**, the resonances for N-C**H$_2$**-C**H$_2$**-Br appear as two triplets at 3.80 and 4.66 ppm. Similarly, the resonances for the carbon atom C8 were detected in the ^{13}C {^{1}H} NMR spectrum at 148 and 149 ppm for compounds **1a** and **1b**, respectively.

2.2.2. Synthesis of di-substituted theophylline

For the investigation, compounds **1a** and **1b**, with various steric and electrical characteristics at the N7 position, were used for alkylating on the N9 position to produce xanthinium salts as NHC precursors. Various alkylating agents were used for this aim, and their effectiveness was examined. The generation of xanthinium salts mainly involves the reaction of substituted xanthinium with alkyl halides. [184,201,202] In most cases, methyl iodide [203] is reacted with caffeine or theophylline in refluxing DMF for 24 hours. [184] The formation of *N*-alkyl xanthinium salts generally occurs through a bimolecular nucleophilic substitution (SN2) process. [204]

In this reaction, the nitrogen atom of the imidazole molecule serves as the electron donor (nucleophile). This nucleophilic nitrogen attacks the carbon atom bonded to the halogen in the alkyl halide, which acts as the electron acceptor (electrophile). This mechanism results in the creation of a new carbon-nitrogen bond, forming the *N*-alkyl xanthinium salt. However, the reaction usually results in a 1:1 mixture of the desired product and the starting material. [205] Therefore, there are more reactive alkylating reagents available that require shorter reaction times and produce products with higher purity and yield, like alkyl tosylate [206] and dialkyl sulfates [206,207] or alkyl trifluoromethanesulfonate [208,209] as the most recent class of alkylating agents. (Alkyl triflates are well-known for their strong alkylating abilities.) [210,211] So, in the second part of this project, the xanthinium salts of **1a** and **1b** were reacted with ROTs, $(RO)_2SO_2$ (R= Et, Me), and $(CF_3)SO_3Me$ under solvent-free conditions (Scheme 3).

The details of the reactions are shown in Table 1.

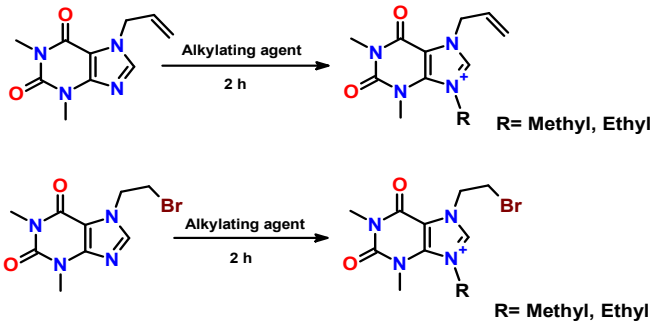

Scheme 3. Alkylating of N9 position of one-substituted theophylline under solvent-free condition.

Table 1. Alkylating on the N9 position with various agents

name	product	T (°C)	Time (h)	Yield (%)
2a	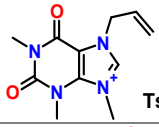	150	2	89
2b	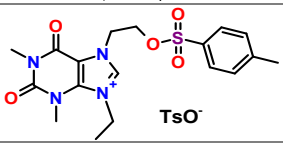	150	2	Not favorable
3a	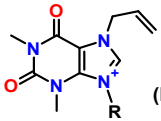	130	2	70-87
3b	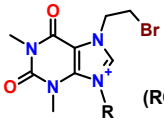	130	2	91-92
4a	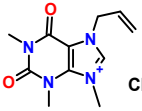	120	2	69
4b	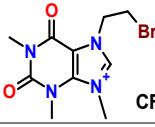	120	2	50

The structures of the synthesized compounds were verified using multiple analytical techniques, including proton (^{1}H) and carbon-13 (^{13}C) Nuclear Magnetic Resonance (NMR) spectroscopy. In the ^{1}H-NMR spectra, the ethyl group's signature was evident, with the -$\mathbf{CH_2}CH_3$ protons appearing as a quartet between 3.90-4.63 ppm and the -$CH_2\mathbf{CH_3}$ protons showing as a triplet in the 1.32-1.55 ppm range. The signals in the 9-10 ppm region identified the imidazolium protons, aligning with the typical acidic proton shift range (8-10 ppm) for xanthinium salts, as reported in the literature. [4] The ^{13}C-NMR spectra revealed the imidazolium carbon (N-**C**-N), the precursor to the carbene center, with a characteristic chemical shift at 138-140 ppm. Additionally, HRMS analysis further confirmed the successful synthesis of the intended products. Our experiments in this part emphasized that alkylating reactions with dialkyl sulfates are superior to alkyl halides. They offer faster reactions (e.g., dimethyl sulfate is 60 times faster than methyl iodide), lower equipment costs, Non-toxic end products, and less corrosive salts, reducing equipment wear. Also, dialkyl sulfates reacted better than alkyl sulfonates and became the preferred choice for efficient and cost-effective alkylation processes in industrial settings. [212] The synthesized salts exhibited high solubility characteristics, demonstrating complete miscibility with water and various polar solvents, including dichloromethane, acetonitrile, and ethanol. This solubility profile is consistent with the behavior observed in other hydrophilic ionic liquids (Ils). [213,214]

2.2.3. Ion exchange reaction of the xanthinium salts

The ionic liquids xanthinium salts synthesized in this study offer dual advantages: They are not only readily prepared through a facile and expeditious process, but they also serve as versatile precursors for the synthesis of other xanthinium salts via ion-exchange reactions. To

demonstrate the utility of these novel water-soluble ILs as intermediates, an ion exchange reaction was conducted using ammonium hexafluorophosphate. This reaction resulted in the successful preparation of a crystalline $(NHC)^{+}PF_6^{-}$ solid, thereby illustrating the potential of these compounds as starting materials for the synthesis of silver-NHC complexes. Notably, this ion-exchange reaction, which forms a hydrophobic xanthinium salt, highlights the versatility and potential advantages of using alkyl sulfate-based IL in synthesis. [212] Also, Chloride salts could be synthesized by treating the corresponding hexafluorophosphate (PF_6^{-}) derivatives of *N*-heterocyclic carbene (NHC) complexes with Amberlite 900(Cl^{-}) resin. [215] This ion exchange process effectively substitutes the hexafluorophosphate anion with a chloride anion, resulting in the formation of the desired chloride salts.

2.2.4. Synthesis of $[NHCH]PF_6$ salts

The xanthinium salts listed in Table 1 undergo facile ion exchange reactions with ammonium hexafluorophosphate ($NH_4^{+}PF_6^{-}$) in aqueous medium. [216] This process, illustrated in Scheme 4, results in the substitution of the original counter-anions with hexafluorophosphate (PF_6^{-}) anions, yielding white crystalline solid products easily separated by filtration.

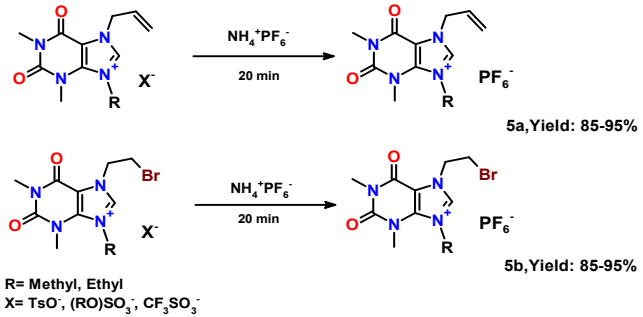

Scheme 4. Ion exchange reaction of xanthinium salts

The structures of the synthesized products **5a** and **5b** were confirmed using ^{1}H, ^{13}C, and ^{31}P NMR spectroscopy, as well as Electrospray Ionization Mass Spectrometry (ESI-MS). The absence of resonance peaks corresponding to TsO^-, $(RO)SO_3^-$, and $CF_3SO_3^-$ in the ^{1}H and ^{13}C NMR spectra, along with the emergence of a septet signal for PF_6^- at -144 ppm in the ^{31}P NMR spectrum, validates the successful synthesis of the expected products.

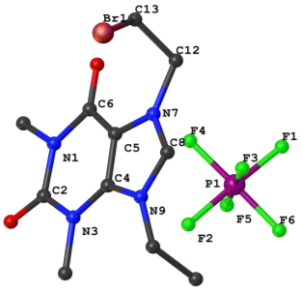

Figure 2.2. The molecular structure of compound **5a** in the solid state. Hydrogen atoms have been excluded for improved clarity,. Selected bond angle [°]: N7-C8-N9 = 111.0 (2)°.

The mass spectra of pro-ligands **5a** and **5b** exhibited base peaks corresponding to their respective mono-cationic xanthinium salts. For compound **5a**, the base peak was observed at m/z 249.13, representing the $[C_{12}H_{17}N_4O_2]^+$ ion. Similarly, for compound **5b**, the base peak appeared at m/z 317.04 $[C_{11}H_{16}BrN_4O_2]^+$, indicative of its mono-cationic xanthinium salt structure. These findings confirm the expected molecular compositions of the synthesized pro-ligands. Crystals of compound **5a**, appropriate for X-ray crystallography, were grown using a slow diffusion method. This involved introducing tetrahydropyran into an acetonitrile solution containing the complex. Figure 2.2 illustrates the solid-state molecular structure of complex **5a**, as determined by this analysis.

2.2.5. Synthesis of [NHCH]Cl salts

The conversion from hexafluorophosphate (PF_6^-) to chloride (Cl^-) salts is motivated by several factors. Halide salts are generally preferred over PF_6^- salts for subsequent reactions. Because in the next step, which involves silver oxide (Ag_2O) for complex formation, xanthinium salts with halide anions exhibit superior reactivity compared to those with non-coordinating anions such as BF_4^- and PF_6^-. [217,218]

Additionally, the C8 proton forms stronger hydrogen bonds with halides than with BF_4^- and PF_6^-, leading to increased acidity of the halide salts relative to their BF_4^- and PF_6^- counterparts. [208] The enhanced acidity of the *N*-heterocyclic carbene (NHC) precursors with halide anions also facilitates more efficient proton abstraction in the reaction with Ag_2O, which acts as a base in this context. [219,220]

Various methodologies exist for the anion exchange from hexafluorophosphate (PF_6^-) to chloride (Cl^-). One such approach involves the addition of tetrabutylammonium chloride in tetrahydrofuran (THF) to a solution of the PF_6^- salt in THF, followed by agitation for 30 minutes. This process typically results in the separation of an oil, which contains the desired Cl^- salt. [198] However, in the context of this research project, this particular method proved unsuccessful in yielding the intended product.

An alternative and environmentally friendly method for anion exchange is based on the work of Zhigang Zou *et al*. [221] This approach involves a two-step ion exchange process. The initial step comprises the substitution of the alkyl sulfate anion (where $ROSO_3^-$ represents an alkyl group) with hydroxide (OH^-) in Ethanol or water as solvent. Subsequently, the reaction proceeds with the addition of HY (where Y denotes the desired anion). Despite multiple attempts to implement

this methodology in our research project, it did not yield the anticipated product. This outcome underscores the challenges often encountered in adapting published protocols to specific research contexts and highlights the need for further optimization of ion exchange techniques in this particular system.

The third method is using ion exchange chromatography by Amberlite® IRA-900(Cl^-form) ion exchange resin. This ion exchange method was investigated for compounds **3a-5d**, representing four different alkylated theophylline derivatives, as shown in Scheme 5. In order to optimize the ion-exchange resin methodology, a comprehensive study was conducted to evaluate the impact of various organic solvents, including both polar protic (e.g., ethanol) and polar aprotic (e.g., tetrahydrofuran, acetonitrile, dichloromethane) solvents. The results of this investigation are presented in Table 2. In each instance, the outcomes were confirmed using ^{1}H NMR, HRMS, and ^{35}Cl NMR to detect the presence of the chloride anion. If the chloride anion is present in the product, it will manifest as a soft singlet in the ^{35}Cl NMR spectrum within the range of 50-100 ppm. Also, the removal of the PF_6^- anion is demonstrated by the elimination of its signals in ^{31}P NMR, which was verified for compounds **6a** and **6b** (Figure 2.3).

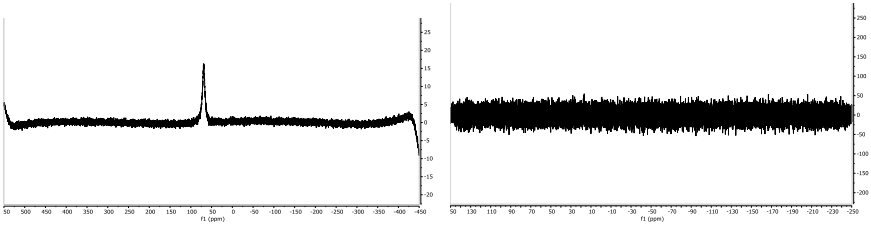

Figure 2.3. ^{35}Cl NMR (left) and ^{31}P NMR (right) of the product as a sign of a successful ion exchange reaction.

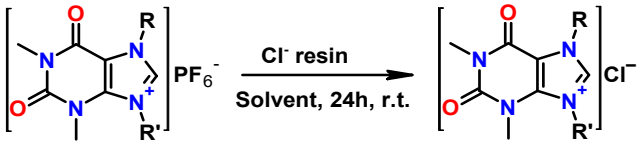

R=Allyl, CH_2-CH_2-Br

(6a) R=Allyl
(6b) R=CH_2-CH_2-Br
R' = Me, Et

Scheme 5. Ion exchange from hexafluorophosphate (PF_6^-) to chloride (Cl^-).

Table 2. Influence of solvent variation on ion exchange reaction using Amberlite IR9200 (Chloride Form)

compound	Cl^- resin eluting solvent	exchanged ion	yield
3a	EtOH	Cl^-	25%
	MeCN	Cl^-	19%
3b	EtOH	×	
	MeCN	×	
4a	EtOH	Cl^-	18%
	MeCN	×	
4b	EtOH	×	
	THF	×	
5a	EtOH	Cl^-	28%
	MeCN	×	
	THF	×	
5b	EtOH	Cl^-	20%
	MeCN	×	
	THF	×	

Theoretically, polar aprotic solvents are generally preferred for ion exchange reactions due to their inability to form hydrogen bonds with ions, thereby reducing ion solvation and potentially facilitating more efficient ion exchange. This is attributed to decreased solvent interference in the ion-resin interactions. Chloride resins, in particular, are known to exhibit favorable performance with aprotic solvents, which are typically more compatible with the resin matrix. However,

our experimental findings revealed that ethanol, a polar protic solvent, demonstrated superior performance compared to acetonitrile (MeCN) and tetrahydrofuran (THF) in the ion exchange reaction from PF_6^- to Cl^- on a chloride resin. This unexpected result may be attributed to several factors: first; Enhanced solubility and swelling properties of the chloride resin in ethanol, and second; Potential ion-pairing effects, where ethanol molecules may stabilize ions in solution, thereby influencing the ion exchange equilibrium and potentially favoring chloride ion selectivity. Furthermore, the inherent strength of the hydrogen bonds formed between the xanthinium cation and the anions is ranked as follows: $CF_3SO_3^-$ > BF_4^- > PF_6^-. [222] This variation in bond strength may influence the ease of their removal and facilitate the ion exchange process in polar protic solvents. Interestingly, for the allyl-substituted theophylline derivatives, both protic and aprotic solvents yielded satisfactory results in the ion exchange process. Also, xanthinium cations paired with weakly coordinating anions [208], such as hexafluorophosphate (PF_6^-) or trifluoromethanesulfonate, exhibit enhanced reactivity in ion exchange processes. However, subsequent reactions of the chloride salts of compounds **3a** and **4a** with silver oxide frequently produced oily products, thereby complicating the isolation and purification of the desired compounds. In some cases, ion exchange to chloride using resin resulted in mixed products or incomplete bromide-to-chloride conversions.

In light of these challenges, we opted to employ iodine for the alkylation step. Although this reaction is relatively time-consuming, it offers the significant advantage of simultaneously achieving N9-substitution and incorporating the desired halogen counter anion.

2.2.6. Synthesis of [NHCH]I salt

Methylation of compounds **1a** and **1b** by reacting with an excess amount of methyl iodide in DMF under reflux conditions [184,193,201] resulted in the formation of xanthinium salts **7a-7b**, with an average yield ranging from 60-80% (Scheme 6). Results are shown in Table 3.

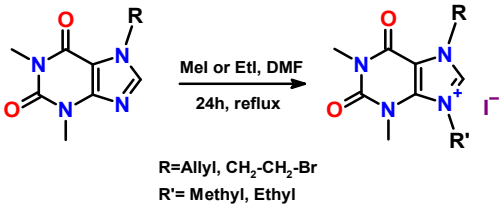

Scheme 6. The Alkylating reaction of mono-substituted theophylline

Table 3. Results of the alkylating reaction of mono-substituted theophylline.

Name	Substitution on N7 position	Alkylating agent	yield
7a-1	Allyl	MeI	62%
7a-2	Allyl	EtI	75%
7b-1	CH_2-CH_2-Br	MeI	74%
7b-2	CH_2-CH_2-Br	EtI	81%

Compounds **7a-1** to **7b-2** are water-soluble solids with low melting points, stable at temperatures up to 7 °C, and are best stored in a

refrigerator. In the ^{1}H NMR spectra, similar to other salts discussed in this section, the imidazolium proton resonates between 9.50 and 9.75 ppm. For compounds **7b-1** and **7b-2**, a halide exchange occurred between bromide and iodide.

This substitution was anticipated and subsequently confirmed through mass spectrometric analysis. Compounds **7a** and **7b** were analyzed using single-crystal X-ray diffraction techniques. To obtain the necessary single crystals, a concentrated solution of each compound in acetonitrile was allowed to evaporate slowly. The resulting crystal structures are depicted in Figure 2.4. Surprisingly, X-ray diffraction analysis of a single crystal obtained during the recrystallization process revealed the presence of triiodide (I_3^-) anions rather than the anticipated iodide (I^-) ions for compound **7a**.

In each instance, the pyrimidinone backbone of the xanthinium salt exhibits a slight torsion from the plane established by the N(7)–C(8)–N(9) bond. This twisting angle may arise due to the steric constraints imposed by bulky substituent. This twist can impact how the molecule interacts with other compounds and its stability. [223]

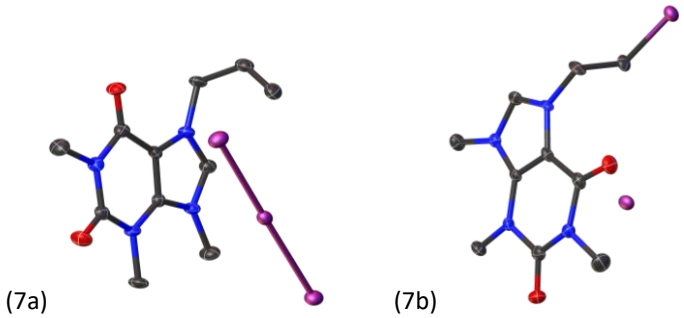

(7a) (7b)

Figure 2.4. Molecular structure of compounds **7a** and **7b**. Hydrogen atoms have been excluded for improved clarity, and ellipsoids are shown at 50% probability. 7a: N7-C8-N9: 110.02(3)°, 7b: N7-C8-N9: 110.03(7)°.

2.2.7. Synthesis of (NHCH)I salts at room temperature

One drawback of using methyl iodide for alkylation is its tendency to decompose at high reflux temperatures (70 °C), despite its boiling point being only 40 °C. This decomposition can generate toxic byproducts, which not only pose a threat to the reaction environment but also diminish the overall yield [224] , necessitating the use of at least five times the amount of methyl iodide in the reaction mixture. The instability of methyl iodide under elevated temperatures can lead to significant losses of both reactants and products due to evaporation or degradation, ultimately decreasing the efficiency of the alkylation process.

To address this issue, conducting the alkylation at lower temperatures can help preserve the stability of methyl iodide and reduce decomposition. Performing reactions at or below its boiling point (40 °C) can improve yields and minimize the formation of toxic byproducts. In our recent experiment conducted at room temperature, as reported in the recent publication of Longo *et al*. [225] We observed a substantial increase in reaction yield for methylation with this adjustment. However, this method proved ineffective for ethylation. The initial phase in the synthesis of an *N*-heterocyclic carbene (NHC) metal complex derived from theophylline involves the preparation of an xanthinium salt precursor, which was accomplished in this segment of the study. The next stage entails the reaction of these precursors with diverse metal precursors, a process that will be elucidated in the following sections.

2.3. Synthesis of $[Ag(NHC)(NH_3)]PF_6$ and $[Ag(NHC)_2]PF_6$ complexes

The initial set of heteroleptic Ag(I)-NHC complexes, represented by the general formula of $[Ag(NHC)(NH_3)]^+PF_6^-$ and homoleptic complexes as $[Ag(NHC)_2]^+PF_6^-$, were synthesized by reaction of corresponding $[NHCH]PF_6$ with Ag_2O [226] in the presence of NH_3 (as outlined in Scheme 7). Additional information can be found in Table 4.

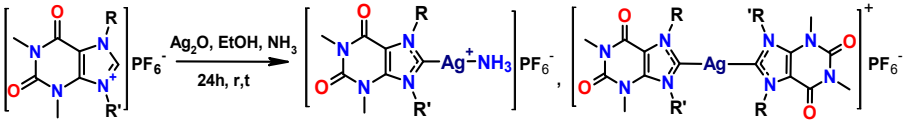

Scheme 7. Synthesis of $[Ag(NHC)(NH_3)]PF_6$ complexes.

Table 4. Synthesis of $[Ag(NHC)(NH_3)]PF_6$ complexes

Name	Anticipated Structure	Yield
Ag1	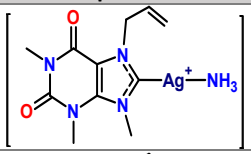	84%
Ag2	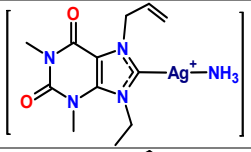	87%
Ag3	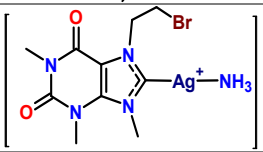	68%
Ag4	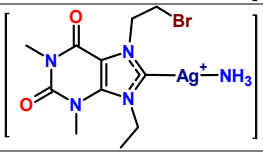	69%

Compounds **Ag1-Ag4** were characterized by NMR and HRMS analyses. The most significant alterations in the ^{1}H-NMR spectrum included the loss of the imidazolium proton signal at 9.30-9.60 ppm and the emergence of a new signal around 3 ppm, with an integral of 3, which can be attributed to the NH_3 ligand. Additionally, the appearance of a signal in the ^{13}C-NMR spectrum at 184-186 ppm, corresponding to the carbene carbon directly attached to Ag, further confirmed the successful synthesis of the anticipated product. It is worth noting that in the absence of ammonia, we will have homoleptic complexes with the formula of $[Ag(NHC)_2]PF_6$, which were also characterized by ESI-MS and crystallography. Complexes **Ag1**, **Ag2,** and **Ag4** were successfully obtained as a monocrystal suitable for X-ray diffraction analysis. Their single crystal was obtained through the slow diffusion of Tetrahydropyran into an acetonitrile solution. The molecular structures of these complexes in their solid state are illustrated in Figure 2.5.

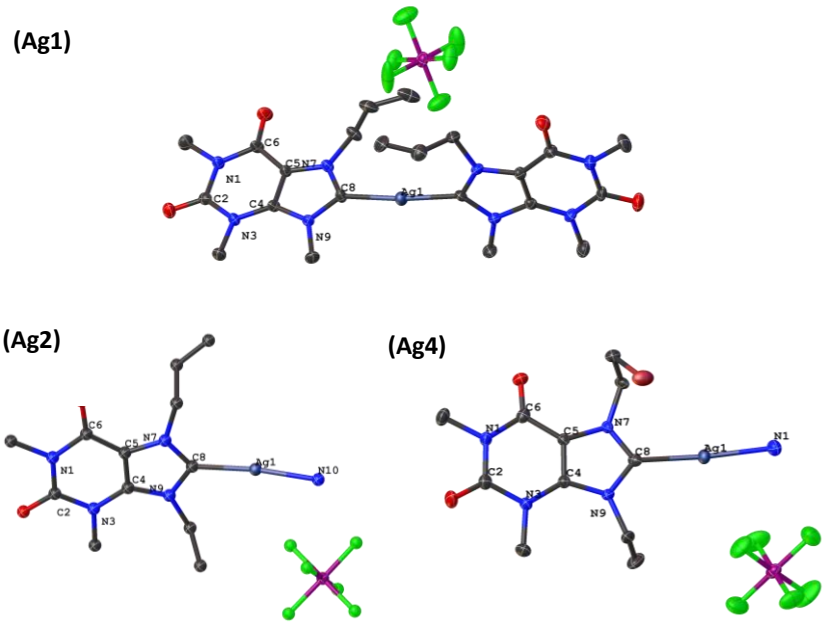

Figure 2.5. Molecular structure of complexes **Ag1**, **Ag2** and **Ag4**. Hydrogen atoms have been excluded for improved clarity, and ellipsoids are shown at 50% probability. Selected interatomic distances [Å] and bond angle [°]: Complex **Ag1**: C8-Ag1: 2.118(10) Å, Ag1-N10: 2.118(4) Å, N7-C8-N9: 106.03(8)°, C8-Ag1-C17: 174.8(4)°. Complex **Ag2**: C8-Ag1: 2.071(4) Å, N7-C8-N9: 106.2(3)°. Complex **Ag4**: C8-Ag1: 2.074(3) Å, Ag1-N10: 2.124(3) Å, N7-C8-N9: 105.8(3)°, C8-Ag1-N10: 175.07(11)°.

2.4. Synthesis of [Ag(NHC)(Cl)] complexes

The synthesis of silver-NHC complexes featuring halogen-coordinating anions was accomplished through the reaction of the corresponding ligands (**6a** and **6b**) with silver(I) oxide in ethanol or DCM, yielding compounds with the general formula of [Ag(NHC)Cl] (scheme 8), designated as complex **Ag5** (Figure 2.6).

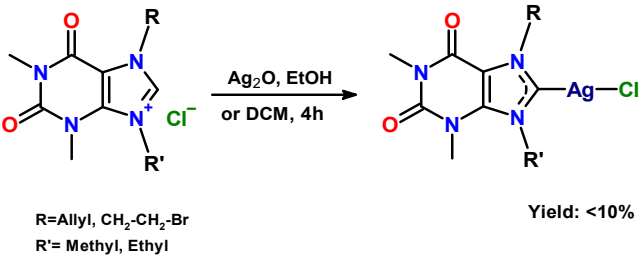

Scheme 8. Synthesis of Ag(NHC)Cl complexes.

Complex **Ag5** exists as a neutral species in solution. [227] The $^{107/109}$Ag-$^{13}C_{NHC}$ resonance was observed at a chemical shift of 183.94 ppm. This complex was the sole product formed from the successful reaction of the (NHCH)Cl salt with silver(I) oxide, which yielded the corresponding [Ag(NHC)Cl]. The complex was thoroughly characterized using NMR and HRMS techniques.

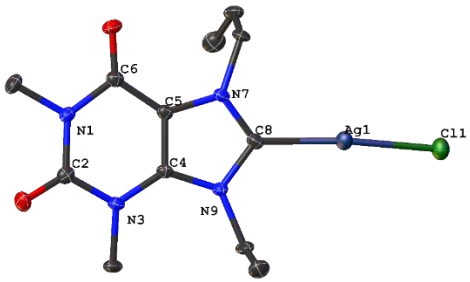

Figure 2.6. Molecular structure of complex **Ag5**. Hydrogen atoms have been excluded for improved clarity, and ellipsoids are shown at 50% probability. C8-Ag1: 2.096(3) Å, Ag1-Cl1: 2.3632(8) Å, N7-C8-N9: 106.03(3)°.

This methodology represents a well-established approach for the preparation of silver-NHC complexes, leveraging the basic nature of silver(I) oxide to facilitate the deprotonation of xanthinium salts and subsequent coordination to the silver center. However, the synthesis of the [NHCH]Cl precursor in this project presented significant challenges in terms of yield optimization. The low yield of this crucial intermediate compound severely limited the scope of subsequent reactions and hampered efforts to conduct comprehensive characterization and reactivity studies of the resulting silver complexes. Similarly, for the bromine-substituted theophylline, no successful outcome was obtained in its reaction with silver. This lack of reactivity might be attributed to steric or electronic effects introduced by the bromine substituent, potentially hindering the formation of the desired silver complex. Further investigation is needed to understand the exact reasons for this failure and to explore alternative reaction conditions or reagents. This limitation in the case of [NHCH]Cl precursor prompted us to explore [NHCH]I precursors, which generally exhibit enhanced reactivity and yield in silver complex formation.

The use of iodide counterions offers several advantages over chloride in this context: (1) Increased solubility: [NHCH]I salts typically demonstrate improved solubility in organic solvents compared to their chloride counterparts, facilitating more efficient reactions. [228] (2) Enhanced leaving group ability: Iodide is a better leaving group than chloride, potentially leading to a more facile formation of the Ag-NHC bond. [229] (3) Reduced tendency for halide bridging: Iodide's larger size and softer nature can minimize unwanted halide bridging in the resulting silver complexes, often resulting in more well-defined monomeric structures. [230] (4) proved yield: The combination of these factors frequently results in higher yields of the desired Ag(I)-NHC complexes when using iodide precursors. [228] (5) Versatility in further transformations: Ag(I)-NHC complexes derived from iodide precursors can serve as effective transmetallation agents for synthesizing other metal-NHC complexes. [229]

2.5. Why are Ag complexes so important?

Coinage Metal-NHCs are extensively researched due to their fascinating structural characteristics and diverse potential applications. Among this group, silver(I)-NHCs have emerged as the most extensively studied subclass. This is primarily attributed to two factors:

The ease of synthesizing Ag(I)-NHCs using the Ag_2O route, which involves the reaction of xanthinium salts with silver(I) oxide. [178] Ag(I)-NHCs also serve as convenient precursors for obtaining other metal-NHCs through a process called transmetallation. [45] In this process, the silver atom is replaced by a different metal, allowing for the preparation of a wide range of metal-NHC complexes.

Additionally, silver-NHC complexes also exhibit biological activity. They have been shown to possess antibacterial properties and have

demonstrated cytotoxicity, which refers to their ability to be toxic or lethal to cancer cells. [63,231–236] Additionally, The Ag_2O method for preparing Ag(I)-NHC complexes has several benefits: (1) Ag_2O is a stable compound that is easily obtained; (2) The reaction can be performed at room temperature in the presence of air; (3) Solvent pretreatments and strong bases are unnecessary. [237,238] These properties have made Ag(I)-NHCs the most extensively studied class within the broader field of metal-NHC research.

The Ag_2O route, typically conducted in organic aprotic solvents, is now regarded as a classic method for synthesizing silver-NHC complexes. In this process, silver(I) oxide is the metal source and the base. [45] In fact, the Ag_2O molecule removes a proton from an xanthinium cation. Then, the Ag(X) atom (X= Cl, Br, I) binds to the carbene to form the first [Ag(NHC)X] complex and AgOH (Scheme 9, equation 2.1). This AgOH removes a proton from a second xanthinium cation, and the silver metal coordinates to the carbene to produce the second [Ag(NHC)X] complex and H_2O (Scheme 9, equation 2.2). [239]

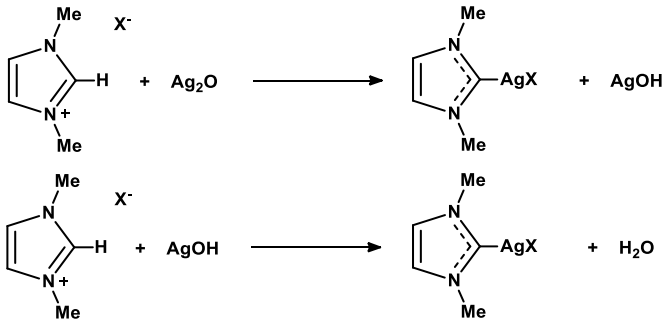

Scheme 9. Mechanism of reaction of Ag_2O with $(NHC)^+X^-$ precursor, X=Cl, Br, I.

The success of this Ag_2O-based method for preparing Ag(I)-NHC complexes may depend on properties like the acidity [149,208,240,241] and

steric hindrance [227,242–245] of the azolium salt precursors, as well as the nucleophilicity [95,146,246] of the NHC ligands. (Chapter 1, part 1.2.3. and 1.2.4). The reactivity and yields could vary depending on the specific azolium salt and NHC employed in the silver-NHC synthesis.

The reaction of xanthinium salts with Ag_2O typically results in the formation of neutral [Ag(NHC)X] complexes or ionic compounds $[Ag(NHC)_2][AgX_2]$. [247] It has been suggested that a dynamic equilibrium exists between these forms in solution [176,178,216] (Equation 2.3) and can be observed using ^{13}C NMR spectroscopy. [178,227,248]

$$2Ag(NHC)X \rightleftharpoons [Ag(NHC)_2][AgX_2] \rightleftharpoons Ag(NHC)_2X + AgX \quad (2.3)$$

The isolation of either the neutral or ionic form primarily relies on the steric size of the NHC and the choice of solvent system. In general, larger NHCs and less polar solvents tend to favor the neutral form. [248] Often, the formation of Ag(I)-NHC complexes is accompanied by the precipitation of AgX, resulting in the isolation of nonstoichiometric $[Ag(NHC)_2][(AgX_2)_n/X_{1-n}]$. [249,250] To avoid this issue, pure $[Ag(NHC)_2]^+$ type salts can be generated through anion metathesis using anions such as BF_4^-, PF_6^-, $B(Ph)_4^-$, or NO_3^-. However, in some instances, extended reaction times can lead to the complete precipitation of AgX, resulting in the formation of three-coordinated $[(Ag(NHC)_2X]$ type compounds. [247]

2.6. Synthesis of [Ag(NHC)(I)] complexes

The [Ag(NHC)I] complexes were synthesized by treating the corresponding (NHCH)I salts (**7a-7b**) with Ag_2O [178] or silver acetate (AgOAc) [209,251] in acetonitrile or methanol. It is well-known that silver complexes may undergo ligand redistribution equilibria [252] using a solvent with a high dielectric constant may favor the formation of the

cationic homoleptic complexes. Several attempts to react xanthinium salts with silver oxide did not succeed, as indicated in Table 5.

Table 5. Synthesis of [Ag(NHC)I] complexes.

Name	Structure	Silver reactant	yield
Ag6	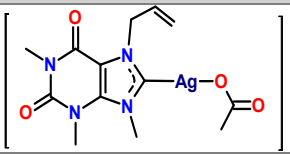	AgOAc	36%
Ag7	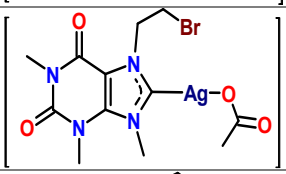	AgOAc	36%
-	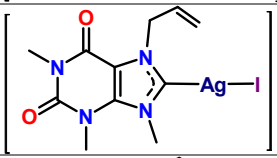	Ag_2O	×
-	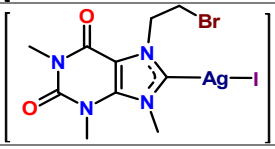	Ag_2O	×

The mechanism remains unclear, although crystallographic data (Figure 2.7) revealed that the xanthinium salt dissociated from C8, which interfered with the formation of a bond between silver and C8. The reasons for this occurrence are not understood. Consequently, this led to the exploration of using silver acetate as an alternative reagent for the reaction.

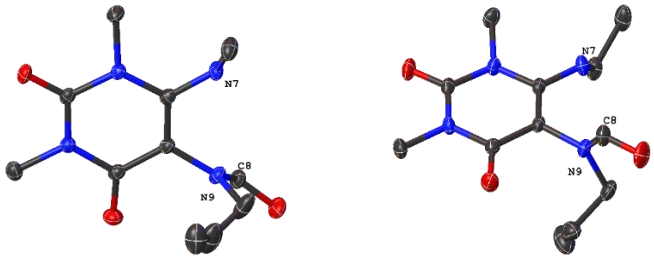

Figure 2.7. Crystal structures showing aldehyde formation at the C8 position of the xanthinium salt.

The process of the reaction between silver acetate and [(NHC)I] precursor is achieved through the addition of two equivalents of silver acetate. The initial equivalent of silver acetate generates silver iodide and acts as a base to deprotonate C8, resulting in the formation of acetic acid and the *in situ* generation of the carbene. Subsequently, the second equivalent of silver acetate reacts with the carbene to yield compounds of type [Ag(NHC)OAc]. [253] The general procedure is shown in Scheme 10.

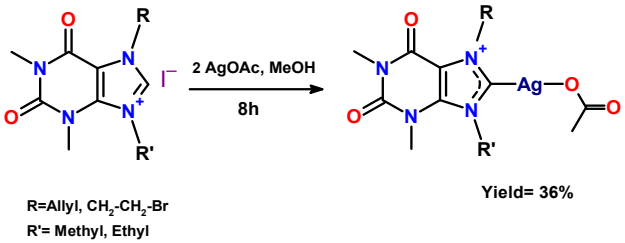

Scheme 10. Synthesis of Silver-NHC complexes through the reaction with silver acetate.

The synthesized products were characterized using NMR and HRMS techniques. In the ^{1}H NMR spectra of complex **Ag6**, the absence of the imidazolium proton (NCHN) signal suggests the successful formation of the silver complexes. The ^{13}C NMR spectra for compounds **Ag6** and **Ag7**

show a characteristic singlet at 185.54 and 184.03 ppm, respectively, corresponding to the $^{107/109}Ag$-$^{13}C_{NHC}$ resonance.

The silver complexes derived from bromo-substituted theophylline exhibited a mixture of product and unreacted starting material (S29-supplementary information), which might indicate a slow reaction. This slow reactivity could be considered a limitation of this particular xanthinium species. One possibility might be a substitution reaction at the C13 position (ion exchange of Br with I), which may interfere with the primary reaction. Furthermore, the mass spectra of Ag7 indicate that only the iodo-substituted xanthinium reacted with silver acetate, resulting in a mixture of unreacted bromo-substituted and reacted iodo-substituted species. The molecular structure of compound **Ag6** was determined using single-crystal X-ray diffraction (Figure 2.7). Selected bond lengths and angles are shown in Table 6.

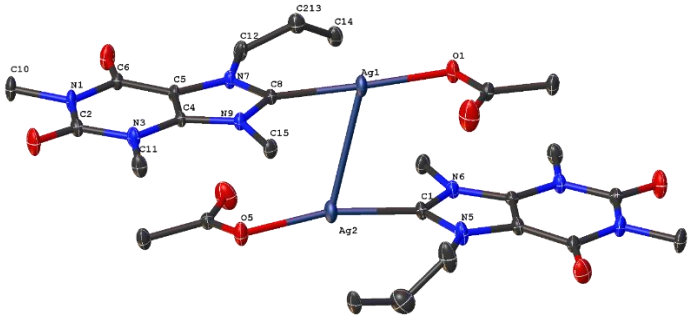

Figure 2.8. Molecular structure of silver(I)-NHC complexes **Ag6**. Hydrogen atoms have been omitted for clarity, and ellipsoids are shown at 50% probability.

Silver carbene complexes of this type are known to have a variety of different structures in the solid state. [178,250,254] In most other instances, we obtained a yellow or colorless, viscous, oily liquid that was unsuitable for high-quality crystallographic analysis.

Table 6. Selected bond lengths (Å) and angles (°) for silver(I)–NHC complexes **Ag6**

	Bond lengths (Å)		Bond angles (°)
Ag1-Ag2	3.1301(4)	C8-Ag1-O1	175.42(14)
Ag2-C1	2.084(4)	C1-Ag2-O5	166.39(5)
Ag1-C8	2.087(3)	O1-Ag1-Ag2	107.1(2)
Ag1-O1	2.140(2)	C1-Ag2-Ag1	80.16(8)
Ag2-O5	2.153(2)	N7-C8-N9	105.8(2)

This kind of crystal can be obtained by slow diffusion of Ethyl acetate into Methanol or a similar combination of DMC/Pentane.

2.7. Transmetalation reactions

The synthesis of Ag(I)-NHC compounds is essential in organometallic chemistry. This is because the carbene can subsequently be transferred to a transition metal complex through transmetallation [22,176,231], thereby producing the desired M-NHC compound. The gold (I) and palladium (II) NHC complexes synthesized by Wang and Lin in 1998 are the first examples of this method. [178]

Due to their strong σ-donor capabilities, *N*-heterocyclic carbenes (NHCs) are among the most commonly used ligands for coordinating transition metal centers. Their effectiveness in forming stable complexes was recognized even before the free NHC ligands themselves were successfully isolated. [4,37,38] It is important to highlight that NHCs predominantly exhibit strong σ-donor properties rather than significant π-acidity, which distinguishes them from routine Schrock or Fischer carbenes. However, despite this, backbonding into the vacant p_z orbital should not be disregarded, particularly when interacting with

electrophilic metal centers, as it still plays a non-negligible role. [54,255] Compared to phosphines, NHCs generally exhibit even stronger σ-donation, as evidenced by lower Tolman electronic parameters. A key distinction between NHCs and phosphorus-based ligands is the coordination environment. While phosphines form a cone-like shape pointing away from the metal, NHCs adopt umbrella-shaped coordination due to the substituents on the adjacent heteroatom(s) (see Figures 1.15 and 1.16). This results in greater steric bulk near the metal, which can significantly influence the binding behavior of other ligands and, consequently, affect the catalytic performance of the metal center. [256]

2.7.1. Synthesis of Au(I)-NHC complexes

In 1997, Lin and his team successfully synthesized the first series of liquid crystalline Au(I)-NHC compounds by reacting long-chain substituted N,N'-dialkyl benzimidazolium salts with $[Au(SMe_2)Cl]$ under phase-transfer catalysis conditions. [257] The following year, in 1998, they introduced a method for synthesizing Au(I)-NHCs by utilizing Ag(I)-NHCs as carbene transfer agents. [178] This approach significantly simplified access to Au(I)-NHCs, providing a highly convenient pathway for their preparation.

General synthetic method:

Scheme 11 illustrates the common approaches for synthesizing Au(I)-NHC complexes: [45] (1) cleavage of electron-rich double bonds, (2) protonation or alkylation of gold carbonate compounds, (3) transfer of NHC ligands from group 6, 7, and 11 complexes, and (4) reaction of Au(I) sources with either free NHCs or those generated *in situ*.

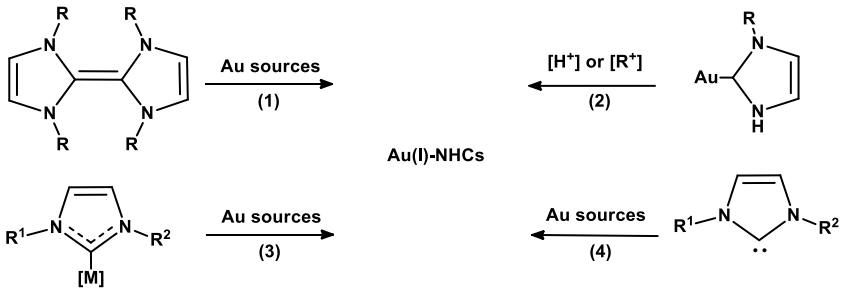

Scheme 11. General methods employed to synthesize Au(I)-NHC complexes. [45]

Among these methods, over 70% of published results utilize the Ag-carbene transfer route (3), while around 20% rely on the free-carbene method (4). [45] In our project, we experimented with both methods 3 and 4 to evaluate and compare their feasibility and reactivity within the context of our case study.

Gold-NHC complexes with the general formula of [Au(NHC)X], where X= PF_6, I were synthesized by the reaction of corresponding silver-NHC complexes with gold precursor [Au(THT)Cl] in acetone or DCM as the solvent (Scheme 12). [178,197] The synthesized complexes are shown in Table 7. When PF_6^- is used, the formation of a gold bis(NHC) salt is expected, whereas the use of I^- typically leads to the formation of a mono(NHC) gold complex, [Au(NHC)I].

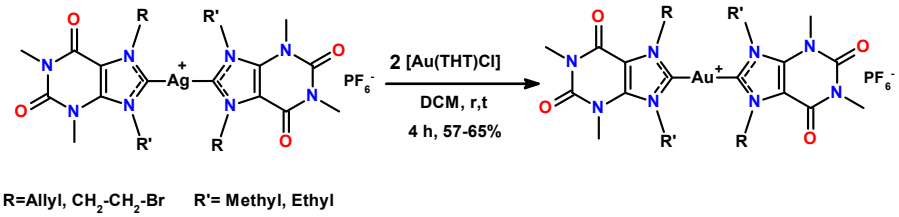

Scheme 12. Synthesis of Au(I)-NHC complex via transmetallation reaction.

Table 7. Synthesis of Au-NHC complexes via transmetallation reaction

Product name	reactant	structure	Yield
Au1	$[Ag(NHC)_2]^+PF_6^-$	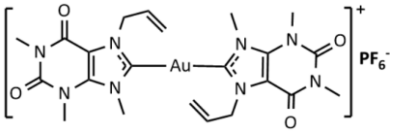	48%
Au2	$[Ag(NHC)_2]^+PF_6^-$	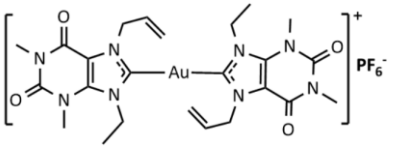	56%
Au3	$[Ag(NHC)_2]^+PF_6^-$	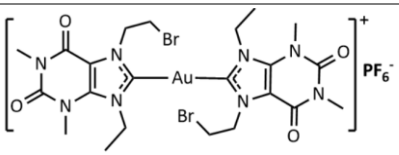	36%

These three complexes were fully characterized using NMR and ESI-MS techniques. In the ^{13}C-NMR spectra, the signal for the carbene carbon attached to the Au atom shifted upfield, from approximately 186 ppm for the Ag-C_{carb} to around 175 ppm.

When reacting $[Ag(NHC)]PF_6$ with a gold precursor, a mixture of unreacted starting material and the desired product is observed. This is clearly evident in the ^{1}H NMR and mass spectra, particularly in the spectra of **Au2** and **Au3**. This suggests that the reaction involving silver-PF_6 complexes proceeds more slowly and may require extended reaction times or additional measures, such as heating, to accelerate the process.

The structure of complex **Au2** was confirmed by X-ray diffraction analysis. A suitable single crystal was grown by slow diffusion of *tert*-butyl methyl ether into a concentrated solution of dichloromethane.

The molecular structure of complex **Au2** in the solid state is illustrated in Figure 2.9.

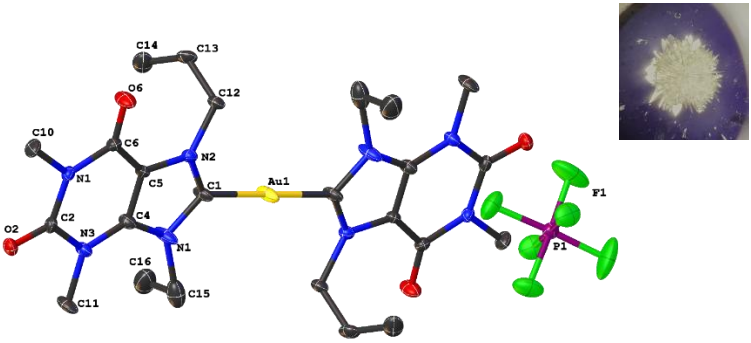

Figure 2.9. Molecular structure of Gold(I)-NHC complexes **Au2**. Hydrogen atoms have been omitted for clarity, and ellipsoids are shown at 50% probability. Selected interatomic distances [Å] and bond angle [°]: C1-Au: 2.016(7) Å. C1-Au-C1 angle: 180.0 (4)°. N(1)-C(1)-N(2): 106.3(5)°.

The Au-C_{carb}. bond length [C_8-Au= 2.016(7) Å] in complex **Au2** is shorter than the Ag-$C_{carb.}$ bond lengths in complexes **Ag5** and **Ag6** (C_8-Ag = 2.096(3) Å and 2.087 Å), indicating that gold forms stronger or more covalent interactions with the carbene carbon than silver.

2.7.2. Synthesis of Rhodium-(NHC) complexes

Various methods for synthesizing rhodium-NHC complexes involve different solvents and adjustments to temperature and reaction time. One effective approach, described by Zinner *et al*. [238], is the synthesis of Ag-NHC complex starting with NHC-PF_6 salt, which is subsequently treated with an excess of potassium iodide and then reacted with a rhodium precursor. This sequence of steps, as shown in Scheme 13, yields the desired rhodium-NHC complex. There is also a gentle carbene transfer method which was initially developed by Wang and Lin [178] for the transmetallation a silver carbene by treatment with

$[RhCl_2(COD)]_2$ in CH_2Cl_2 as the solvent in room temperature for 24 hours. This method is known as the classical transmetallation route (especially for ligands with halogen counterions). In our experiment, we examined the formation of Rh-Complex utilizing both methods. Results are shown in Table 8.

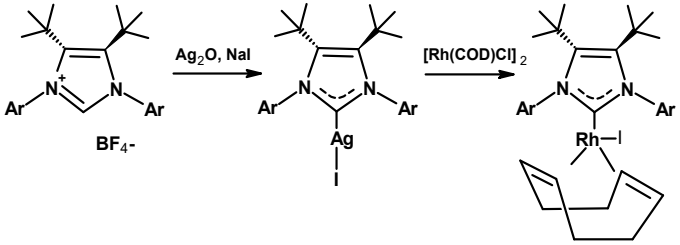

Scheme 13. Synthesis of Rh-NHC complex, by Zinner *et al.* [238]

Table 8. Synthesis of rhodium-(NHC)-complexes via transmetallation reactions

Product name	reactant	Product structure	yield
Rh1	$[Ag(NHC)_2]PF_6$	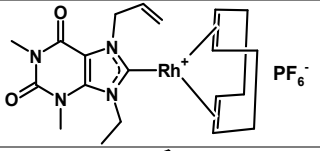	89%
Rh2	[Ag(NHC)Cl]	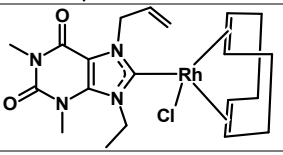	38%

For each synthesis, the complex was purified using gradient column chromatography. Initially, a fraction eluted with CH_2Cl_2 captured a minor amount of unreacted $[Rh(COD)Cl]_2$. Following this, subsequent elution with acetone [238] and THF [237] yielded complexes **Rh1** and **Rh2**, respectively. The synthesized complexes underwent thorough characterization through NMR and ESI-MS techniques. In the ^{1}H-NMR

analysis of the synthesized complexes, distinct proton behaviors were observed that align with established data for similar rhodium complexes. Specifically, the methylene (CH_2) protons of the cyclooctadiene (COD) ligand exhibited a splitting pattern ranging from 1.72 to 2.52 ppm. This pattern is consistent with what has been previously reported for [RhCl(NHC)(COD)] complexes [258], confirming the expected chemical environment around the COD ligand. Furthermore, the methine (CH) protons of the COD ligand were identified as two inequivalent protons. These protons presented resonances between 2.92 and 4.62 ppm, demonstrating the complex electronic interactions within the molecule. This detailed spectroscopic characterization helps in confirming the structural integrity and purity of the synthesized complexes. Figure 2.10 illustrates the variations in the ^{1}H-NMR proton signals between the starting material (xanthinium salt) and the Rh-complex of **Rh2**.

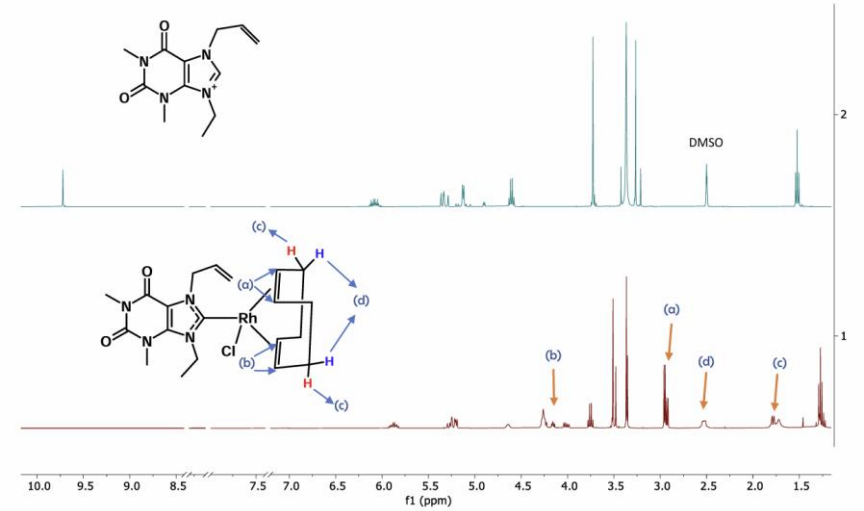

Figure 2.10. Comparative ^{1}H-NMR Spectra of xanthinium Salt (2) and Rhodium Complex (1).

Figure 2.10 presents a visual comparison of the ^{1}H-NMR spectra for an initial xanthinium salt and the resulting Rh-complex. The diagram highlights the splitting of the proton signals from the COD ligand, labeled a to d, which proves the structural transformations and the impact of metal coordination on the proton environment. The disappearance of the imidazolium hydrogen is additional evidence of successful synthesis. Unfortunately, due to the oily nature of the product, possibly resulting from the presence of iodide, we were unable to crystallize the rhodium-NHC complexes.

2.8. Weak base reaction as an eco-friendly route

Although the transmetalation route is convenient to execute, it is hindered by poor atom economy and should only be considered for large-scale applications if the silver or copper by-products are recycled. [168] Therefore, employing a weak base (such as K_2CO_3, NEt_3, or NaOAc) presents an alternative strategy to the free carbene and transmetalation methods, allowing for reactions to be conducted in air, under mild conditions, and in environmentally friendly solvents. This approach yields a diverse array of carbene compounds with various transition metals, achieving high yields and purity. [168] Following this, the successful synthesis of gold and palladium complexes using this method is described.

2.8.1. Synthesis of Au(NHC)I complexes via weak base route reactions

Gold-carbene complexes were the first to be thoroughly investigated using the weak base method. [168] The synthesis of Au(NHC)I complexes is achieved through the direct reaction between gold precursors (such

as [Au(DMS)Cl] or [Au(THT)Cl]) and NHC salts, facilitated by the presence of a weak inorganic base [180,259–261] (Scheme 14).

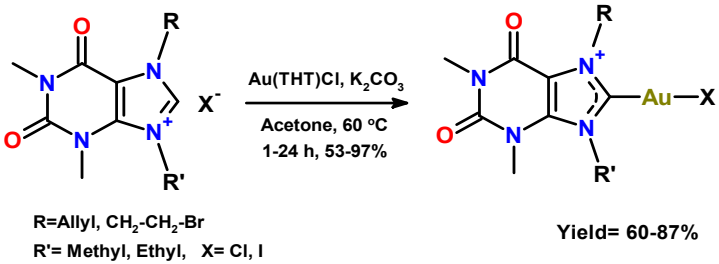

Scheme 14. Synthesis of [Au(NHC)I] complexes via a weak base route.

The synthesis of complexes **Au4** and **Au5** (Table 9), both with the general formula of [Au(NHC)I], was accomplished using this method from their respective (NHCH)I salts **7a-1** and **7a-2**. Unfortunately, the reaction with **7b-1** and **7b-2** was unsuccessful. These synthesized complexes underwent thorough characterization through NMR and ESI-MS spectrometry.

Table 9. Synthesis of Au-NHC complexes via weak base route

Product name	structure	yield
Au4	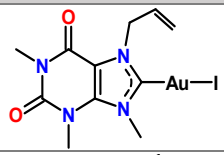	60%
Au5	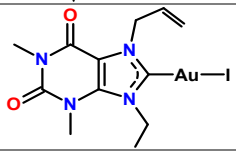	87%

The ^{1}H-NMR spectra displayed patterns similar to those of the corresponding silver-NHC complexes. Interestingly, the carbene carbon signal for the Au atom in compound **Au5** was observed at 186.54 ppm,

a value comparable to that of Ag complexes. This is unexpected, as no silver was involved in the weak base route, and this value is in the range of bis-NHC-Au complexes.

Although mass spectrometry indicated complete conversion to homoleptic $[Au(NHC)_2]^+$ complexes, crystallographic analysis of complex **Au4** and **Au5** revealed that the structure actually crystallized as [Au(NHC)I] through the slow diffusion of *tert*-butyl methyl ether into a dichloromethane solution. (usually for counterion is halogen). Here, it is evident once again that the C8-M bond distances in Au-NHC complexes are shorter compared to those in Ag-NHC complexes. This observation highlights the higher reactivity of gold with the carbene center compared to silver. Another straightforward method for synthesizing Au-NHC complexes, which operates at **room temperature** and does not require elevated temperatures, was introduced by Gimeno *et al.* in their 2013 publication, [262] in which an equimolar mixture of NHC·HCl and [AuCl(tht)] is prepared in dichloromethane. After 15 minutes of stirring, 20 equivalents of a weak base, such as K_2CO_3, are added (which is typically utilized in nucleophilic substitution reactions with an acidic reactant with [AuCl(L)] [263]).

The reaction is completed within 1.5 hours under this mild condition. This method was utilized for compound **6b**, and the results from ^1H NMR and mass spectrometry confirmed the successful conversion to the Au-NHC complex. Notably, the mass spectrum **exclusively** displayed the homoleptic Au-$(NHC)_2$ complex, where the bromine atom was replaced by chlorine at the C^{13} position (Figure 2.11).

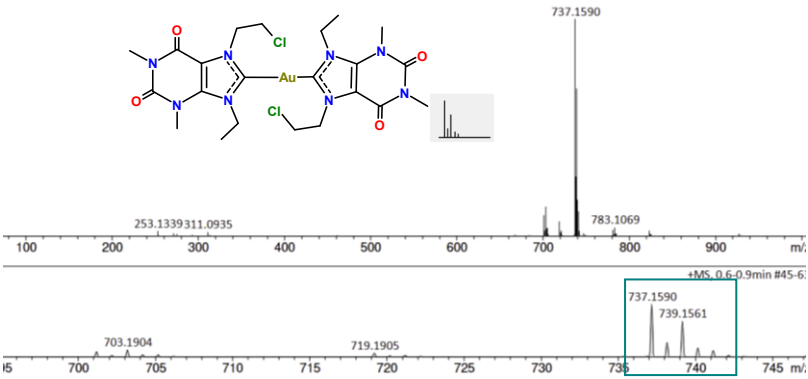

Figure 2.11. Synthesis of $[Au\text{-}(NHC)_2]^+$ complexes via weak base route by Gimeno *et al.*

The solid-state molecular structure of complex **Au4** and **Au5** is depicted in Figures 2.12 and 2.13.

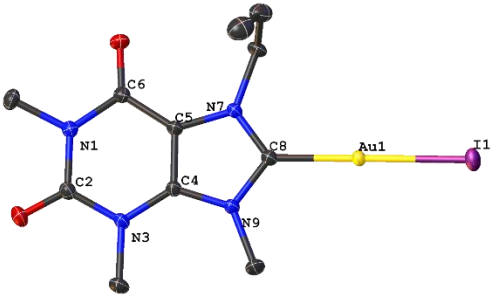

Figure 2.12. The molecular structures of complex **Au4** in the solid state. Hydrogen atoms have been excluded for improved clarity, and ellipsoids are shown at 50% probability. Selected bond lengths [Å] and angles [°]: Au1-C8 = 2.0016 (13) Å, Au1-I(1)= 2.5479 (3) Å. C8-Au1-I1 angle: 178.55(4)°.

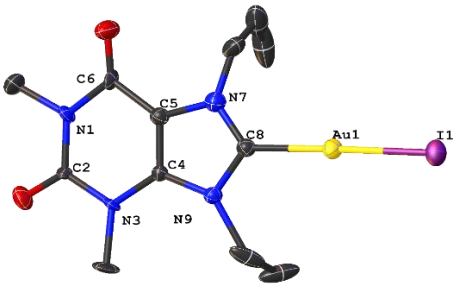

Figure 2.13. The molecular structures of complex **Au5** in the solid state. Hydrogen atoms have been excluded for improved clarity, and ellipsoids are shown at 50% probability. Selected bond lengths [Å] and angles [°]: Au1-C8= 2.059(18) Å, Au1-I(1)= 2.500(5) Å. C8-Au1-I1 angle: 177.6(5)°.

Using this mild base method, superior results could be achieved compared to the previous route, not only due to the significantly shorter reaction times but also because of the higher yields obtained.

2.8.2. Synthesis of Pd(II)-NHC complexes

The development of palladium-NHC complexes has garnered significant interest among researchers due to their versatile applications and cost-effectiveness compared to gold and platinum complexes. Palladium-NHC complexes, often featuring bulky substituents, are particularly valued for their catalytic properties in various organic transformations. Researchers have focused on understanding the steric effects [264] of these bulky substituents [265] by calculating the %V_{bur} values, which quantify the percentage of the coordination sphere occupied by the ligand. [13] This parameter helps in fine-tuning the reactivity and selectivity of the complexes, making palladium-NHC complexes a crucial area of study in the field of organometallic chemistry.

Palladium-PEPPSI complexes

In 2006, Organ and colleagues[266,267] developed a class of palladium-NHC complexes known as PEPPSI (Pyridine Enhanced Precatalyst Preparation Stabilization and Initiation) catalysts. These complexes are characterized by their ease of handling, stability against moisture, and the use of an NHC ligand paired with a palladium atom, two anionic ligands (such as OAc, Br, or Cl), and a fourth, easily removable pyridine ligand.

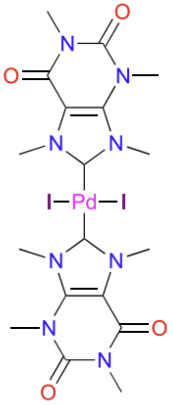

Scheme 15. Pd-bis(NHC) complex derived from caffein, synthesized by Luo and Lo in 2011

The pyridine ligands, or their substituted versions, were found to be effective replacements for traditional ligands, allowing the preparation of these metal complexes without the need for a glove box.

Additionally, including pyridine facilitated the straightforward synthesis of stable palladium (II) complexes that could potentially dissociate into active palladium-NHC (0) species upon activation. This innovation paved the way for the exploration of new NHC-Pd-Py complexes, expanding their utility across a broad range of organic transformations. [13] In 2011, Luo and Lo [268] synthesized a palladium bis(NHC) complex derived from caffeine and evaluated its performance in various cross-coupling reactions, including Suzuki–Miyaura, Heck, and Sonogashira (Scheme 15). The complex demonstrated efficacy in these catalytic

processes, showcasing the potential of caffeine-derived NHC ligands in palladium-catalyzed organic transformations. The NHC is an excellent *σ*-donor and facilitates the oxidative addition of substrates to the palladium center, which enhances the reactivity of the resulting Pd–bis(NHC) complex and improves the efficiency of the reaction. [21]

In this work, we reported the preparation of two novel Pd-PEPPSI complexes bearing NHC ligands derived from Theophylline based on the reaction shown in Scheme 16.

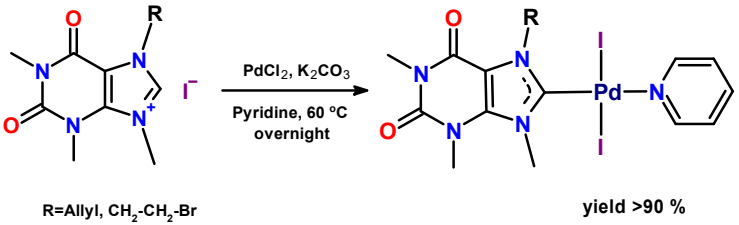

Scheme 16. Optimized synthesis of Pd-PEPPSI complexes **Pd1** and **Pd2**

Compounds **7a-1** and **7b-1** were subjected to an overnight reaction with $PdCl_2$ and K_2CO_3 in neat pyridine at 60°C, with no special precautions to exclude air or moisture. The reaction products were then separated using column chromatography on silica gel and eluted with 100% CH_2Cl_2. Following the work-up, a shiny orange solid of **Pd1** and **Pd2** was isolated in nearly quantitative yield, as shown in Table 10.

^1H and ^{13}C NMR analyses confirmed the formation of two distinct complexes. In comparison to silver(I) and gold(I) complexes, the signal for the carbene carbon attached to palladium in the palladium-NHC complexes appeared around 155-157 ppm. [21] X-ray diffraction analysis further indicated that, in complex **Pd2**, the bromide at the N7 position was replaced by iodide during the reaction with methyl iodide used for synthesizing the xanthinium salt.

Table 10. Synthesis of Pd-PEPSI complexes via the weak base route.

Product name	Structure	Yield
Pd1	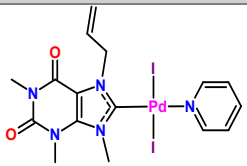	94%
Pd2	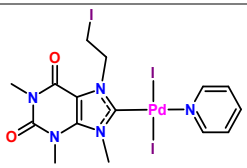	91%

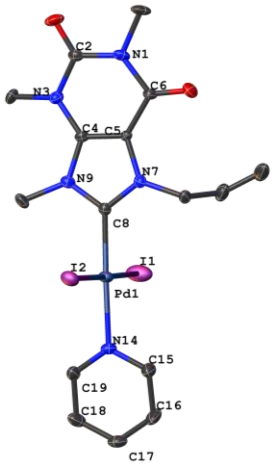

(Pd1)

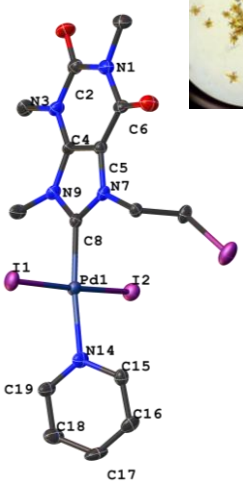

(Pd2)

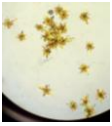

Figure 2.14. The molecular structures of complexes **Pd1** and **Pd2** in their solid state. Hydrogen atoms were omitted for clarity, and ellipsoids are shown at 50% probability. Selected bond lengths [Å] and angles [°]: complex **Pd1**: Pd-I1: 2.5963(6) Å, Pd-I2: 2.5951(6) Å, Pd-C8: 1.976(5) Å, Pd-N14: 2.092(4) Å, I1-Pd-I2: 177.82(2)° , C8-Pd-N14: 177.95(18)° , [N7– C8–Pd–I1]: -83.5(4)°, [C15–N14–

Pd–I1]: 80.3(3)° , N7-C8-N9: 107.6(4)° , complex **Pd2**: Pd-I1: 2.5995(7) Å, Pd-I2: 2.6064(7) Å, Pd-C8: 1.963(6) Å, Pd-N14: 2.089(5) Å, I1-Pd-I2: 174.83(2)° , C8-Pd-N14: 173.6(2)° , [N7– C8–Pd–Cl1] -96.4(4)° , [C15–N14–Pd–Cl1] 68.6(3)°.

The slow diffusion of the product in a DCM/tert-butyl methyl ether solution yielded yellow prismatic crystals suitable for X-ray diffraction analysis (Fig. 2.14). The alignment between the carbenic carbon of the NHC, the metal center, and the nitrogen atom of pyridine was nearly perfect, forming a C8–Pd–N14 angle of 177.95(18)° and 173.6(2)°. In contrast, the two iodide atoms were slightly tilted towards the NHC, resulting in an I1–Pd–I2 angle of 177.82(2)° and 174.83(2)°.

2.9. Further functionalization of Theophylline: Thiophenol Substitution and Reactivity Exploration

In the final phase of this study, modifications were made to bromo-substituted theophylline. Given that the bromine atom exhibited a tendency to be easily replaced by other atoms or groups during the experimental processes, we chose to substitute it with thiophenol. This allowed us to investigate the reactivity of the newly functionalized theophylline in complex formation reactions. Replacing bromine with thiophenol introduces a soft nucleophilic site with increased electron density, potentially enhancing the interaction with silver and promoting the formation of stable silver complexes. However, steric effects and possible side reactions, such as oxidation, could also influence the outcome of the reaction. Experimental results would be needed to confirm the exact impact of this substitution on the silver complex formation.

2.9.1. Synthesis of [NHCH]PF_6 salts of thiophenol-substituted theophylline

Various methods were explored to achieve this, and ultimately, the straightforward reaction of $(NHC)^+PF_6^-$ with thiophenol in the presence of NaOH for SH deprotonation in an aqueous solution yielded the desired outcome. Further investigation showed that deprotonation could also be achieved using a weaker base, such as triethylamine, in an aqueous solution. This approach simplified the separation process, as the product remained insoluble in water while the thiophenolate dissolved. Additionally, employing this method resulted in an improved yield. Compounds **T-1** and **T-2** were successfully synthesized and thoroughly characterized using NMR analysis and Mass spectroscopy techniques. The results are shown in Table 11.

Table 11. Synthesis of PF_6 salts of thiophenol-substituted theophylline.

Product name	Structure	Yield
T-1	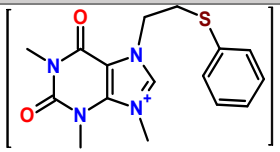	90%
T-2	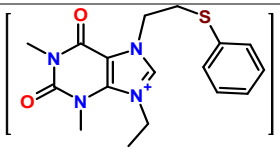	92%

2.9.2. Synthesis of [NHCH]I salts of thiophenol-substituted theophylline

To have halogen salts of thiophenol-substituted theophylline, it is possible to do the exchange reaction with compound **1b** in the presence of thiophenol and triethylamine, and then do the alkylating reaction with methyl or ethyl iodide as we did and could have the following structure listed in Table 12.

Table 12. Synthesis of Iodide salts of thiophenol-substituted theophylline.

Product name	Structure	Yield
T-3	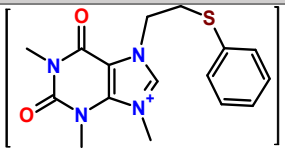	68%
T-4	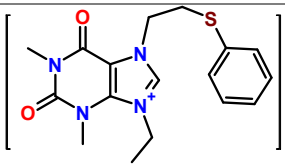	79%

All the synthesized structures were characterized by NMR and Mass spectroscopy techniques, which are available in the supplementary data file. The next step is for this new generation of "thiophenol-substituted theophylline" to react with silver and gold, based on the method represented in parts 2.3 and 2.8.1, respectively.

2.10. Synthesis of $Ag(NHC)PF_6$ complexes of thiophenol-substituted theophylline

The $[Ag(NHC)_2]PF_6$ complexes derived from thiophenol-functionalized theophylline were synthesized following the procedure outlined in Section 2.3. Both Ag_2O and AgOAc were tested as silver sources, and

both successfully facilitated the reaction. However, the use of silver acetate resulted in a higher yield compared to silver oxide. The X-ray diffraction analysis of a single crystal obtained through the recrystallization process (**Ag8**) verified the presence of a homoleptic structure, with no detectable interaction between the sulfur atom and the silver center (Figure 2.15).

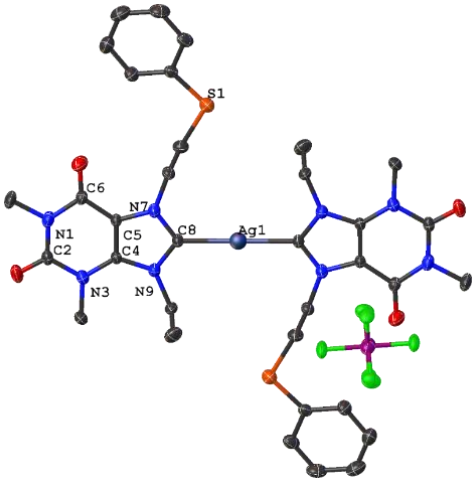

Figure 2.15. Molecular structure of complex **Ag8**. Hydrogen atoms have been excluded for improved clarity, and ellipsoids are shown at 50% probability. Selected bond lengths [Å] and angles [°]: Ag1-C8= 2.0790(17) Å, C8-Ag1-C8' angle: 180.00(4)°.

However, further investigation into crystal growth revealed variations in crystal packing for **Ag9**, which exhibits a *cis*-homoleptic arrangement. This structural shift suggests the possibility of weak internal interactions between the sulfur atoms and the metal center (Figure 2.16).

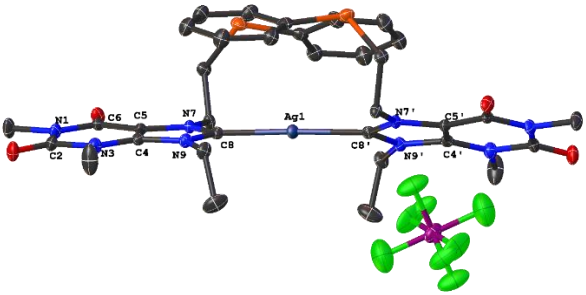

Figure 2.16. Molecular structure of complex **Ag9**. Hydrogen atoms have been excluded for improved clarity, and ellipsoids are shown at 50% probability. Selected bond lengths [Å] and angles [°]: Ag1-C8= 2.085(5) Å, C8-Ag1-C8' angle: 178.3(3)°. N7-C8-C8'-N9' torsion angle: 26.6(4)°.

Quite contrary to complex **Ag8**, which shows a total symmetrical linear geometry with no interaction between the silver center and sulfur atoms, complex **Ag9** exhibits a slightly distorted geometry with a torsion angle of 26.6(4)°, which shows twisting around the center.

2.11. Synthesis of Au-(NHC)-X, (X=PF_6, I) complexes of Thiophenol-substituted Theophylline

To obtain gold complexes with PF_6^- or iodide counterions, the methods outlined in sections 2.7.1 and 2.8.1 were followed accordingly. In this study, gold complex **Au6** was successfully synthesized with a good yield (80%) and characterized using NMR and mass spectrometry techniques.

Table 13. Synthesis of Au(NHC)Cl complex of thiophenol-substituted theophylline.

Product name	structure	yield
Au6	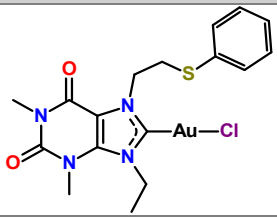	80%

Surprisingly, there were no traces of PF_6^- anion in the mass spectra, which shows PF_6^- might be replaced with chloride anions from the gold source.

2.12. Switching from thiophenol to tosylate: Enabling silver-driven polymerization via ligand and counterion design

Despite incorporating a thiophenol substituent into the theophylline scaffold with the expectation of promoting internal Ag–S coordination, no direct interaction between the sulfur atom and the silver center was observed in the resulting complex. Motivated by this limitation, we explored an alternative approach using a tosylate-substituted theophylline derivative, which was obtained as an unfavorable product during the alkylation reaction of compound 1b by alkyl tosylate (section 2.2.2). As shown in Scheme 17, the tosylate-substituted theophylline, without undergoing ion exchange to PF_6^- or iodide salts, reacts directly with silver oxide in acetonitrile as the solvent.

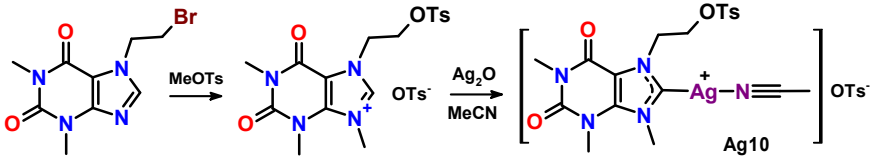

Scheme 17. Synthesis of tosylate-substituted theophylline-silver complexes.

Although the formation of a bis-carbene complex was expected for **Ag10**, and both NMR and mass spectrometry confirmed the deprotonation of the imidazolium group, crystallographic analysis revealed a different structure. Remarkably, the reaction of this tosylated theophylline ligand with silver oxide led to the formation of a well-defined polymeric coordination structure (Figure 2.17). In this system, the tosylate group acted as a μ_2-bridging ligand through its sulfonyl oxygen atoms, effectively linking multiple silver centers and enabling the formation of extended S–O–Ag–O–Ag linkages. In contrast, anions such as PF_6^- or halides (e.g., I^-) lack this bridging capability and do not support polymerization to the same extent. [269] Furthermore, Ag(I) ions have a known preference for soft or borderline donor atoms, particularly nitrogen and oxygen. [270]

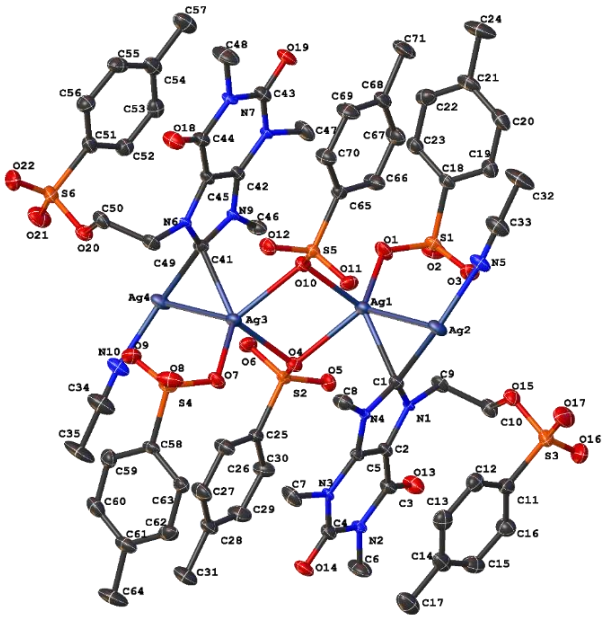

Figure 2.17. molecular structure of complex **Ag10** as a polymeric structure. Hydrogen atoms have been excluded for improved clarity, and ellipsoids are shown at 50% probability.

The combination of tosylate-O and theophylline-N donors creates a favorable coordination environment that supports the formation of stable and extended silver-based polymeric structures. The result was not only structurally distinct from the thiophenol-based system but also demonstrated the crucial role of counterions and subtle electronic factors in directing metal–ligand assembly. This outcome highlights the potential of tosylate-functionalized ligands in constructing extended silver-based architectures.

In addition, a silver–toyslate coordination polymer was observed as a side product and isolated in crystalline form (Figure 2.18).

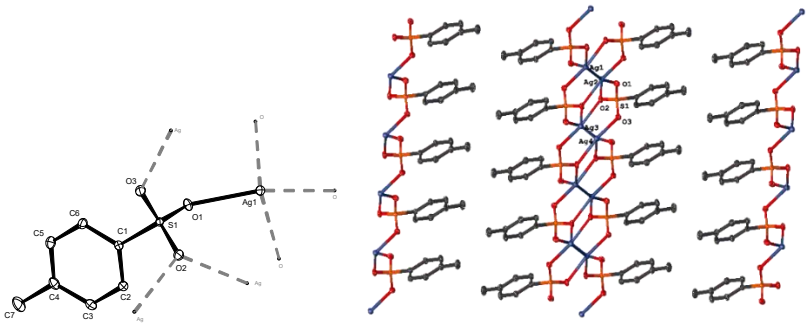

Figure 2.18. The molecular structure of silver-tosylate coordination polymer. Hydrogen atoms have been excluded for improved clarity, and ellipsoids are shown at 50% probability.

While the coordination chemistry of silver(I) sulfonates remains insufficiently explored, particularly in the presence of neutral ligands, [271] the results of this study provide complementary perspectives. In one case, the coordination polymer highlights the synergistic role of a neutral ligand like theophylline alongside the underexplored potential of tosylate ligands in silver-based assemblies. In the other, the formation of a polymeric silver–tosylate side product underscores the intrinsic bridging ability of sulfonate groups, even in the absence of strong neutral donors.

2.13. Idea for Future Work

To investigate the potential interaction between sulfur atoms at the N7-substituted position and the silver center, or more broadly, any metal center, these precursors could be reacted with rhodium or ruthenium. Given that both metals possess vacant orbitals, they may engage in weak intramolecular interactions with the lone electron pairs of sulfur. This approach presents a promising strategy for developing

Metal–NHC complexes featuring additional internal coordination, potentially enhancing their overall stability.

It is also noteworthy to consider the synthesis of Pd(II)-NHC complexes featuring sulfur-functionalized NHC ligands and to examine their coordination behavior. In a study by Vinh Huynh and colleagues [272], it was demonstrated that, in addition to the carbene center, the sulfur moiety of the thioether-NHC ligand also participates in coordination with the palladium center. X-ray crystallographic analysis confirmed the formation of a Pd–S bond, with a bond length of 2.3079(3) Å as depicted in Figure 2.19.

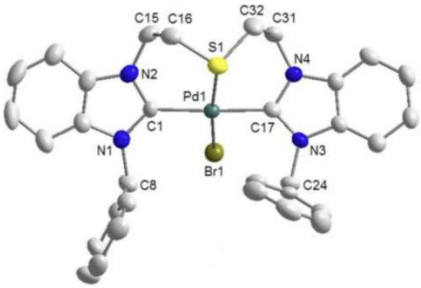

Figure 2.19. Molecular structure of Pd(II)-NHC complex synthesised by Huynh *et al.* [272]

Chapter 3

Experimental

3.1. General considerations

All reactions were conducted at room temperature unless otherwise specified, with some requiring heating up to 150 °C under reflux conditions. Reactions involving silver and gold were carried out in the dark. Key reagents such as [Au(tht)Cl] and $[Rh(COD)Cl]_2$ were synthesized by known methods, while other substances were procured from commercial suppliers and used as received without further purification.

NMR spectrometry

NMR characterizations were performed at 298 K using a Bruker AVANCE 400 operating at 400 MHz for ^{1}H and 151 MHz for ^{13}C, or a Bruker AM 600 operating at 600 MHz for ^{1}H and 151 MHz for ^{13}C. Chemical shifts were referenced to tetramethylsilane ($SiMe_4$, δ = 0), with residual proton impurities from deuterated solvents serving as internal standards (δ 2.50 for DMSO, δ 5.32 for CD_2Cl_2, δ 7.26 for $CDCl_3$). In the ^{13}C NMR spectra, the solvent peaks used were δ 39.51 for DMSO, δ 54.00 for CD_2Cl_2, and δ 77.23 for $CDCl_3$. The multiplicities are denoted as follows: singlet (s), doublet (d), triplet (t), multiplet (m), broad (br), and overlapped (o).

Mass spectrometry

ESI-MS analysis was conducted using a Bruker Daltonics MicroTOF mass spectrometer, operating in either positive or negative mode with acetonitrile or water as the solvent.

X-ray Crystallography analysis

The crystal data were obtained using an Oxford Diffraction Gemini E Ultra Diffractometer equipped with a Mo-Kα source (λ = 0.71073 Å), an EOS CCD detector, and a four-circle kappa goniometer at 150 K. Data processing, which included integration, scaling, and empirical absorption correction, was handled by the CrysAlis Pro software (Oxford Diffraction Ltd., CrysAlis Pro 171.33.42, 2009). The crystal structures were determined through direct methods and standard difference map techniques, and then refined using full-matrix least-squares procedures on F^2. Hydrogen atom positions were calculated from the geometrical environment and adjusted at each refinement cycle. All computational work was performed using Olex2 software (Olex2-1.5 © OlexSys Ltd, 2004-2024).

3.2. Synthesis of *N*-heterocyclic carbene ligands:

3.2.1. Synthesis of mono-substituted theophylline- general procedure

In this section, two different mono-substituted theophylline derivatives were synthesized following the method outlined in the 2020 patent (WO 2020/157668). [199] Theophylline monohydrate (3.66 g, 16.65 mmol) was suspended in 55 mL of DMF and stirred for 10 minutes. Subsequently, 83.25 mmol of dibromoethane or allyl bromide (7.2 mL) was added dropwise. The reaction mixture was stirred at room temperature for 24 hours. After the reaction was complete, it was quenched by diluting the mixture with EtOAc and washing the organic phase three times with water and once with brine. The organic layer was dried and filtered, and the solvent was evaporated. The final product was obtained after trituration with heptane, yielding a 75% recovery.

- **Synthesis of 7-allyl-1,3-dimethyl-1H-purine-2,6(3H,7H)-dione (1a)**

To synthesize **1a**, theophylline monohydrate (3.66 g, 16.65 mmol) was reacted with allyl bromide (7.2 ml, 83.65 mmol) in DMF. Yield: 2.67 g, 72%.

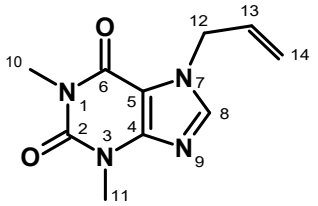

^{1}H NMR (400 MHz, DMSO): δ=[ppm]= 8.07 (s, 1H, C^{8}**H**), 6.05 (ddd, J_{HH} = 22.6, 10.6, 5.5 Hz, 1H, C^{13}**H**), 5.19 (dd, J_{HH} = 10.4, 1.4 Hz, 1H, C^{14}**H**), 5.07 (dd, J_{HH} = 17.2, 1.5 Hz, 1H, C^{14}**H**), 4.89 (d, J_{HH} = 5.7 Hz, 2H, C^{12}**H$_2$**), 3.42 (s, 3H, C^{10}**H$_3$**), 3.21 (s, 3H, C^{11}**H$_3$**).

^{13}C{^{1}H} NMR (151 MHz, DMSO): δ=[ppm]= 154.21 (C_6=O), 150.99 (C_2=O), 148.25 (C8), 142.20 (C4), 133.61 (C13), 117.70 (C14), 105.88 (C5), 47.96 (C12), 39.92-39.09 (DMSO), 29.37 (C11), 27.46(C10).

ESI-MS (CH_3CN *m/z*) = calculated for $[C_{10}H_{12}N_4O_2Na]^+$: 243.0852 found: 243.0948.

- **Synthesis of 7-(2-bromoethyl)-1,3-dimethyl-1H-purine-2,6(3H,7H)-dione (1b)**

To synthesize **1b**, theophylline monohydrate (3.66 g, 16.65 mmol) was reacted with 1,2-diboromoethane (7.2 ml, 83.65 mmol) in DMF. The yield was 3.72 g, 78%.

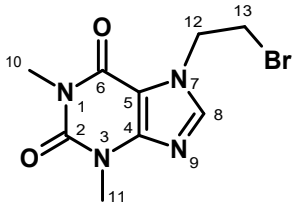

^{1}H NMR (400 MHz, $CDCl_3$): δ=[ppm]= 7.66 (s, 1H, C^{8}**H**), 4.66 (t, J_{HH}= 5.6 Hz, 2H, C^{12}**H_2**), 3.81 (t, J_{HH}= 5.8 Hz, 2H, C^{13}**H_2**), 3.62 (s, 3H, C^{11}**H_3**), 3.42 (s, 3H, C^{10}**H_3**).

^{13}C{^{1}H} NMR (151 MHz, CDCl3): δ=[ppm]= 155.21 (C_6=O), 151.58 (C_2=O), 149.29 (C8), 141.98 (C4), 106.39 (C5), 48.82 (C13), 31.61 (C12), 29.94 (C11), 28.04 (C10)

ESI-MS (CH_3CN *m/z*) = calculated for $[C_9H_{11}BrN_4O_2Na]^+$: 308.9958 found: 309.0111.

3.2.2. Synthesis of xanthinium salts:

3.2.2.1. Synthesis of xanthinium tosylate salts- general procedure

A 4 mL vial was loaded with the xanthine derivative (1 equivalent) and EtOTs or MeOTs (3.6 equivalents), then heated at 150 °C for 2 hours under solvent-free conditions. After cooling to room temperature, diethyl ether was added to the vial to precipitate the product as a white solid. The product was washed multiple times with diethylether and then air-dried at room temperature. [206]

- **Synthesis of 7-allyl-1,3,9-trimethyl-2,6-dioxo-2,3,6,7-tetrahydro-1H-purin-9-ium 4-methylbenzenesulfonate (2a)**

Compound **2a** was synthesized by the reaction of 1a (0.1 g, 0.45 mmol) and MeOTs (0.301 g, 1.62 mmol, 3.6 eq) with a yield of 0.16 g., 89%.

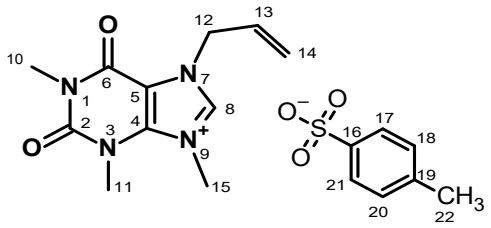

^{1}H NMR (600 MHz, DMSO): δ=[ppm]= 9.42 (s, 1H, C^{8}**H**), 7.76 (d, *J* = 8.4 Hz, 2H, C^{18}**H**, C^{20}**H**), 7.09 (d, *J* = 8.2 Hz, 2H, C^{17}**H**, C^{21}**H**), 6.03 (ddt, *J* = 16.5, 11.2, 5.8 Hz, 1H, C^{13}**H**), 5.37 – 5.29 (m, 2H, C^{14}**H$_2$**), 5.01 (d, *J* = 6.1 Hz, 2H, C^{12}**H$_2$**), 4.13 (s, 3H, C^{15}**H$_3$**), 3.67 (s, 3H, C^{11}**H$_3$**), 3.19 (s, 3H, C^{10}**H$_3$**), 2.26 (s, 3H, C^{22}**H$_3$**).

^{13}C{^{1}H} NMR (151 MHz, DMSO): δ=[ppm]= 152.84 (C6=O), 150.01 (C2=O), 144.85 (C19), 139.53 (C8), 130.81 (C13), 128.30 (C16), 125.93 (C17, C21), 124.82 (C18, C20), 120.45 (C14), 106.95 (C5), 56.83 (C4), 50.21 (C12), 37.51 (C15), 31.59 (C11), 28.77 (C10), 21.22 (C22).

ESI-MS (CH_3CN m/z) = attributed to the cationic part of xanthinium proligand $[C_{11}H_{15}N_4O_2]^+$, calculated: 235.1190, found: 235.1351.

- **Synthesis of 9-ethyl-1,3-dimethyl-2,6-dioxo-7-(2-(tosyloxy)ethyl)-2,3,6,7-tetrahydro-1H-purin-9-ium (2b)**

Compound **2b** was produced by the reaction of 1b (0.1 g, 0.35 mmol) and EtOTs (0.251 g, 1.25 mmol, 3.6 eq), which did not yield a favorable product.

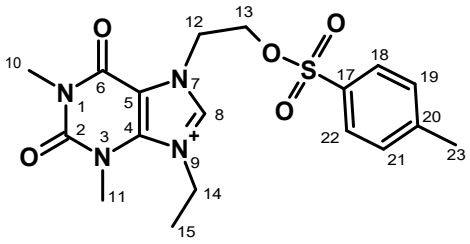

^{1}H NMR (400 MHz, $CDCl_3$): δ=[ppm]= 9.96 (s, 1H, C^{8}**H**), 7.82 (d, 2H, C^{18}**H**, C^{22}**H**), 7.36 (d, 2H, C^{19}**H**, C^{21}**H**), 5.00 (t, *J* = 5.2 Hz, 2H, C^{12}**H$_2$**), 4.53 (t, *J* = 4.9 Hz, 2H, C^{13}**H$_2$**), 4.13 (q, *J* = 7.1 Hz, 2H, C^{14}**H$_2$**), 3.82 (s, 3H, C^{11}**H$_3$**), 3.37 (s, 3H, C^{10}**H$_3$**), 1.71 (t, *J* = 7.6 Hz, 3H, C^{23}**H$_3$**) 1.32 (t, *J* = 7.1 Hz, 3H, C^{15}**H$_3$**).

ESI-MS (CH_3CN m/z) = attributed to the cationic part of xanthinium proligand $[C_{18}H_{23}N_4O_5S]^+$, calculated: 407.1384, found: 407.1694.

3.2.2.2. Synthesis of xanthinium sulfate salts- general procedure

xanthinium sulfate salts were synthesized by gradually adding 2 equivalents of diethyl sulfate (>99.8%) to 1 equivalent of mono-substituted imidazole in a 4 mL vial. [221] The mixture was heated at 130 °C for 2 hours under solvent-free conditions while stirring. After the reaction, the mixture was cooled to room temperature and washed with an excess of diethyl ether. The resulting sulfate salts appeared as a yellow-brown oily liquid.

- **Synthesis of 7-allyl-1,3,9-trimethyl-2,6-dioxo-2,3,6,7-tetrahydro-1H-purin-9-ium methyl sulfate (3a-1)**

Compound **3a-1** was prepared by the reaction of 1a (0.1 g, 0.45 mmol) and $(MeO)_2SO_2$ (80 µL, 0.90 mmol, 2 eq). Yield: 0.1 g (70%).

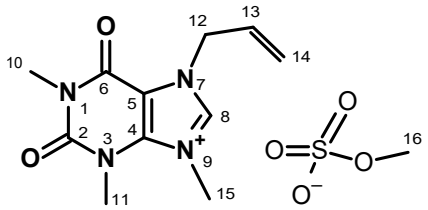

^{1}H NMR (400 MHz, DMSO): δ=[ppm]= 9.37 (s, 1H, C^{8}**H**), 6.13 – 5.99 (m, 1H, C^{13}**H$_2$**), 5.38 – 5.26 (m, 2H, C^{14}**H$_2$**), 5.09 (d, *J* = 5.6 Hz, 2H, C^{12}**H$_2$**), 4.15 (s, 3H, C^{15}**H$_3$**), 3.98 (s, 3H, C^{16}**H$_3$**), 3.73 (s, 3H, C^{11}**H$_3$**), 3.25 (s, 3H, C^{10}**H$_3$**).

^{13}C{^{1}H} NMR (101 MHz, DMSO): δ=[ppm]= 153.09 (C6=O), 150.29 (C2=O), 139.88 (C8), 139.41 (C4), 131.09 (C13), 120.22 (C14), 107.18 (C5), 52.98 (C16), 50.28 (C12), 37.06 (C15), 31.35 (C11), 28.49 (C10).

ESI-MS (CH_3CN m/z) = attributed to the cationic part of xanthinium proligand $[C_{11}H_{15}N_4O_2]^+$, calculated: 235.1190, found: 235.1351.

- **Synthesis of 7-allyl-9-ethyl-1,3-dimethyl-2,6-dioxo-2,3,6,7-tetrahydro-1H-purin-9-ium ethyl sulfate (3a-2)**

Compound **3a-2** was prepared by the reaction of 1a (0.09 g, 0.40 mmol) and $(EtO)_2SO_2$ (106.7 µL, 0.81 mmol, 2 eq). Yield: 0.13 g (87%).

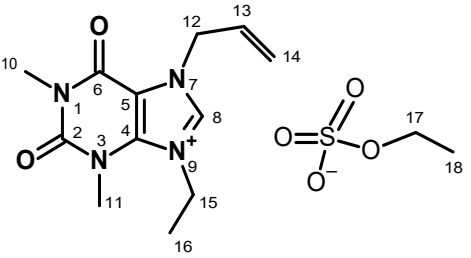

^{1}H NMR (400 MHz, DMSO): δ=[ppm]= 9.72 (s, 1H, C^{8}**H**), 6.16 – 5.99 (m, 1H, C^{13}**H**), 5.40 – 5.25 (m, 2H, C^{14}**H$_2$**), 5.12 (d, *J* = 5.6 Hz, 2H, C^{12}**H$_2$**), 4.60 (q, *J* = 7.3 Hz, 2H, C^{15}**H$_2$**), 3.74 (q, *J* = 7.0, 2H, C^{17}H$_2$), 3.73 (s, 3H, C^{11}**H$_3$**), 3.27 (s, 3H, C^{10}**H$_3$**), 1.52 (t, *J* = 7.3 Hz, 3H, C^{16}**H$_3$**), 1.09 (t, J = 7.01, 3H,C^{18}**H$_3$**).

^{13}C{^{1}H} NMR (151 MHz, DMSO): δ=[ppm]= 153.11 (C$_6$=O), 150.43 (C$_2$=O), 139.52, 138.46 (C8), 131.17 (C4), 120.19 (C14), 107.37 (C5), 61.39 (C17), 50.45 (C12), 45.35 (C15), 31.75 (C11), 28.47 (C10), 18.59 (C16), 15.11 (C18).

ESI-MS (CH_3CN m/z) = attributed to the cationic part of xanthinium proligand $[C_{12}H_{17}N_4O_2]^+$, calculated: 249.1346, found: 249.1353.

- **7-(2-bromoethyl)-1,3,9-trimethyl-2,6-dioxo-2,3,6,7-tetrahydro-1H-purin-9-ium methyl sulfate (3b-1)**

Compound **3b-1** was prepared by reacting **1b** (0.12 g, 0.42 mmol) with $(MeO)_2SO_2$ (80 µL, 0.84 mmol, 2 eq.). The yield was 0.15 g, 91%.

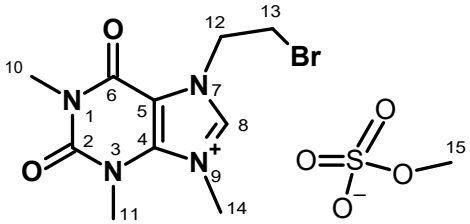

^{1}H NMR (400 MHz, DMSO): δ=[ppm]= 9.47 (s, 1H, C^{8}**H**), 4.84 (t, *J* = 5.9 Hz, 2H, C^{12}**H$_2$**), 4.19 (s, 3H, C^{14}**H$_3$**), 3.92 (t, *J* = 5.9 Hz, 2H, C^{13}**H$_2$**), 3.74 (s, 3H, C^{11}**H$_3$**), 3.26 (s, 3H, C^{10}**H$_3$**), 3.15 (s, 3H, C^{15}**H$_3$**).

$^{13}C\{^{1}H\}$ NMR (101 MHz, DMSO): δ=[ppm]= 153.33 (C_6=O), 150.23 (C_2=O), 139.91 (C8), 139.86 (C4), 107.20 (C5), 53.02 (C15), 49.89 (C12), 48.71 (C14), 37.14 (C11), 31.39 (C13), 28.59 (C10).

ESI-MS (CH_3CN m/z) = attributed to the cationic part of xanthinium proligand $[C_{10}H_{14}BrN_4O_2]^+$, calculated: 301.0295, found: 301.0253.

- **Synthesis of 7-(2-bromoethyl)-9-ethyl-1,3-dimethyl-2,6-dioxo-2,3,6,7-tetrahydro-1H-purin-9-ium ethyl sulfate (3b-2)**

Compound **3b-2** was prepared by the reaction between **1b** (0.12 g, 0.42 mmol) and $(EtO)_2SO_2$ (110 µL, 0.84 mmol). Yield: 0.17 g, 92%.

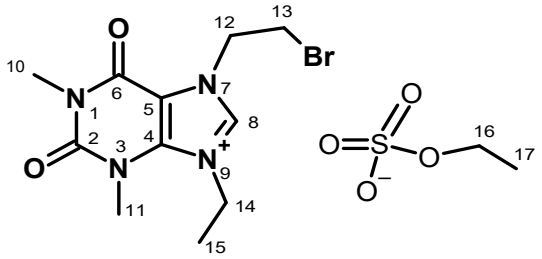

^{1}H NMR (600 MHz, DMSO): δ=[ppm]= 9.57 (s, 1H, $C^{8}\mathbf{H}$), 4.85 (t, *J* = 6.2 Hz, 2H, $C^{12}\mathbf{H_2}$), 4.62 (q, *J* = 7.2 Hz, 2H, $C^{14}\mathbf{H_2}$), 3.94 (t, *J* = 6.2 Hz, 2H, $C^{13}\mathbf{H_2}$), 3.73 (s, 3H, $C^{11}\mathbf{H_3}$), 3.43 (q, *J* = 7.0 Hz, 2H, $C^{16}\mathbf{H_2}$), 3.27 (s, 3H, $C^{10}\mathbf{H_3}$), 1.53 (t, *J* = 7.3 Hz, 3H, $C^{15}\mathbf{H_3}$), 1.05 (t, *J* = 7.0 Hz, 3H, $C^{17}\mathbf{H_3}$).

$^{13}C\{^{1}H\}$ NMR (151 MHz, DMSO): δ=[ppm]= 153.25 (C_6=O), 150.29 (C_2=O), 139.37(C8), 138.92 (C4), 107.26 (C5), 56.01 (C16), 49.73 (C12), 45.38 (C14), 31.67 (C11), 30.33 (C13), 28.39 (C10), 18.50 (C15), 15.05 (C17).

ESI-MS (CH_3CN m/z) = attributed to the cationic part of xanthinium proligand $[C_{11}H_{16}N_4O_2]^+$, calculated: 317.0431, found: 317.0421.

3.2.2.3. Synthesis of xanthinium triflate salts- general procedure

xanthinium triflate salts were synthesized like sulfate and tosylate salts by gradually adding 2 equivalents of methyl trifluoromethanesulfinate (CF_3SO_2Na) (>99.8%) to 1 equivalent of mono-substituted imidazole in a 4 mL vial. The mixture was heated at 120 °C for 2 hours under solvent-free conditions while stirring. After the reaction, the mixture was cooled to room temperature and washed with an excess of diethyl ether. The resulting sulfate salts appeared as a dark brown oily liquid.

- **Synthesis of 7-allyl-1,3,9-trimethyl-2,6-dioxo-2,3,6,7-tetrahydro-1H-purin-9-ium trifluoromethanesulfinate (4a)**

Compound **4a** was prepared by the reaction between **1a** (0.186 g, 0.84 mmol) and methyl trifluoromethane sulfonate (0.18 ml, 1.68 mmol) in solvent-free condition at 120 °C for 2 hours while stirring. Then, the mixture was cooled down and washed several times with diethyl ether. The product appeared as a dark brown oily liquid with low viscosity. Yield: 0.2 g, 69%.

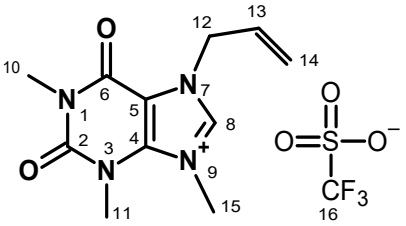

^{1}H NMR (400 MHz, DMSO): δ=[ppm]= 9.34 (s, 1H, C^8**H**), 6.16 – 5.99 (m, 1H, C^{13}**H**), 5.42 – 5.22 (m, 2H, C^{14}**H$_2$**), 5.11 (d, *J* = 5.7 Hz, 2H, C^{12}**H$_2$**), 4.15 (s, 3H, C^{15}**H$_3$**), 3.74 (s, 3H, C^{11}**H$_3$**), 3.27 (s, 3H, C^{10}**H$_3$**).

$^{13}C\{^{1}H\}$ NMR (101 MHz, DMSO): δ=[ppm]: 152.94 (C6=O), 150.15 (C2=O), 140.33 (C8), 139.66 (C4), 138.03 (C16), 130.08 (C13), 120.19 (C14), 107.13 (C5), 49.81 (C12), 36.53 (C15), 30.77 (C11), 27.18 (C10).

ESI-MS (CH_3CN m/z) = attributed to the cationic part of xanthinium proligand $[C_{11}H_{15}N_4O_2]^+$, calculated: 235.1190, found: 235.1351.

- **Synthesis of 7-(2-bromoethyl)-1,3,9-trimethyl-2,6-dioxo-2,3,6,7-tetrahydro-1H-purin-9-ium trifluoromethanesulfinate (4b)**

Compound **4b** was prepared by the reaction between 1a (0.263 g, 0.92 mmol) and methyl trifluoromethane sulfonate (0.2 ml, 1.83 mmol) in solvent-free condition at 120 °C for 2 hours while stirring. Then, the mixture was cooled down and washed several times with diethyl ether. The product appeared as a dark brown oily liquid with low viscosity. Yield: (0.2 g, 0.46 mmol) 50%. In this case, data analysis revealed that we have a mixture of reacted and unreacted material.

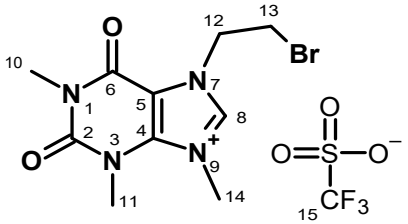

^{1}H NMR (600 MHz, DMSO): δ=[ppm]= 9.46 (s, 1H, $C^{8}\mathbf{H}$), 4.64 (t, *J* = 6.0 Hz, 2H, $C^{12}\mathbf{H_2}$), 4.21 (s, 3H, $C^{14}\mathbf{H_3}$), 3.90 (t, *J* = 6.0 Hz, 2H, $C^{13}\mathbf{H_2}$), 3.76 (s, 3H, $C^{11}\mathbf{H_3}$), 3.43 (s, 3H, $C^{10}\mathbf{H_3}$).

$^{13}C\{^{1}H\}$ NMR (151 MHz, DMSO): δ=[ppm]= 153.52 (C_6=O), 150.33 (C_2=O), 140.80 (C8), 139.88 (C4), 129.73 (C15), 107.40 (C5), 49.91 (C13), 42.47 (C12), 37.14 (C14), 31.21 (C11), 28.24 (C10).

ESI-MS (CH_3CN m/z) = attributed to the cationic part of xanthinium proligand $[C_{10}H_{14}BrN_4O_2]^+$, calculated: 301.0295, found: 301.0426.

3.2.2.4. Synthesis of xanthinium hexafluorophosphate salts- general procedure

[NHCH]PF_6 was obtained through an ion-exchange process, where [NHCH]X (X: TsO^-, $EtOSO_3^-$, OTf^-) was reacted with $NH_4^+PF_6^-$ using either water or ethanol as the solvent. The reaction was stirred at room temperature for a designated period (20 minutes to 2 hours). After completion, the mixture was filtered, and the solid was thoroughly washed with water or ethanol, followed by diethyl ether, and then dried at room temperature.

- **Synthesis of 7-allyl-1,3,9-trimethyl-2,6-dioxo-2,3,6,7-tetrahydro-1H-purin-9-ium hexafluorophosphate(V) (5a-1)**

Compound **5a-1** was prepared according to the previously described method using three different substrates: **2a**, **3a-1**, and **4a-1**.

In each experiment, the xanthinium salt was dissolved in water or ethanol, and a saturated Ammonium hexafluorophosphate solution (in water or ethanol) was added to the mixture to precipitate the desired white solid. This process was continued until no further precipitation occurred. The resulting suspension was then filtered, washed sequentially with ethanol and diethyl ether, and dried at room temperature. Yield: 85-95%.

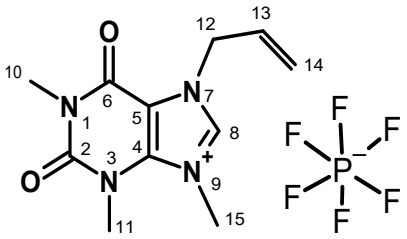

^{1}H NMR (600 MHz, DMSO): δ=[ppm]= 9.36 (s, 1H, C^{8}**H**), 6.09 (ddt, *J* = 17.2, 10.4, 5.6 Hz, 1H, C^{13}**H**), 5.45 – 5.28 (m, 2H, C^{14}**H$_2$**), 5.13 (dt, *J* = 5.8, 1.6 Hz, 2H, C^{12}**H$_2$**), 4.17 (s, 3H, C^{15}**H$_3$**), 3.75 (s, 3H, C^{11}**H$_3$**), 3.29 (s, 3H, C^{10}**H$_3$**).

^{13}C{^{1}H} NMR (151 MHz, DMSO): δ=[ppm]= 152.92 (C_6=O), 150.15 (C_2=O), 139.68 (C8), 139.26 (C4), 130.87 (C13), 120.21 (C14), 107.05 (C5), 50.22 (C12), 36.94 (C15), 31.27 (C11), 28.38 (C10).

ESI-MS (CH_3CN m/z) = attributed to the cationic part of xanthinium proligand $[C_{11}H_{15}N_4O_2]^+$, calculated: 235.1190, found: 235.1264.

- **Synthesis of 7-allyl-9-ethyl-1,3-dimethyl-2,6-dioxo-2,3,6,7-tetrahydro-1H-purin-9-ium hexafluorophosphate(V) (5a-2)**

Compound **5a-2** was prepared by the reaction between **3a-2** and a saturated solution of $NH_4^+PF_6^-$ in water. Adding the solution continued until no more white precipitation was seen. yield: 85-95%.

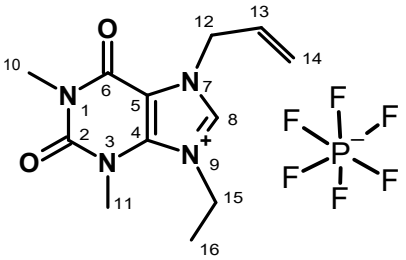

^{1}H NMR (400 MHz, DMSO): δ=[ppm]= 9.44 (s, 1H, C^{8}**H**), 6.08 (ddt, *J* = 17.1, 10.3, 5.6 Hz, 1H, C^{13}**H**), 5.42 – 5.23 (m, 2H, C^{14}**H$_2$**), 5.11 (dt, *J* = 5.6, 1.6 Hz, 2H, C^{12}**H$_2$**), 4.58 (q, *J* = 7.2 Hz, 2H, C^{15}**H$_2$**), 3.72 (s, 3H, C^{11}**H$_3$**), 3.27 (s, 3H, C^{10}**H$_3$**), 1.52 (t, *J* = 7.2 Hz, 3H, C^{16}**H$_3$**).

^{13}C{^{1}H} NMR (101 MHz, DMSO) δ=[ppm]= 152.98 (C_6=O), 150.37 (C_2=O), 139.35 (C8), 138.37 (C4), 131.05 (C13), 120.07 (C14), 107.24 (C5), 50.41 (C12), 45.24 (C15), 31.65 (C11), 28.43 (C10), 15.15 (C16).

ESI-MS (CH_3CN m/z) = attributed to the cationic part of xanthinium proligand $[C_{12}H_{17}N_4O_2]^+$, calculated: 249.1346, found: 249.1353.

- **Synthesis of 7-(2-bromoethyl)-1,3,9-trimethyl-2,6-dioxo-2,3,6,7-tetrahydro-1H-purin-9-ium hexafluorophosphate(V) (5b-1)**

Compound **5b-1** was prepared based on the previously described method using compounds **3b-1** and **4b** with ammonium hexafluorophosphate solution. yield: 85-95%.

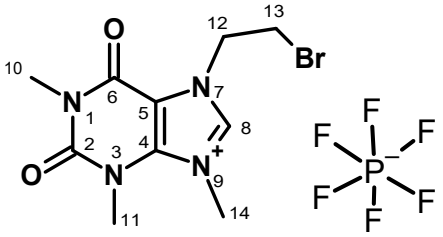

^{1}H NMR (400 MHz, DMSO): δ=[ppm]= 9.46 (s, 1H, C^{8}**H**), 4.87 (t, *J* = 5.8 Hz, 2H, C^{12}**H$_2$**), 4.21 (s, 3H, C^{14}**H$_3$**), 3.95 (t, *J* = 5.7 Hz, 2H, C^{13}**H$_2$**), 3.75 (s, 3H, C^{11}**H$_3$**), 3.28 (s, 3H, C^{10}**H$_3$**).

^{13}C{^{1}H} NMR (101 MHz, DMSO): δ=[ppm]= 153.20 (C_6=O), 150.13 (C_2=O), 139.77 C4, C8), 107.05 (C5), 49.96 (C13), 37.09 (C14), 31.34 (C12), 30.79 (C11), 28.55 (C10).

ESI-MS (CH_3CN m/z) = attributed to the cationic part of xanthinium proligand $[C_{10}H_{14}BrN_4O_2]^+$, calculated: 301.0295, found: 301.0426.

- **Synthesis of 7-(2-bromoethyl)-9-ethyl-1,3-dimethyl-2,6-dioxo-2,3,6,7-tetrahydro-1H-purin-9-ium hexafluorophosphate(V) (5b-2)**

Compound **5b-2** was prepared based on the previously described method using compound **3b-2** with ammonium hexafluorophosphate solution. yield: 85-95%.

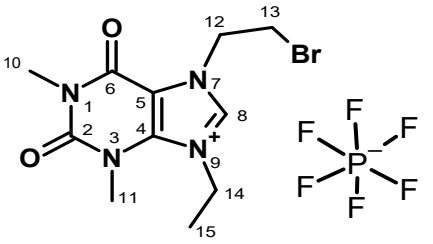

^{1}H NMR (600 MHz, DMSO): δ=[ppm]= 9.54 (s, 1H, C^{8}**H**), 4.87 (t, *J* = 5.9 Hz, 2H, C^{12}**H$_2$**), 4.63 (q, *J* = 7.2 Hz, 2H, C^{14}**H$_2$**), 3.96 (t, *J* = 5.9 Hz, 2H, C^{13}**H$_2$**), 3.74 (s, 3H, C^{11}**H$_3$**), 3.29 (s, 3H, C^{10}**H$_3$**), 1.52 (t, *J* = 7.2 Hz, 3H, C^{15}**H$_3$**).

^{13}C{^{1}H} NMR (151 MHz, DMSO): δ=[ppm]= 153.18 (C_6=O), 150.24 (C_2=O), 139.32 (C8), 138.82 (C4), 107.18 (C5), 49.93 (C12), 45.34 (C14), 31.67 (C11), 30.64 (C10), 28.47 (C13), 15.18 (C15).

ESI-MS (CH_3CN m/z) = attributed to the cationic part of xanthinium proligand $[C_{11}H_{16}BrN_4O_2]^+$, calculated: 317.0431, found: 317.0492.

3.2.2.5. Synthesis of xanthinium Chloride salts- general procedure

[NHCH]Cl was synthesized from [NHCH]PF_6 by an ion-exchange reaction. To synthesize xanthinium chloride salts, a predetermined quantity of [NHCH]PF_6 salt was dissolved in 20 mL of ethanol. This solution was subsequently subjected to column chromatography utilizing Amberlite® IRA-900 (Cl^- form) ion exchange resin, where the chloride resin serves as a medium that contains fixed chloride ions, which can be exchanged for other anions present in the solution. Following the chromatography process, the solvent was evaporated by a rotary evaporator, yielding an oily yellow product identified as xanthinium chloride salt.

- **Synthesis of 7-allyl-1,3,9-trimethyl-2,6-dioxo-2,3,6,7-tetrahydro-1H-purin-9-ium chloride (6a-1)**

Compound **6a-1** was synthesized through an ion exchange reaction involving the corresponding PF_6 salt (**5a-1**) and a chloride ion exchange resin. Yield: 15-25% (0.018 g, 0.06 mmol).

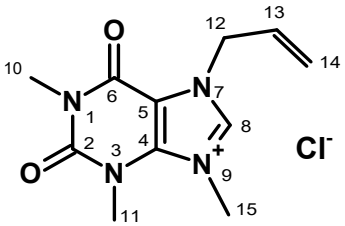

^{1}H NMR (600 MHz, DMSO): δ=[ppm]= 9.92 (s, 1H, C^{8}**H**), 6.14 – 6.04 (m, 1H, C^{13}**H**), 5.39 – 5.30 (m, 2H, C^{14}**H$_2$**), 5.14 (d, *J* = 5.6 Hz, 2H, C^{12}**H$_2$**), 4.24 (s, 3H, C^{15}**H$_3$**), 3.77 (s, 3H, C^{11}**H$_3$**), 3.26 (s, 3H, C^{10}**H$_3$**).

^{13}C{^{1}H} NMR (151 MHz, DMSO): δ=[ppm]= 153.00 (C_6=O), 150.20 (C_2=O), 139.77 (C8), 139.51 (C4), 130.99 (C13), 120.18 (C14), 106.99 (C5), 50.17 (C12), 37.06 (C15), 31.38 (C11), 28.39 (C10).

^{35}Cl NMR (39 MHz, DMSO): δ=[ppm]= 49.93 (Cl^- anion).

ESI-MS (CH_3CN m/z) = attributed to the cationic part of xanthinium proligand $[C_{11}H_{15}N_4O_2]^+$, calculated: 235.1190, found: 235.1197.

- **Synthesis of 7-allyl-9-ethyl-1,3-dimethyl-2,6-dioxo-2,3,6,7-tetrahydro-1H-purin-9-ium chloride (6a-2)**

Compound **6a-2** was prepared by the ion exchange reaction as previously mentioned method involving the corresponding PF_6 salt (**5a-2**) and a chloride resin, yielding 0.01 g (0.048 mmol) of the xanthinium chloride salt **6a-2**, corresponding to a 19% yield.

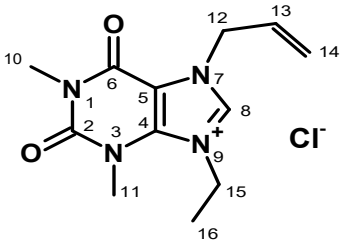

^{1}H NMR (400 MHz, DMSO): δ=[ppm]= 9.86 (s, 1H, C^{8}**H**), 6.09 (ddt, *J* = 17.1, 10.4, 5.6 Hz, 1H, C^{13}**H**), 5.39 – 5.26 (m, 2H, C^{14}**H$_2$**), 5.14 (dt, *J* = 5.7, 1.5 Hz, 2H, C^{12}**H$_2$**), 4.62 (q, *J* = 7.2 Hz, 2H, C^{15}**H$_2$**), 3.73 (s, 3H, C^{11}**H$_3$**), 3.26 (s, 3H, C^{10}**H$_3$**), 1.53 (t, *J* = 7.2 Hz, 3H, C^{16}**H$_3$**).

^{13}C{^{1}H} NMR (151 MHz, DMSO): δ=[ppm]= 153.11 (C_6=O), 149.98 (C_2=O), 139.93 (C8), 138.46 (C4), 131.16 (C13), 120.60 (C14), 107.37 (C5), 56.12 (C12), 50.86 (C15), 31.75(C11), 28.47 (C10), 18.59 (C16).

^{35}Cl NMR (39 MHz, DMSO): δ=[ppm]= 70.43 (Cl^- anion).

ESI-MS (CH_3CN m/z) = attributed to the cationic part of xanthinium proligand $[C_{12}H_{17}N_4O_2]^+$, calculated: 249.1346, found: 249.1374.

- **7-(2-bromoethyl)-1,3,9-trimethyl-2,6-dioxo-2,3,6,7-tetrahydro-1H-purin-9-ium chloride (6b-1)**

Compound **6b-1** was prepared by the ion exchange reaction between the corresponding PF_6 salt (**5b-1**) and a chloride ion exchange resin. NMR and mass spectrometry analyses confirmed substituting the C^{13}-Br group with C^{13}-Cl.

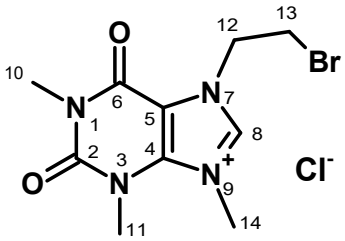

^{1}H NMR (600 MHz, DMSO): δ=[ppm]= 9.81 (s, 1H, C^{8}**H**), 4.85 (dt, *J* = 26.7, 6.0 Hz, 2H, C^{12}**H$_2$**), 4.25 (s, 3H, C^{14}**H$_3$**), 4.01 (dt, *J* = 96.3, 6.0 Hz, 2H, C^{13}**H$_2$**), 3.75 (s, 3H, C^{11}**H$_3$**), 3.24 (s, 3H, C^{10}**H$_3$**).

^{13}C{^{1}H} NMR (151 MHz, DMSO): δ=[ppm]= 153.47 (C_6=O), 150.37 (C_2=O), 140.13 (C8), 139.97 (C4), 107.30 (C5), 50.13 (C13), 42.43 (C12), 37.48 (C14), 31.67 (C11), 28.70 (C10).

^{35}Cl NMR (39 MHz, DMSO): δ=[ppm]= 60.96 (Cl^- anion).

ESI-MS (CH_3CN m/z) = attributed to the cationic part of xanthinium proligand $[C_{10}H_{14}BrN_4O_2]^+$, calculated: 301.0295, found: 301.0337, and for proligand $[C_{10}H_{14}ClN_4O_2]^+$, calculated: 257.0800, found: 257.0837.

- **7-(2-bromoethyl)-9-ethyl-1,3-dimethyl-2,6-dioxo-2,3,6,7-tetrahydro-1H-purin-9-ium chloride (6b-2)**

Compound **6b-2** was obtained through an ion exchange reaction between the PF_6 salt (**5b-2**) and a chloride ion exchange resin. NMR and mass spectrometry analyses confirmed the partial substitution of the C^{13}-Br group with C^{13}-Cl.

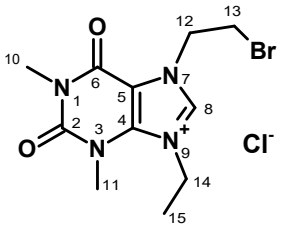

^{1}H NMR (600 MHz, DMSO): δ=[ppm]= 10.01 (s, 1H, C^{8}**H**), 4.90 (t, *J* = 6.1 Hz, 2H, C^{12}**H$_2$**), 4.67 (q, *J* = 7.2 Hz, 2H, C^{14}**H$_2$**), 3.98 (t, *J* = 6.1 Hz, 2H, C^{13}**H$_2$**), 3.74 (s, 3H, C^{11}**H$_3$**), 3.28 (s, 3H, C^{10}**H$_3$**), 1.54 (t, *J* = 7.2 Hz, 3H, C^{15}**H$_3$**).

^{13}C{^{1}H} NMR (151 MHz, DMSO): δ=[ppm]= 153.23 (C_6=O), 150.24 (C_2=O), 139.20 (C8), 139.04 (C4), 107.22 (C5), 49.99 (C12), 45.38 (C14), 31.72 (C11), 30.48 (C13), 28.45 (C10).

^{35}Cl NMR (39 MHz, DMSO): δ=[ppm]= 66.87 (Cl^- anion).

ESI-MS (CH_3CN m/z) = attributed to the cationic part of xanthinium proligand $[C_{11}H_{16}BrN_4O_2]^+$, calculated: 315.0452, found: 317.0492, and for proligand $[C_{11}H_{16}ClN_4O_2]^+$, calculated: 271.0956, found: 271.0996.

3.2.2.6. Synthesis of xanthinium Iodide salt- general procedure

xanthinium 2a (2.11 g, 9.6 mmol) and 2b (2.75 g, 9.6 mmol) were dissolved in dimethylformamide (3 mL) in an ampoule, and methyl iodide (11.89 mL, 191 mmol) or Ethyl iodide was added. The mixture was heated at 70 °C for 24 hours in a closed system, resulting in a clear red solution. Excess diethyl ether was added to the flask to precipitate an orange powder, which was filtered. Further recrystallization using dichloromethane–diethyl ether and acetonitrile–diethyl ether resulted in the product as a yellow solid. [223] We also found a more eco-friendly

method at low or room temperature to produce xanthinium iodide salts, introduced recently by Longo *et al*. [225] By this method, compounds **7a-1** and **7b-1** were achieved through reaction with methyl iodide in DMF at 24-35 °C for 72 hours. The xanthinium salts were obtained after trituration with DCM/diethyl ether and AN/diethyl ether and kept in the refrigerator to avoid getting oily.

- **Synthesis of 7-allyl-1,3,9-trimethyl-2,6-dioxo-2,3,6,7-tetrahydro-1H-purin-9-ium iodide (7a-1)**

Compound **7a-1** was prepared by the reaction between **1a** (2 g, 9.08 mmol) and methyl iodide (2.26 ml, 36.32 mmol, 4 eq.) in 5 ml DMF in 24-36 °C. 2.03 g, yield: 62%.

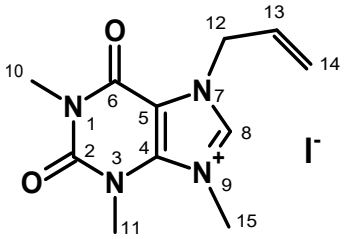

^{1}H NMR (600 MHz, DMSO): δ=[ppm]= 9.38 (s, 1H, C^{8}**H**), 6.07 (ddt, *J* = 17.1, 11.3, 5.6 Hz, 1H, C^{13}**H**), 5.35 (dd, *J* = 30.0, 13.7 Hz, 2H, C^{14}**H$_2$**), 5.11 (d, *J* = 7.1 Hz, 2H, C^{12}**H$_2$**), 4.16 (s, 3H, C^{15}**H$_3$**), 3.74 (s, 3H, C^{11}**H$_3$**), 3.27 (s, 3H, C^{10}**H$_3$**).

^{13}C{^{1}H} NMR (151 MHz, DMSO): δ=[ppm]= 152.21 (C_6=O), 149.42 (C_2=O), 139.24(C8), 137.74 (C4), 129.66 (C13), 119.54 (C14), 106.34 (C5), 49.54 (C12), 35.87 (C15), 31.13 (C11), 28.17 (C10).

ESI-MS (CH_3CN m/z) = attributed to the cationic part of xanthinium proligand $[C_{11}H_{15}N_4O_2]^+$, calculated: 235.1190, found: 235.1264.

- **Synthesis of 7-allyl-9-ethyl-1,3-dimethyl-2,6-dioxo-2,3,6,7-tetrahydro-1H-purin-9-ium iodide (7a-2)**

Compound **7a-2** was prepared by reaction of **1a** (0.528 g, 2.4 mmol) with Ethyl iodide (3.83 mL, 47.75 mmol). Yield: 0.67 g, 75%.

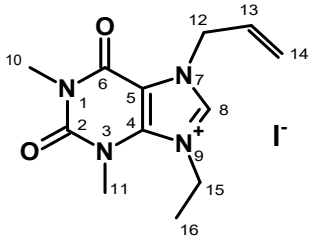

^{1}H NMR (400 MHz, DMSO): δ=[ppm]= 9.72 (s, 1H, C^8**H**), 6.19 – 5.97 (m, 1H, C^{13}**H**), 5.42 – 5.26 (m, 2H, C^{14}**H$_2$**), 5.12 (d, *J* = 5.6 Hz, 2H, C^{12}**H$_2$**), 4.60 (q, *J* = 7.3 Hz, 2H, C^{15}**H$_2$**), 3.73 (s, 3H, C^{11}**H$_3$**), 3.27 (s, 3H, C^{10}**H$_3$**), 1.52 (t, *J* = 7.3 Hz, 3H, C^{16}**H$_3$**).

^{13}C{^{1}H} NMR (151 MHz, DMSO): δ=[ppm]= 153.11 (C_6=O), 150.48 (C_2=O), 139.96 (C8), 138.02 (C4), 131.17 (C13), 120.19 (C14), 108.22 (C5), 49.72 (C12), 46.38 (C15), 28.47 (C11), 18.59 (C10), 14.27 (C16).

ESI-MS (CH_3CN m/z) = attributed to the cationic part of xanthinium proligand $[C_{12}H_{17}N_4O_2]^+$, calculated: 249.1346, found: 249.1374.

- **Synthesis of 7-(2-iodoethyl)-1,3,9-trimethyl-2,6-dioxo-2,3,6,7-tetrahydro-1H-purin-9-ium iodide (7b-1)**

Compound **7b-1** was prepared by the reaction of **1b** (1 g, 3.48 mmol) and methyl iodide (0.9 mL, 13.9 mmol, 4 eq.) in 4 mL DMF. Yield: (1.19 g, 2.5 mmol), 74%.

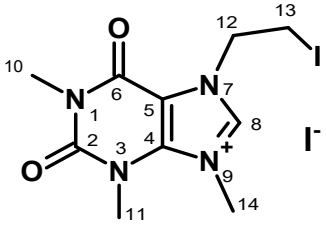

^{1}H NMR (600 MHz, DMSO): δ=[ppm]= 9.44 (s, 1H, C^{8}**H**), 4.78 (t, *J* = 6.7 Hz, 2H, C^{12}**H$_2$**), 4.20 (s, 3H, C^{14}**H$_3$**), 3.75 (s, 3H, C^{11}**H$_3$**), 3.63 (t, *J* = 6.6 Hz, 2H, C^{13}**H$_2$**), 3.29 (s, 3H, C^{10}**H$_3$**).

^{13}C{^{1}H} NMR (151 MHz, DMSO): δ=[ppm]= 152.39 (C_6=O), 149.43 (C_2=O), 139.90 (C8), 138.52 (C4), 106.39 (C5), 49.71 (C12), 35.80 (C14), 30.15 (C11), 27.31 (C10), 1.44 (C13).

ESI-MS (CH_3CN m/z) = attributed to the cationic part of xanthinium proligand $[C_{11}H_{16}IN_4O_2]^+$, calculated: 349.0156, found: 349.0223.

- **Synthesis of 7-(2-iodoethyl)-9-ethyl-1,3-dimethyl-2,6-dioxo-2,3,6,7-tetrahydro-1H-purin-9-ium iodide (7b-2)**

Compound **7b-2** was prepared by the reaction between **1b** (0.689 g, 2.4 mmol) and ethyliodide (3.84 mL, 47.75 mmol) in 4mL DMF. Yield: (0.95 g, 1.94 mmol) 81%.

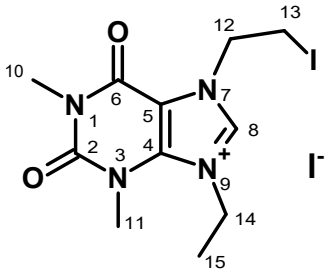

^{1}H NMR (600 MHz, DMSO): δ=[ppm]= 9.53 (s, 1H, C^{8}**H**), 4.72 (t, *J* = 6.9 Hz, 2H, C^{12}**H$_2$**), 4.58 (q, *J* = 7.2 Hz, 2H, C^{14}**H$_2$**), 3.68 (s, 3H, C^{11}**H$_3$**), 3.58 (t, *J* = 6.9 Hz, 2H, C^{13}**H$_2$**), 3.22 (s, 3H, C^{10}**H$_3$**), 1.48 (t, *J* = 7.2 Hz, 3H, C^{15}**H$_3$**).

^{13}C{^{1}H} NMR (151 MHz, DMSO): δ=[ppm]= 152.44 (C_6=O), 149.51 (C_2=O), 138.33 (C8), 136.86 (C4), 106.41 (C5), 50.18 (C12), 44.74 (C14), 31.49 (C11), 28.35 (C10), 14.80 (C15), 2.24 (C13).

ESI-MS (CH_3CN m/z) = attributed to the cationic part of xanthinium proligand $[C_{11}H_{16}IN_4O_2]^+$, calculated: 363.0312, found: 363.0281.

3.3. Synthesis of [Ag(NHC)(NH$_3$)]PF$_6$ and [Ag(NHC)$_2$]PF$_6$ complexes

[NHCH]PF_6 (1.0 mmol) was suspended in 5 mL of ethanol. Silver(I) oxide (64.3 mg, 0.277 mmol) and ammonia (0.65 mL, 15.3 mol/L, 9.9 mmol) were then added to the mixture. The solution was stirred at room temperature for a duration ranging from 30 minutes to 4 hours before being filtered. The resulting white solid was washed sequentially with cold ethanol and diethyl ether and then dried at room temperature. [226]

- **Synthesis of [Ag(7-allyl-1,3,9-thrimethylxanthine-8-ylidene)(NH$_3$)]PF$_6$ (Ag1)**

Complex **Ag1** was prepared by the reaction between **5a-1** (0.12 g, 0.31 mmol) and Ag_2O (0.03 g, 0.15 mmol) in the presence of ammonia, yield: (0.13 g, 0.26 mmol), 84%.

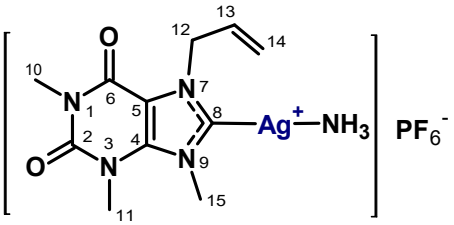

^{1}H NMR (400 MHz, DMSO): δ=[ppm]= 6.07 (ddd, *J* = 22.5, 10.4, 5.4 Hz, 1H, C^{13}**H**), 5.26 – 5.07 (m, 4H, C^{14}**H$_2$**, C^{12}**H$_2$**), 4.21 (s, 3H, C^{15}**H$_3$**), 3.76 (s, 3H, C^{11}**H$_3$**), 3.25 (s, 3H, C^{10}**H$_3$**).

^{13}C{^{1}H} NMR (101 MHz, DMSO): δ=[ppm]= 184.97 ($C_{8\text{-}Ag}$), 152.77 (C_6=O), 151.95 (C_2=O), 140.81 (C4), 133.94 (C13), 117.86 (C14), 108.31 (C5), 52.01 (C12), 48.81 (C15), 31.56 (C11), 28.25 (C10).

ESI-MS (CH_3CN m/z): Calculated for $C_{11}H_{14}AgN_4O_2^+$ [Ag-NHC]$^+$: 341.0168, found: 341.0232 and calculated for $C_{22}H_{28}AgN_8O_4^+$ [Ag(NHC)$_2$]$^+$: 575.1284, found: 575.1414.

- **Synthesis of [Ag(7-allyl-9-ethyl-1,3-dimethylxanthine-8-ylidene)(NH$_3$)]PF$_6$ (Ag2)**

Complex **Ag2** was prepared by the reaction between **5a-2** (0.12 g, 0.30 mmol) and Ag_2O (0.03 g, 0.15 mmol) in the presence of ammonia. Yield: (0.13 g, 0.26 mmol), 87%.

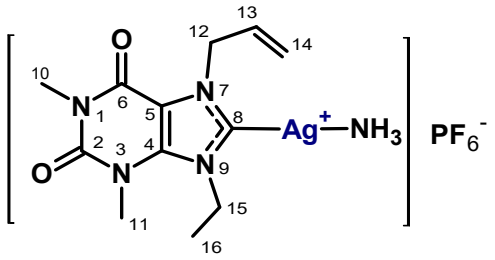

^{1}H NMR (400 MHz, DMSO): δ=[ppm]= 6.06 (ddd, *J* = 22.2, 10.2, 5.2 Hz, 1H, C^{13}**H**), 5.28 – 5.13 (m, 2H, C^{14}**H$_2$**), 5.11 (d, *J* = 4.9 Hz, 2H, C^{12}**H$_2$**), 4.60 (q, *J* = 7.5 Hz, 2H, C^{15}**H$_2$**), 3.72 (s, 3H, C^{11}**H$_3$**), 3.24 (s, 3H, C^{10}**H$_3$**), 1.44 (t, *J* = 7.2 Hz, 3H, C^{16}**H$_3$**).

^{13}C{^{1}H} NMR (101 MHz, DMSO): δ=[ppm]= 152.28 (C_6=O), 150.70 (C_2=O), 140.10 (C4), 133.83 (C13), 122.45 (C14), 108.20 (C5), 52.99 (C12), 46.34 (C15), 31.41 (C11), 28.24 (C10), 17.38 (C16).

ESI-MS (CH_3CN m/z): Calculated for $C_{12}H_{16}AgN_4O_2^+$ [Ag-NHC]$^+$: 355.0324, found: 355.0390, and calculated for $C_{24}H_{32}AgN_8O_4^+$ [Ag(NHC)$_2$]$^+$: 603.1597, found: 603.1703.

- **Synthesis of [Ag(7-(2-bromoethyl)-1,3,9-trimethylxanthine-8-ylidene)(NH$_3$)]PF$_6$ (Ag3)**

Complex **Ag3** was prepared by the reaction between **5b-1** (0.11 g, 0.24 mmol) and Ag_2O (0.03 g, 0.123 mmol) in the presence of ammonia. Yield: (0.09 g, 0.16 mmol), 68%.

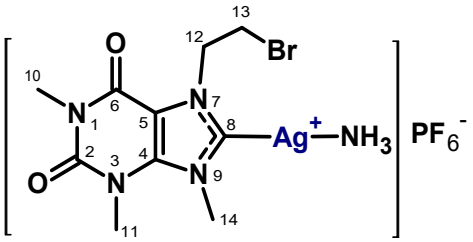

^{1}H NMR (400 MHz, DMSO): δ=[ppm]= 4.90 (t, *J* = 5.7 Hz, 2H, C^{12}**H$_2$**), 4.26 (s, 3H, C^{14}**H$_3$**), 3.96 (t, *J* = 5.7 Hz, 2H, C^{13}**H$_2$**), 3.78 (s, 3H, C^{11}**H$_3$**), 3.27 (s, 3H, C^{10}**H$_3$**).

^{13}C{^{1}H} NMR (101 MHz, DMSO): δ=[ppm]= 153.10 (C_6=O), 150.52 (C_2=O), 140.99 (C4), 108.09 (C5), 51.77 (C12), 32.30 (C14), 30.87 (C13), 29.05 (C11), 27.63 (C10).

ESI-MS (CH_3CN m/z): Calculated for $C_{10}H_{13}AgBrN_4O_2$ $[Ag\text{-}NHC]^+$: 408.9252, found: 408.9382 and calculated for $C_{20}H_{26}AgBr_2N_8O_4$ $[Ag(NHC)_2]^+$: 708.9474, found: 708.9690.

- **Synthesis of [Ag(7-(2-bromoethyl)-9-ethyl-1,3-dimethylxanthine-8-ylidene)(NH_3)]PF_6 (Ag4)**

Complex **Ag4** was prepared by the reaction between **5b-2** (0.12 g, 0.26 mmol) and Ag_2O (0.030 g, 0.14 mmol) in the presence of ammonia. Yield: (0.1 g, 0.17 mmol), 69%.

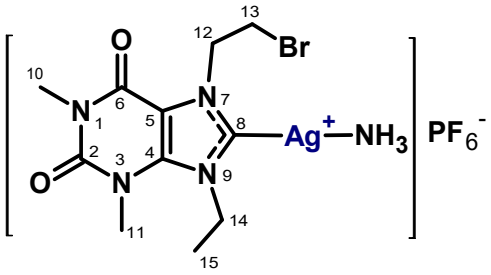

^{1}H NMR (600 MHz, DMSO) δ 4.89 (t, *J* = 5.9 Hz, 2H, C^{12}**H$_2$**), 4.65 (q, *J* = 7.2 Hz, 2H, C^{14}**H$_2$**), 3.94 (t, *J* = 5.9 Hz, 2H, C^{13}**H$_2$**), 3.75 (s, 3H, C^{11}**H$_3$**), 3.28 (s, 3H, C^{10}**H$_3$**), 1.48 (t, *J* = 7.2 Hz, 3H, C^{15}**H$_3$**).

^{13}C{^{1}H} NMR (151 MHz, DMSO): δ=[ppm]= 186.38 ($C_{8\text{-}Ag}$), 153.25 (C_6=O), 150.66 (C_2=O), 140.20 (C4), 108.07 (C5), 51.77 (C12), 46.38 (C14), 32.44 (C13), 31.58 (C11), 27.98 (C10), 17.40 (C15).

ESI-MS (CH_3CN m/z): Calculated for $C_{11}H_{15}AgBrN_4O_2^+$ [Ag-NHC]$^+$: 420.9429, found: 422.9503, and calculated for $C_{22}H_{30}AgBr_2N_8O_4^+$ [Ag(NHC)$_2$]$^+$: 736.9787, found: 736.9929.

3.4. Synthesis of [Ag(NHC)]Cl complexes

[NHCH]Cl (1.0 mmol) was dissolved in a specified volume of ethanol or CH_2Cl_2 as the solvent and reacted with Ag_2O (0.50 mmol) at room temperature for 24 hours. The reaction mixture was then filtered through Celite, and the resulting filtrate was concentrated to 3 mL using a rotary evaporator. To precipitate the product, an excess of diethyl ether or *n*-hexane was added, forming a white solid. This solid was filtered, washed with diethyl ether, and dried at room

temperature. [273–275] However, this procedure was successful in some cases, while others did not yield favorable results.

- **Synthesis of [Ag(7-allyl-9-ethyl-1,3-dimethylxanthine-8-ylidene)(Cl)] (Ag5)**

Complex **Ag5** was synthesized through the reaction of [NHCH]Cl (0.03 g, 0.10 mmol) and Ag_2O (0.012 g, 0.052 mmol) as prescribed above, yield (0.003 g, 0.01 mmol) <10%.

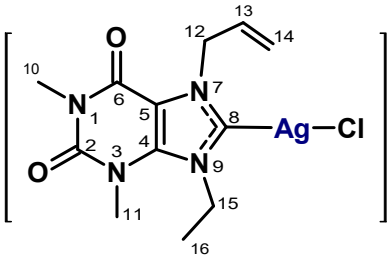

^{1}H NMR (400 MHz, DMSO): δ=[ppm]= 6.12 – 5.96 (m, 1H, C^{13}**H**), 5.22 (d, *J* = 11.7 Hz, 1H, C^{14}**H**), 5.12 (d, *J* = 1.5 Hz, 1H, C^{14}**H**), 5.08 (d, *J* = 5.6 Hz, 2H, C^{12}**H$_2$**), 4.56 (q, *J* = 7.1 Hz, 2H, C^{15}**H$_2$**), 3.70 (s, 3H, C^{11}**H$_3$**), 3.23 (s, 3H, C^{10}**H$_3$**), 1.43 (t, *J* = 7.3 Hz, 3H, C^{16}**H$_3$**).

^{13}C{^{1}H} NMR (101 MHz, DMSO): δ=[ppm]= 183.94 (C_8-Ag), 152.76 (C_6=O), 150.99 (C_2=O), 139.99 (C4), 132.92 (C13), 119.44 (C14), 108.14 (C5), 52.13 (C12), 46.42 (C15), 30.69 (C11), 27.52 (C10), 17.76 (C16).

^{35}Cl NMR (39 MHz, DMSO): δ=[ppm]= 50.05 (Cl^- anion).

ESI-MS (CH_3CN m/z): calculated for $C_{24}H_{32}AgN_8O_4$ [$Ag(NHC)_2$]: 603.1597, found: 603.1597.

3.5. Synthesis of [Ag(NHC)]I complexes, (AgOAc route)

xanthinium salt [NHCH]I (0.61 mmol) was added to silver acetate (0.2 g, 1.2 mmol) in a mixture of methanol or acetonitrile (10 ml). the mixture was stirred at room temperature for two hours in the dark. The mixture was filtered, with the solid being washed with acetonitrile, and the filtrate was dried in vacuo to give the product as a white solid, which was recrystallized from acetonitrile-diethyl ether. [223]

- **Synthesis of [Ag(7-allyl-1,3,9-thrimethylxanthine-8-ylidene)(acetate)] (Ag6)**

Complex **Ag6** was synthesized through the method described above by the reaction between compound **7a-1** (0.08 g, 0.22 mmol) and AgOAc (0.07 g, 0.44 mmol). The yield was 36% (0.03 g, 0.07 mmol).

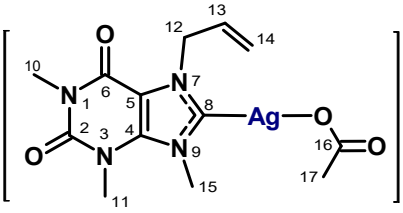

^{1}H NMR (400 MHz, $CDCl_3$): δ=[ppm]= 6.08 – 5.94 (m, 1H, C^{13}H), 5.39 (d, *J* = 0.9 Hz, 1H, C^{14}**H**), 5.34 (d, *J* = 1.4 Hz, 1H, C^{14}**H**), 5.14 (d, *J* = 6.1 Hz, 2H, C^{12}**H$_2$**), 4.26 (s, 3H, C^{15}**H$_3$**), 3.86 (s, 3H, C^{11}**H$_3$**), 3.43 (s, 3H, C^{10}**H$_3$**), 2.08 (s, 3H, C^{17}**H$_3$**).

^{13}C{^{1}H} NMR (101 MHz, DMSO): δ=[ppm]= 185.54 ($C_{8\text{-Ag}}$), 175.79 (C16), 152.86 (C_6=O), 150.54 (C_2=O), 140.74 (C4), 134.48 (C13), 118.15 (C14), 108.25 (C5), 52.05 (C12), 40.44 (C15), 30.80 (C11), 27.53 (C10), 22.68 (C17).

ESI-MS (CH_3CN m/z): Calculated for $C_{11}H_{14}AgN_4O_2$ [Ag-NHC]: 341.0168, found: 341.0354 and calculated for $C_{22}H_{28}AgN_8O_4$ [$Ag(NHC)_2$]: 575.1284, found: 575.1585.

- **Synthesis of [Ag(7-(2-iodoethyl)-1,3,9-trimethylxanthine-8-ylidene)(Acetate)] (Ag7)**

Complex **Ag7** was synthesized through the method described above by the reaction between compound **7b-1** (0,11 g, 0,36 mmol) and AgOAc (0.122 g, 0.73 mmol). yield: (0.067 g, 0.12 mmol), 36%.

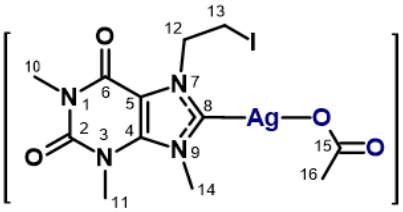

^{1}H NMR (400 MHz, DMSO): δ=[ppm]= 4.56 (t, *J* = 6.6 Hz, 2H, $C^{12}\mathbf{H_2}$), 3.94 (s, 3H, $C^{14}\mathbf{H_3}$), 3.69 (s, 3H, $C^{11}\mathbf{H_3}$), 3.63 (t, *J* = 6.6 Hz, 2H, $C^{13}\mathbf{H_2}$), 3.44 (s, 3H, $C^{10}\mathbf{H_3}$), 3.09 (s, 3H, $C^{16}\mathbf{H_3}$).

$^{13}C\{^1H\}$ NMR (151 MHz, DMSO): δ=[ppm]= 184.03 ($C_{8\text{-}Ag}$), 176.28 (C15), 154.32 (C_6=O), 150.87 (C_2=O), 142.66 (C4), 104.43 (C5), 47.93 (C12), 34.15 (C14), 29.43 (C11), 27.57 (C10), 13.45 (C16), 4.97 (C13).

ESI-MS (CH_3CN m/z): Calculated for $C_{10}H_{13}AgIN_4O_2$ [Ag-NHC]: 454.9134, found: 454.9260, and calculated for $C_{20}H_{26}AgI_2N_8O_4$ [$Ag(NHC)_2$]: 802.9217, found: 802.9484.

3.6. Synthesis of [Ag(NHC)]I complexes, (Ag_2O route)

A mixture containing imidazolinium iodide (1.12 mmol) and Ag_2O (0.56 mmol) in dichloromethane (25 mL) was stirred at room temperature for 24 hours in the dark, covered with aluminum foil. Afterward, the mixture was filtered through Celite, and the solvent was removed under reduced pressure to obtain the product. The crude product underwent purification by recrystallization using dichloromethane: hexane mixture (1:2) at room temperature. [276] (Unfortunately, the favorable product was not obtained.)

3.7. Synthesis of [Au(NHC)]PF_6 complexes from [Ag(NHC)PF_6, general procedure

A 25 mL round-bottom flask was charged with $[Ag(NHC)_2]PF_6$ (1.44 mmol) and 10 mL of dichloromethane. To this solution, 0.923 g (2.88 mmol, 2 eq.) of Au(tht)Cl dissolved in 5 mL of dichloromethane was added, leading to the immediate formation of a fine white precipitate. The mixture was stirred in the dark for 25 minutes and then filtered through Celite. The clear, colorless filtrate was evaporated to dryness using a rotary evaporator. The resulting white solid was dissolved in a minimal amount of CH_3CN and precipitated with diethylether, yielding $[Au(NHC)_2]PF_6$ as a microcrystalline product. [178,197]

- **Synthesis of [Au(7-allyl-1,3,9-thrimethylxanthine-8-ylidene)$_2$]PF_6 (Au1)**

For synthesising **Au1**, **Ag1** (0,07 g, 0,143 mmol) was reacted with Au(tht)Cl (0.09 g, 0.286 mmol) in 30 ml CH_2Cl_2. Yiled: (0.05 g, 0.06 mmol), 48%.

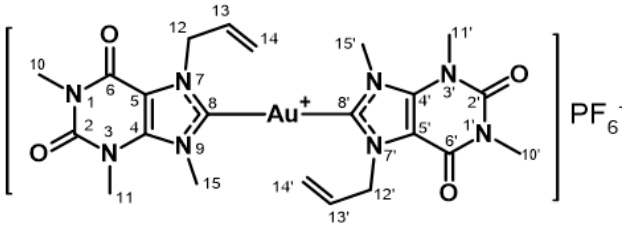

^{1}H NMR (400 MHz, DMSO): δ=[ppm]= 6.14 – 5.96 (m, 1H, C^{13}**H**), 5.23 (dd, *J* = 10.4, 1.2 Hz, 2H, C^{14}**H$_2$**), 5.09 (s, 2H, C^{12}**H$_2$**), 4.20 (s, 3H, C^{15}**H$_3$**), 3.74 (s, 3H, C^{11}**H$_3$**), 3.24 (s, 3H, C^{10}**H$_3$**).

^{13}C{^{1}H} NMR (101 MHz, DMSO) δ= 175.03 ($C_{8\text{-}Au}$), 152.72 (C_6=O), 150.43 (C_2=O), 140.35 (C4), 133.03 (C13), 117.72 (C14), 107.38 (C5), 51.45 (C12), 48.53 (C15), 31.57 (C11), 28.24 (C10).

ESI-MS (CH_3CN m/z): Calculated for $C_{22}H_{28}AuN_8O_4^+$ $[Au(NHC)_2]^+$: 665.1899, found: 665.1817.

- **Synthsis of [Au(7-allyl-9-ethyl-1,3-dimethylxanthine-8-ylidene)$_2$]PF$_6$ (Au2)**

Au2 was synthesized when **Ag2** (0.054 g, 0.11 mmol) was reacted with Au(tht)Cl (0.07 g, 0.22 mmol) in 30 ml CH_2Cl_2, and the reaction was followed as described in part 3.7. yield: (0.05 g, 0.0616 mmol), 56%

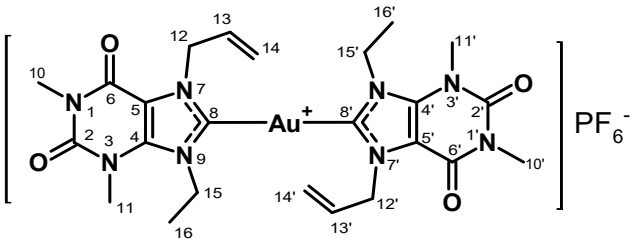

^{1}H NMR (400 MHz, DMSO): δ=[ppm]= 6.21 – 6.02 (m, 1H, C^{13}**H**), 5.40 – 5.23 (m, 1H, C^{14}**H$_2$**), 5.10 (d, *J* = 1.1 Hz, 2H, C^{12}**H$_2$**), 4.74 – 4.54 (m, 2H, C^{15}**H$_2$**), 3.74 (s, 3H, C^{11}**H$_3$**), 3.26 (s, 3H, C^{10}**H$_3$**), 1.57 – 1.46 (m, 3H, C^{16}**H$_3$**).

^{13}C{^{1}H} NMR (101 MHz, DMSO): δ=[ppm]= 186.55 ($C_{8\text{-}Au}$), 152.82 (C_6=O), 150.58 (C_2=O), 140.12 (C4), 133.41 (C13), 117.59 (C14), 107.88 (C5), 51.50 (C12), 46.17 (C15), 31.44 (C11), 28.30 (C10), 17.23 (C16).

ESI-MS (CH_3CN m/z): Calculated for $C_{24}H_{32}AuN_8O_4^+$ $[Au(NHC)_2]^+$: 693.2212, found: 693.2306.

- **Synthesis of [Au(7-(2-bromoethyl)-9-ethyl-1,3-dimethylxanthine-8-ylidene)$_2$]PF$_6$ (Au3)**

For synthesizing **Au3**, **Ag4** (0.045 g, 0.050 mmol) was reacted with Au(tht)Cl (0.032 g, 0.10 mmol) in 30 ml CH_2Cl_2, and the reaction was done as described in part 3.7. yield: (0.01 g, 0.018 mmol), 36%

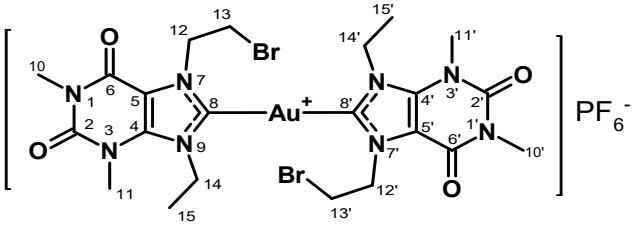

^{1}H NMR (600 MHz, DMSO): δ=[ppm]= 5.00 (t, *J* = 5.7 Hz, 2H, C^{12}**H$_2$**), 4.77 (q, *J* = 7.2 Hz, 2H, C^{14}**H$_2$**), 4.02 (t, *J* = 5.8 Hz, 2H, C^{13}**H$_2$**), 3.77 (s, 3H, C^{11}**H$_3$**), 3.30 (s, 3H, C^{10}**H$_3$**), 1.57 (t, *J* = 7.3 Hz, 3H, C^{15}**H$_3$**).

^{13}C{^{1}H} NMR (151 MHz, DMSO): δ=[ppm]= 186.37 ($C_{8\text{-}Ag}$), 177.39 ($C_{8\text{-}Au}$), 153.03 (C_6=O), 149.94 (C_2=O), 140.07 (C4), 106.71 (C5), 51.56 (C12), 46.22 (C14), 32.11 (C13), 31.05 (C11), 28.64 (C10), 17.24 (C15).

ESI-MS (CH_3CN m/z): Calculated for $C_{22}H_{30}AuBr_2N_8O_4^+$ $[Au(NHC)_2]^+$: 827.0402, found: 827.0636.

3.8. Synthesis of [(COD)Rh(Cl)(NHC)] complexes

- **Synthesis of [(7-allyl-9-ethyl-1,3-dimethylxanthine-8-ylidene)Rh(COD)] PF_6 (Rh1)**

In a darkened environment, 5a-2 (473 mg, 1.2 mmol) was dissolved in 15 mL of anhydrous CH_3CN, to which Ag_2O (301 mg, 1.3 mmol) and NaI (225 mg, 1.5 mmol) were subsequently added. The mixture was heated under reflux at 60°C for 1 hour under an argon atmosphere. The silver precipitate formed was filtered off through Celite. The solvent was then evacuated under reduced pressure, and the resulting complex was used directly without additional purification. The solid was redissolved in 15 mL of CH_2Cl_2, and $[Rh(COD)Cl]_2$ (301 mg, 0.6 mmol) was introduced. This mixture was stirred for 16 hours in the dark. The complex was purified by passing it through a Celite pad and then subjected to gradient column chromatography on silica gel. Eluting with CH_2Cl_2 first produced a fraction of $[Rh(COD)Cl]_2$, and further elution with acetone isolated compound **Rh1**. After the solvents were evaporated, the yellow solid was recrystallized from an acetone and Et_2O (1:1) mixture. [238] The final yield was 397 mg, 0.53 mmol. Yield: 88%.

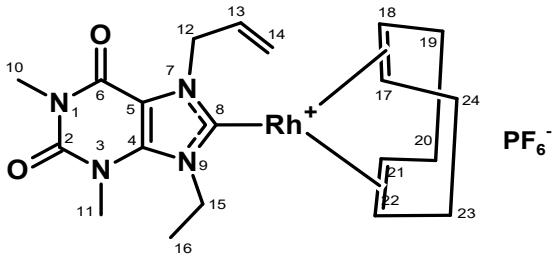

^{1}H NMR (400 MHz, DMSO): δ=[ppm]= 6.19 – 6.02 (m, 1H, C^{13}**H**), 5.25 (d, *J* = 11.7 Hz, 1H) and 5.11 (d, *J* = 15.5 Hz, 1H) (C^{14}**H$_2$**), 5.17 (d, *J* = 5.2 Hz, 2H, C^{12}**H$_2$**), , 4.63 (q, *J* = 7.1 Hz, 2H, C^{15}**H$_2$**), 3.74 (s, 3H, C^{11}**H$_3$**), 3.70 – 3.53 (m, 1H, C^{COD}), 3.39 (q, *J* = 7.1 Hz, 3H, C^{COD}), 3.26 (s, 3H, C^{10}**H$_3$**), 3.16 (d, *J* = 24.5 Hz, 1H, C^{COD}), 2.50 (s, 3H, C^{COD}), 1.48 (t, *J* = 7.2 Hz, 3H, C^{16}**H$_3$**), 1.43 – 1.33 (m, 1H, C^{COD}), 1.09 (t, *J* = 7.0 Hz, 1H, C^{COD}).

^{13}C{^{1}H} NMR (151 MHz, DMSO): δ=[ppm]= 190.45 ($C_{8\text{-}Rh}$), 152.53 (C_6=O), 151.07 (C_2=O), 150.69, 150.43 (d, *J* = 39.1 Hz, C14) , 139.75 (C4), 138.96, 138.33 (d, *J* = 95.1 Hz, C^{COD}), 132.07 (C13), 124.01, 123.9 (d, *J* = 15.4 Hz, C^{COD}), 109.32 (C5), 91.49 (C^{COD} (CH)), 70.78 (C^{COD} (CH)), 51.53 (C12), 41.45 (C15), 35.65 (C11), 31.27, 31.05 (d, *J* = 34.1 Hz, C^{COD}), 28.15, 28.10 (d, *J* = 6.6 Hz, C^{COD}) , 28.03 (C10), 16.70 (C16).

ESI-MS (CH_3CN m/z): Calculated for $C_{24}H_{32}N_8O_4Rh^+$ $[Rh(NHC)_2]^+$: 599.1602, found: 599.1816.

- **Synthesis of [(7-allyl-9-ethyl-1,3-dimethylxanthine-8-ylidene)Rh(COD)] Cl (Rh2)**

The synthesis employed the carbene transfer method through transmetallation from a silver complex. **Ag2** (0.07 g, 0.1 mmol), prepared as described in section 3.4, was dissolved in an excess of CH_2Cl_2, and $[Rh(COD)Cl]_2$ (0.025 g, 0.05 mmol) was subsequently added. The mixture was stirred continuously for three days. The extended reaction duration is attributed to the steric hindrance of the carbenes, a factor that Hahn and colleagues have identified as a common constraint in transmetallation reactions. [277] After the reaction was complete, the precipitate was filtered through Celite, and the complex was isolated using gradient column chromatography. Initially, the starting material was collected using CH_2Cl_2 as the eluent. Further

purification involved using THF to obtain the complex as a yellow powder. Yield: (9.38 mg, 0.019 mmol) 38%.

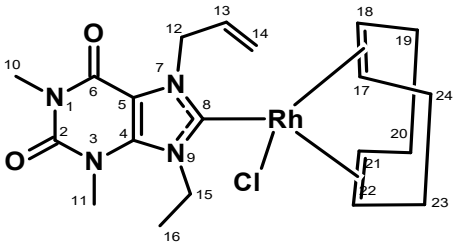

^{1}H NMR (400 MHz, $CDCl_3$): δ=[ppm]= 5.98 – 5.78 (m, 1H, C^{13}**H**), 5.37 – 5.15 (m, 2H, C^{14}**H$_2$**), 4.64 (d, *J* = 4.8 Hz, 1H, cod^{17}(**CH**)), 4.29 – 4.24 (m, 2H, C^{12}**H$_2$**), 4.19 – 4.13 (m, 1H, cod^{18}(**CH**)), 4.01 (dd, *J* = 14.3, 7.3 Hz, 1H, cod^{21}(**CH**)), 3.75 (q, *J* = 7.0 Hz, 1H, cod^{22}(**CH**)), 3.51 (s, 3H, C^{11}**H$_3$**), 3.37 (s, 3H, C^{10}**H$_3$**), 2.94 (dd, *J* = 11.7, 5.6 Hz, 3H, cod^{19,24}(**CH$_2$**)), 2.59 – 2.47 (m, 2H, cod^{23}(**CH$_2$**)), 1.85 – 1.67 (m, 3H, cod^{19,20}(**CH$_2$**)), 1.27 (t, *J* = 7.0 Hz, 3H, C^{16}**H$_3$**).

^{13}C{^{1}H} NMR (101 MHz, $CDCl_3$): δ=[ppm]= 185.93 (d, $J_{C\text{-}Rh}$ = 39.1 Hz, C8-Rh), 155.42 (C6=O), 151.33 (C2=O), 142.85 (C4), 139.25 (d, *J* = 84.7 Hz, C14), 132.44 [d, $J_{Rh\text{-}COD}$ = 26.3 Hz, cod(CH)], 127.35 [d, $J_{Rh\text{-}COD}$ = 29.6 Hz, cod(CH)], 119.64 (cod-CH2), 104.91 (C5), 96.43 (cod-CH2), 78.61 (cod-CH_2), 58.44 (cod-CH2), 52.09(C12), 48.56 (C15), 33.67 (C11), 32.31 (d, *J* = 17.3 Hz, cod-CH_2), 30.85 (cod-CH_2), 28.41 (C10), 18.41 (C16).

ESI-MS (CH_3CN m/z): calculated for $C_{20}H_{24}ClN_4O_2Rh^+$ $[Rh(NHC)_2]^+$: 599.1602, found: 599.1769.

3.9. Synthesis of [Au(NHC)I] complexes -general procedure

The gold NHC iodide complexes were produced following a method established by Nolan and Gimeno's research team. [261,262] This approach involved synthesizing gold NHC complexes with a mild and cost-effective base like K_2CO_3.

The xanthinium salts were combined with the gold precursor [$Au(SMe_2)Cl$] (1 equivalent) in either acetonitrile or acetone and reacted for three hours at room temperature. Subsequently, a substantial excess of base (10 equivalents) was introduced to the mixture to facilitate the deprotonation of the salt and ensure the coordination of the NHC to the metal center. Upon completion of the reaction, the solvent was evaporated using a rotary evaporator, resulting in the formation of a crude orange solid with a satisfactory yield. [225]

- **Synthesis of [Au(7-allyl-1,3,9-thrimethylxanthine-8-ylidene)I] (Au4)**

xanthinium salt **7a-1** (0.036 g, 0.1 mmol) was subjected to reaction with Au(tht)Cl (0.032 g, 0.1 mmol) in 20 ml of acetone under reflux conditions. Subsequently, K_2CO_3 (0.05 g, 0.35 mmol) was added to the mixture. The reaction was allowed to proceed for 24 hours. Afterward, the solvent was evaporated to yield an orange solid. yield: (0.03 g, 0.06 mmol) 60%.

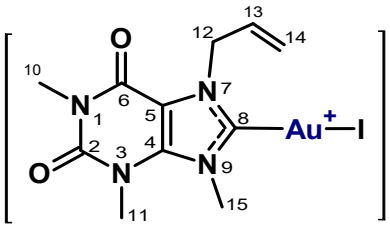

^{1}H NMR (600 MHz, DMSO): δ=[ppm]= 6.05 (ddt, *J* = 16.0, 10.4, 5.2 Hz, 1H, C^{13}**H**), 5.28 – 5.20 (m, 2H, C^{14}**H$_2$**), 5.10 (d, *J* = 5.1 Hz, 2H, C^{12}**H$_2$**), 4.20 (s, 3H, C^{15}**H$_3$**), 3.74 (s, 3H, C^{11}**H$_3$**), 3.25 (s, 3H, C^{10}**H$_3$**).

^{13}C{^{1}H} NMR (151 MHz, DMSO): δ=[ppm]= 152.81 (C_6=O), 150.49 (C_2=O), 140.38 (C4), 133.04 (C13), 117.81 (C14), 107.38 (C5), 51.40 (C12), 40.04 (C15), 31.62 (C11), 28.28 (C10).

ESI-MS (CH_3CN m/z): calculated for $C_{22}H_{28}AuN_8O_4$ [Au(NHC)$_2$]: 665.1899, found: 665.2004.

- **Synthesis of [Au(7-allyl-9-ethyl-1,3-dimethylxanthine-8-ylidene)I] (Au5)**

xanthinium salt **7a-2** (0.075 g, 0.2 mmol) was reacted with Au(tht)Cl (0.064 g, 0.2 mmol) and K_2CO_3 (0.1 g, 0.7 mmol) following the previously described procedure. Yield: (99.3 mg, 0.17 mmol), 87%.

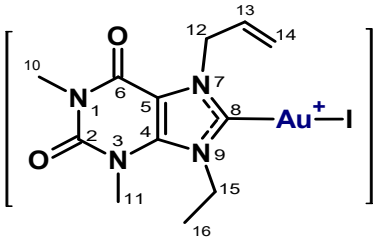

^{1}H NMR (600 MHz, $CDCl_3$): δ=[ppm]= 6.14 – 5.97 (m, 1H, C^{13}**H**), 5.48 – 5.29 (m, 2H, C^{14}**H_2**), 5.25 (d, *J* = 6.0 Hz, 2H, C^{12}**H_2**), 4.74 (q, *J* = 7.2 Hz, 2H, C^{15}**H_2**), 3.85 (s, 3H, C^{11}**H_3**), 3.44 (s, 3H, C^{10}**H_3**), 1.63 (t, *J* = 7.2 Hz, 3H, C^{16}**H_3**).

^{13}C NMR (151 MHz, $CDCl_3$): δ=[ppm]= 186.54 ($C_{8\text{-}Au}$), 153.81 (C_6=O), 150.34 (C_2=O), 138.93 (C4), 131.81 (C13), 120.50 (C14), 107.94 (C5), 52.53 (C12), 46.21 (C15), 31.74 (C11), 28.80 (C10), 17.69 (C16).
ESI-MS (CH_3CN m/z): calculated for $C_{24}H_{32}AuN_8O_4$ $[Au(NHC)_2]$: 693.2212, found: 693.2316.

3.10. Synthesis of [(NHC)-Pd(I)-Py]I complexes- general procedure

In a 25 mL round-bottom flask, Palladium (II) chloride (100 mg, 0.56 mmol), a xanthinium salt (1.1 mmol), and K_2CO_3 (194 mg, 1.41 mmol) were combined. After adding 3 mL of pyridine, the reaction mixture was stirred at 60 °C overnight within an oil bath. Subsequent purification involved column chromatography on silica gel with dichloromethane as the eluent. Afterward, the solvent was removed under vacuum, and the residue was dissolved in 3 mL of dichloromethane. This solution was then slowly added to 50 mL of *n*-pentane to extract the pyridine. The resulting precipitate was filtered, washed repeatedly, and dried under a high vacuum to obtain the final solid product. [21]

- **Synthesis of (7a)(Pd)(PEPPSI) (Pd1)**

Compound **7a-1** (0.398 g, 1.1 mmol) was combined with $PdCl_2$ (0.1 g, 0.56 mmol) and K_2CO_3 (0.194 g, 1.41 mmol) in 3 mL of pyridine. The

reaction proceeded as previously described, resulting in a yield of 94% (0.696 g, 1.03 mmol).

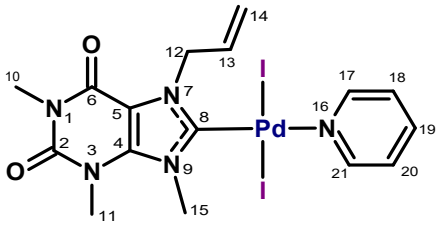

^{1}H NMR (400 MHz, DMSO): δ=[ppm]= 8.92 (d, *J* = 4.8 Hz, 2H, C^{17}**H**, C^{21}**H**), 7.97 (t, *J* = 7.6 Hz, 1H, C^{19}**H**), 7.63 – 7.46 (m, 2H, C^{18}**H**, C^{20}**H**), 6.36 – 6.20 (m, 1H, C^{13}**H**), 5.59 – 5.36 (m, 2H, C^{14}**H$_2$**), 5.33 (d, *J* = 8.8 Hz, 2H, C^{12}**H$_2$**), 4.42 (s, 3H, C^{15}**H$_3$**), 3.75 (s, 3H, C^{11}**H$_3$**), 3.22 (s, 3H, C^{10}**H$_3$**).

^{13}C{^{1}H} NMR (101 MHz, DMSO) δ 155.98 ($C_{8\text{-Pd}}$), 153.21 (C17,21), 151.93 (C_6=O), 150.07 (C_2=O), 140.64 (C19), 138.68 (C4), 131.58 (C13), 125.04 (C18,20), 119.93 (C14), 109.21 (C5), 52.18 (C12), 45.45 (C15), 31.57 (C11), 28.17 (C10).

ESI-MS (CH_3CN m/z): Calculated for $C_{16}H_{19}IN_5O_2Pd^+$ [NHC-Pd-Py]$^+$: 545.9618, found: 545.9428.

- **Synthesis of (7b)(Pd)(PEPPSI) (Pd2)**

A mixture of compound **7b-1** (0.52 g, 1.1 mmol), $PdCl_2$ (0.1 g, 0.056 mmol), and K_2CO_3 (0.194 g, 1.41 mmol) in 3 mL of pyridine was reacted according to the established method, resulting in a 91% yield (0.78 g, 1.0 mmol).

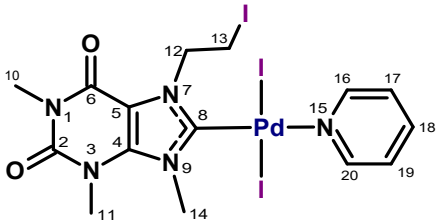

^{1}H NMR (600 MHz, DMSO): δ=[ppm]= 8.91 (d, *J* = 5.3 Hz, 2H, C^{16}**H**, C^{20}**H**), 7.98 (t, *J* = 7.7 Hz, 1H, C^{18}**H**), 7.58 (t, *J* = 7.0 Hz, 2H, C^{17}**H**, C^{19}**H**), 5.06 (t, *J* = 8.2 Hz, 2H, C^{12}**H$_2$**), 4.41 (s, 3H, C^{14}**H$_3$**), 3.79 – 3.76 (m, 2H, C^{13}**H$_2$**), 3.75 (s, 3H, C^{11}**H$_3$**), 3.23 (s, 3H, C^{10}**H$_3$**).

^{13}C{^{1}H} NMR (151 MHz, DMSO): δ=[ppm]= 156.21 ($C_{8\text{-Pd}}$), 153.19 (C16,20), 152.10 (C_6=O), 149.93 (C_2=O), 140.27 (C4), 138.72 (C18), 124.89 (C17,19), 109.10 (C5), 51.69 (C12), 39.87 (C14), 31.52 (C11), 28.40 (C10), -0.88 (C13).

ESI-MS (CH_3CN m/z): Calculated for $C_{15}H_{18}I_3N_5O_2Pd^+$ [NHC-Pd-Py]$^+$: 659.8585, found: 659.8805.

3.11. Synthesis of thiophenol-substituted theophyllinium salts

Compound **5b** (0.1 mmol) was combined with thiophenol (3.6 mmol) and NaOH (3.6 mmol) in an aqueous solution. The reaction mixture was stirred at room temperature for three days. Following this, the mixture was filtered, washed sequentially with ethanol and diethyl ether, and then dried at room temperature.

3.11.1. Synthesis of [NHCH]PF_6 salts of thiophenol-substituted theophylline

The PF_6 salt was prepared using the same procedure outlined for other functionalized theophylline derivatives in section 2.2.4.

- **Synthesis of 1,3,9-trimethyl-2,6-dioxo-7-(2-(phenylthio) ethyl)-2,3,6,7-tetrahydro-1H-purin-9-ium hexafluorophosphate (T-1)**

Compound **T-1** was prepared following the previously described procedure by reacting **5b-1** (0.1 g, 0.2 mmol) with thiophenol (73 µL, 0.72 mmol) and NaOH (0.02 g, 0.72 mmol). The reaction yielded 0.08 g (0.18 mmol), corresponding to a 90% yield.

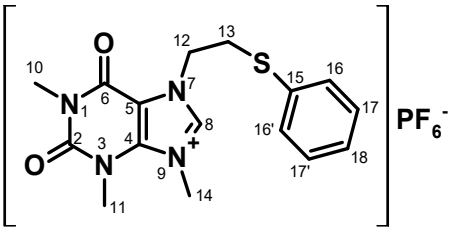

^{1}H NMR (400 MHz, DMSO): δ=[ppm]= 9.37 (s, 1H, C^8**H**), 7.40 – 7.27 (m, 4H, C^{16}**H**, $C^{16'}$**H**, C^{17}**H**, $C^{17'}$**H**), 7.20 (t, *J* = 7.1 Hz, 1H, C^{18}**H**), 4.65 (t, *J* = 6.2 Hz, 2H, C^{12}**H$_2$**), 4.13 (s, 3H, C^{14}**H$_3$**), 3.67 (s, 4H, C^{11}**H$_3$**), 3.56 (t, *J* = 6.1 Hz, 2H, C^{13}**H$_2$**), 3.26 (s, 3H, C^{10}**H$_3$**).

^{13}C{^{1}H} NMR (101 MHz, DMSO): δ=[ppm]= 152.91 (C_6=O), 149.83 (C_2=O), 139.84 (C8), 139.11 (C4), 133.93 (C15), 129.44 (C16, C16'), 128.89 (C17, C17'), 126.60 (C18), 107.16 (C5), 49.21 (C12), 36.82 (C14), 32.41 (C13), 31.17 (C11), 28.48 (C10).

ESI-MS (CH_3CN m/z): Calculated for $C_{16}H_{19}N_4O_2S^+$ [NHC]$^+$: 331.1223, found: 331.1205.

- **Synthesis of 9-ethyl-1,3-dimethyl-2,6-dioxo-7-(2 (phenylthio)ethyl)-2,3,6,7-tetrahydro-1H-purin-9-ium hexafluorophosphate (T-2)**

Compound **T-2** was prepared using the same procedure as described earlier by reacting **5b-2** (0.43 g, 0.2 mmol) with thiophenol (73 µL, 0.72 mmol) and NaOH (0.02 g, 0.72 mmol). The reaction resulted in a yield of 0.09 g (0.184 mmol), equating to 92%.

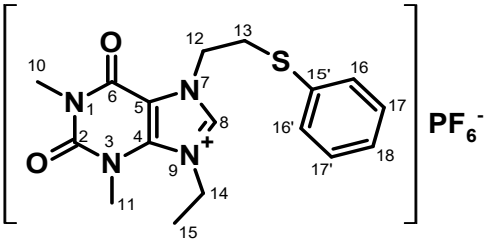

^{1}H NMR (600 MHz, DMSO): δ=[ppm]= 9.43 (s, 1H, C^8**H**), 7.53 (d, *J* = 7.8 Hz, 1H, C^{16}**H**), 7.39 (t, *J* = 7.8 Hz, 1H, C^{17}**H**), 7.36 (d, *J* = 7.7 Hz, 1H, C$^{16'}$**H**), 7.30 (t, *J* = 7.7 Hz, 1H, C$^{17'}$**H**), 7.20 (t, *J* = 7.3 Hz, 1H, C^{18}**H**), 4.66 (t, *J* = 6.3 Hz, 2H, C^{12}**H$_2$**), 4.54 (q, *J* = 7.2 Hz, 2H, C^{14}**H$_2$**), 3.66 (s, 3H, C^{11}**H$_3$**), 3.56 (t, *J* = 6.4 Hz, 2H, C^{13}**H$_2$**), 3.27 (s, 3H, C^{10}**H$_3$**), 1.50 (t, *J* = 7.2 Hz, 3H, C^{15}**H$_3$**).

^{13}C{^{1}H} NMR (151 MHz, DMSO): δ=[ppm]: 152.97 (C_6=O), 150.03 (C_2=O), 138.88 (C8), 135.76 (C4), 133.95 (C15'), 129.30 (C16, C16'), 127.59 (C17, C17'), 126.56 (C18), 107.37 (C5), 49.20 (C12), 45.15 (C14), 32.22 (C13), 31.56 (C11), 28.50 (C10), 15.14 (C15).

ESI-MS (CH_3CN m/z): Calculated for $C_{17}H_{21}N_4O_2S^+$ [NHC]$^+$: 345.1380, found: 345.136.

3.11.2. Synthesis of [NHCH]I salts of thiophenol-substituted theophylline

The iodide salt was prepared using the same procedure outlined for other functionalized theophylline derivatives in section 2.2.6.

- **Synthesis of 1,3,9-trimethyl-2,6-dioxo-7-(2-(phenylthio) ethyl)-2,3,6,7-tetrahydro-1H-purin-9-ium Iodide (T-3)**

Compound **1b** (0.2 g, 0.696 mmol) was combined with thiophenol (0.2 mL, 2.5 mmol, 3.6 eq.) and triethylamine (1.5 mL, 2.5 mmol, 3.6 eq.) in ethanol and stirred for 24 hours. Following the reaction, the mixture was filtered, thoroughly washed multiple times with water and diethyl ether, and subsequently dried at room temperature. The resulting thiophenol-functionalized theophylline was then subjected to methylation using methyl iodide (0.2 mL, 3.5 mmol, 5 eq.) in 5 mL of DMF at a controlled temperature range of 24–36°C for 72 hours. After completion, the suspension was cooled, and an excess of diethyl ether was introduced to induce the formation of a yellow precipitate. Further purification was carried out using sequential solvent extractions with DCM/diethyl ether and AN/diethyl ether, ultimately yielding a pale-yellow solid as the final product. Yield: 68%. (0.2 g, 0.47 mmol).

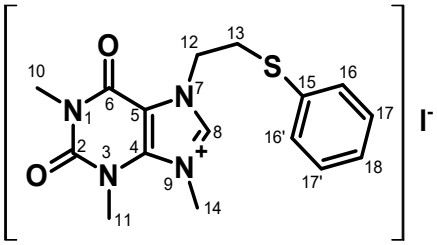

^{1}H NMR (600 MHz, DMSO): δ=[ppm]: 9.41 (s, 1H, C^{8}**H**), 7.37 (d, *J* = 8.2 Hz, 2H, C^{16}**H**, C$^{16'}$**H**), 7.32 (t, *J* = 7.0 Hz, 2H, C^{17}**H**, C$^{17'}$**H**), 7.21 (t, *J* = 7.0

Hz, 1H, $C^{18}\mathbf{H}$), 4.66 (t, *J* = 6.1 Hz, 2H, $C^{12}\mathbf{H_2}$), 4.15 (s, 3H, $C^{14}\mathbf{H_3}$), 3.68 (s, 3H, $C^{11}\mathbf{H_3}$), 3.57 (t, *J* = 6.6 Hz, 2H, $C^{13}\mathbf{H_2}$), 3.26 (s, 3H, $C^{10}\mathbf{H_3}$).

$^{13}C\{^1H\}$ NMR (151 MHz, DMSO): δ=[ppm]= 152.65 (C6=O), 149.61 (C2=O), 139.85 (C8), 139.63 (C4), 133.78 (C15), 129.22 (C16, C16'), 128.42 (C17, C17'), 126.40 (C18), 107.10 (C5), 49.40 (C12), 36.95 (C14), 32.48 (C13), 31.18 (C11), 28.58 (C10).

ESI-MS (CH_3CN m/z): Calculated for $C_{16}H_{19}N_4O_2S^+$ $[NHC]^+$: 331.1223, found: 331.1235.

- **Synthesis of 9-ethyl-1,3-dimethyl-2,6-dioxo-7-(2 (phenylthio)ethyl)-2,3,6,7-tetrahydro-1H-purin-9-ium Iodide (T-4)**

Compound **T-4** was prepared by the same procedure explained above, by the reaction between 1b (0.2 g, 0.696 mmol) and Thiophenol (0.2 mL, 3.6 eq.) and triethylamine (1.5 mL, 3.6 eq.), and a subsequent step with ethyliodide (0.3 mL, 3.5 mmol, 5 eq.). Yield: 79%, (0.25 g, 0.55 mmol).

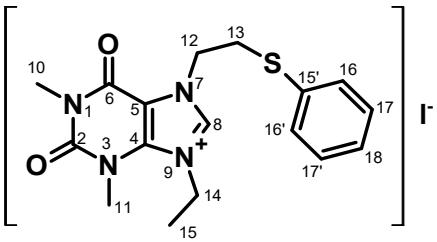

^1H NMR (600 MHz, DMSO): δ=[ppm]= 9.50 (s, 1H, $C^8\mathbf{H}$), 7.37 (d, *J* = 8.1 Hz, 2H, $C^{16,16'}\mathbf{H}$), 7.31 (t, *J* = 7.5 Hz, 2H, $C^{17,17'}\mathbf{H}$), 7.21 (t, *J* = 7.2 Hz, 1H, $C^{18}\mathbf{H}$), 4.67 (t, *J* = 6.4 Hz, 2H, $C^{12}\mathbf{H_2}$), 4.57 (q, *J* = 7.3 Hz, 2H, $C^{14}\mathbf{H_2}$), 3.67

(s, 3H, $C^{11}\mathbf{H_3}$), 3.58 (t, *J* = 6.4 Hz, 2H, $C^{13}\mathbf{H_2}$), 3.27 (s, 3H, $C^{10}\mathbf{H_3}$), 1.52 (t, *J* = 7.2 Hz, 3H, $C^{15}\mathbf{H_3}$).

$^{13}C\{^1H\}$ NMR (151 MHz, DMSO): δ=[ppm]= 152.89 (C6=O), 150.05 (C2=O), 139.21 (C8), 138.67 (C4), 134.03 (C15'), 129.65 (C16, 16'), 128.78 (C17,17'), 124.58 (C18), 107.59 (C5), 49.65 (C12), 45.47 (C14), 32.12 (C13), 31.68 (C11), 28.40 (C10), 15.49 (C15).

ESI-MS (CH_3CN m/z): Calculated for $C_{17}H_{21}N_4O_2S^+$ $[NHC]^+$: 345.1380, found: 345.1374.

3.12. Synthesis of $[Ag(NHC)_2]PF_6$ complexes of thiophenol-substituted theophylline (Ag8)

Complex **Ag8** was obtained by reacting **T-2** (0.1 g, 0.2 mmol) with either silver acetate (0.016 g, 0.1 mmol) or silver(I) oxide (0.02 g, 0.1 mmol) as the silver source in ethanol or methanol as the solvent. The reaction was allowed to proceed for 24 hours. Upon completion, the mixture was filtered, and the solid phase was dissolved in DCM and subjected to trituration using a DCM/Et_2O mixture, leading to the precipitation of the desired white solid product. Yield: 47% (0.07 g, 0.09 mmol).

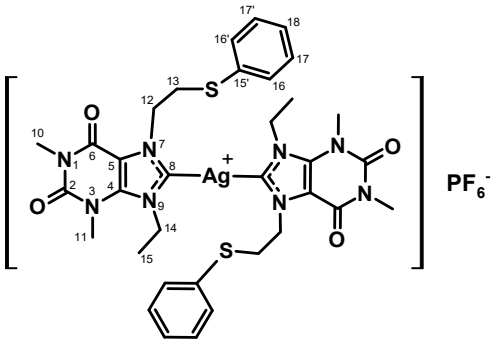

^{1}H NMR (600 MHz, DMSO): δ=[ppm]= 7.21 (d, *J* = 7.6 Hz, 2H, C^{16}**H**, C$^{16'}$**H**), 7.17 (t, *J* = 7.8 Hz, 2H, C^{17}**H**, C$^{17'}$**H**), 7.04 (t, *J* = 7.3 Hz, 1H, C^{18}**H**), 4.67 (t, *J* = 6.1 Hz, 2H, C^{12}**H$_2$**), 4.51 (q, *J* = 7.3 Hz, 2H, C^{14}**H$_2$**), 3.66 (s, 3H, C^{11}**H$_3$**), 3.55 (t, *J* = 6.0 Hz, 2H, C^{13}**H$_2$**), 3.28 (s, 3H, C^{10}**H$_3$**), 1.44 (t, *J* = 7.2 Hz, 3H, C^{15}**H$_3$**).

^{13}C{^{1}H} NMR (151 MHz, DMSO): δ=[ppm]= 185.65 ($C_{8\text{-}Ag}$), 152.87 (C6=O), 150.04 (C2=O), 139.63 (C4), 129.21 (C17,17'), 128.63 (C16,16'), 126.29 (C18), 97.50 (C5), 51.87 (C12), 46.70 (C14), 33.11 (C13), 31.81 (C11), 28.90 (C10), 40.55 (DMSO), 17.90 (C15).

ESI-MS (CH_3CN m/z): Calculated for $C_{34}H_{40}AgN_8O_4S_2$ Ag[NHC]$_2$: 797.1661, found: 797.1640.

3.13. Synthesis of Au-(NHC) complex of thiophenol-substituted theophylline (Au6)

In this part, Ag-(NHC)PF_6 was applied to the synthesis of gold-corresponding complexes, and the reaction was conducted in DCM for 24 hours, based on section 3.7.

Au6 was prepared by reacting compound Ag8 (0.05 g, 0.06 mmol) with Au(tht)Cl (0.04 g, 0.12 mmol, 2 equivalents) in 5 mL of dichloromethane (DCM). After 24 hours, the resulting solution was filtered, and the filtrate was concentrated to approximately 3 mL. The product was then precipitated by adding an excess amount of diethyl ether and subsequently dried at room temperature. Yield: 80%. (0.027 g, 0.04 mmol).

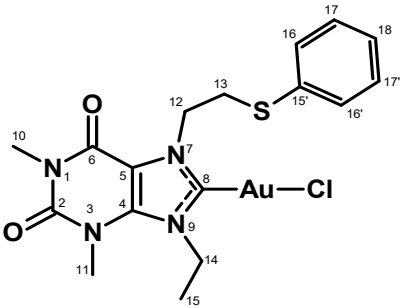

^{1}H NMR (600 MHz, DMSO): δ=[ppm]= 7.33 (d, *J* = 8.1 Hz, 2H, C^{16}**H**, C$^{16'}$**H**), 7.27 (t, *J* = 7.8 Hz, 2H, C^{17}**H**, C$^{17'}$**H**), 7.15 (t, *J* = 6.8 Hz, 1H, C^{18}**H**), 4.71 (t, *J* = 6.6 Hz, 2H, C^{12}**H$_2$**), 4.55 (q, *J* = 8.3, 7.8 Hz, 2H, C^{14}**H$_2$**), 3.63 (s, 3H, C^{11}**H$_3$**), 3.53 (t, *J* = 6.4 Hz, 2H, C^{13}**H$_2$**), 3.24 (s, 3H, C^{10}**H$_3$**), 1.45 (t, *J* = 7.2 Hz, 3H, C^{15}**H$_3$**).

^{13}C{^{1}H} NMR (151 MHz, DMSO): δ=[ppm]= 174.66 ($C_{8\text{-}Au}$), 152.69 (C_6=O), 150.25 (C_2=O), 139.37 (C4), 134.50 (C15'), 128.79 (C16, C16'), 128.58 (C17, C17'), 125.97 (C18), 107.54 (C5), 50.98 (C12), 46.14 (C14), 32.60 (C13), 31.37 (C11), 28.42 (C10), 16.74 (C15).

ESI-MS (CH_3CN m/z): Calculated for $[C_{17}H_{20}AuClN_4O_2S]Na^+$: 599.0559, found: 599.0586.

3.14. Synthesis of tosylate-substituted theophylline-silver complexes

xanthinium tosylate salt (1.0 mmol) was prepared from section 3.2.2.1 and suspended in 5 mL of acetonitrile. Silver(I) oxide (64.3 mg, 0.277 mmol) was added then. The solution was stirred at room temperature for 24 hours before being filtered. The resulting white solid was washed sequentially with cold ethanol and diethylether and then dried at room temperature.

- **Synthesis of (1,3,9-trimethyl-2,6-dioxo-7-(2-(tosyloxy)ethyl)-2,3,6,7,8,9-hexahydro-1H-purin-8-yl)silver (Ag10)**

Complex **Ag10** was prepared by the reaction of xanthinium tosylate salt (methyl form) (0.03 g, 0.1 mmol) and Ag_2O (0.0115 g, 0.05 mmol) in acetonitrile. Yield: (0.01 g, 0.021 mmol, 42%).

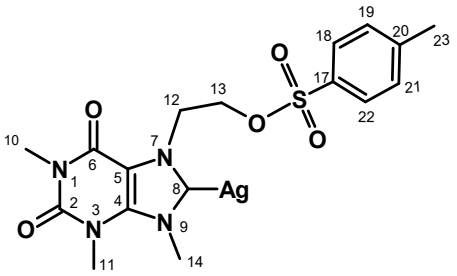

^{1}H NMR (600 MHz, DMSO): δ=[ppm]= 7.49 (d, *J* = 8.1 Hz, 2H, C^{18}**H**, C^{22}**H**), 7.12 (d, *J* = 7.9 Hz, 2H, C^{19}**H**, C^{21}**H**), 4.71 (t, *J* = 4.8 Hz, 2H, C^{13}**H$_2$**), 4.56 – 4.49 (m, 2H, C^{12}**H$_2$**), 4.22 (s, 3H, C^{14}**H$_3$**), 3.78 (s, 3H, C^{11}**H$_3$**), 3.29 (s, 3H, C^{10}**H$_3$**), 2.30 (s, 3H, C^{23}**H$_3$**).

^{13}C{^{1}H} NMR (151 MHz, DMSO): δ=[ppm]= 155.54 (C_6=O), 153.97 (C_2=O), 145.79 (C17), 141.10 (C4), 137.46 (C20), 127.96 (C18, C22), 125.44 (C19, C21), 106.13 (C5), 58.40 (C12), 47.37 (C14), 39.23 (C11), 33.40 (C13), 26.04 (C10).

ESI-MS (CH_3CN m/z): Calculated for $[C_{18}H_{22}AgN_4O_5S]^+$: 499.205, found: 499.0107.

References

[**1**] Gudimetla, V. B.; Joy, B. P.; Sudeep, P.: Imidazolium-Based N-Heterocyclic Carbenes (NHCs) and Metal-Mediated Catalysis. *Carbene*, 1-16, **2022**; IntechOpen: Rijeka. DOI: *10.5772/intechopen.102561*.

[**2**] Enders, D.; Niemeier, O.; Henseler, A. *Organocatalysis by N-Heterocyclic Carbenes* **2007**, *107*, 5606–5655. DOI: *10.1021/cr068372z*.

[**3**] Freeman, R.; Morris, G. A. *Experimental chemical shift correlation maps in nuclear magnetic resonance spectroscopy* **1978**, 684–686. DOI: *10.1039/C39780000684*.

[**4**] Herrmann, W. A.; Köcher, C. *N-Heterocyclic Carbenes* **1997**, *36*, 2162–2187. DOI: *10.1002/anie.199721621*.

[**5**] Nolan, S. P. *N-Heterocyclic Carbenes*; Wiley-VCH Verlag GmbH & Co. KGaA, **2014.** ISBN 978-3-527-33490-2.

[**6**] Kirmse, W. *Neues über Carbene* **1961**, *73*, 161–166. DOI: *10.1002/ange.19610730503*.

[**7**] Ing, P. D.; Wanzlick, H. W. *Nucleophile Carben-Chemie* **1962**, *74*, 129–164.

[**8**] Henkel, S. *Solvatation von Carbenen* **2017**, *51*, 40–43. DOI: *10.1002/CIUZ.201700782*.

[**9**] Bertrand, G. *Carbene Chemistry, From Fleeting Intermediates to Powerful Reagents*; Marcel Dekker: New York, **2002.** ISBN 9780824743215.

[**10**] Herrmann, W. A. *N-Heterocyclic Carbenes: A New Concept in Organometallic Catalysis* **2002**, *41*, 1290–1309. DOI: *10.1002/1521-3773(20020415)41:8%3C1290*.

[**11**] Bourissou, D.; Guerret, O.; Gabbaï, F. P.; Bertrand, G. *Stable Carbenes* **2000**, *100*, 39–92. DOI: *10.1021/cr940472u*.

[**12**] Frémont, d. P.; Marion, N.; Nolan, S. P. *Carbenes: Synthesis, properties, and organometallic chemistry* **2009**, *253*, 862–892. DOI: *10.1016/j.ccr.2008.05.018*.

[**13**] Peddiahgari Vasu, G. R.; Motakatla Venkata, K. R.; Kakarla, R. R.; Ranganath, K. V.; Aminabhavi, T. M. *Recent advances in sustainable N-heterocyclic carbene-Pd(II)-pyridine (PEPPSI) catalysts: A review* **2023**, *225*, 115515. DOI: *10.1016/j.envres.2023.115515*.

[**14**] Jahnke, M. C.; Hahn, F. E. *N-Heterocyclic Carbenes: From Laboratory Curiosities to Efficient Synthetic Tools*; The Royal Society of Chemistry, **2016**.

[**15**] Pauling, L. *Some Guidelines for Radical Reactions* **1980**, 668.

[**16**] Hahn, F. E.; Jahnke, M. C. *Heterocyclic Carbenes: Synthesis and Coordination Chemistry* **2008**, *47*, 3122–3172. DOI: *10.1002/anie.200703883*.

[**17**] Bellotti, P.; Koy, M.; Hopkinson, M. N.; Glorius, F. *Recent advances in the chemistry and applications of N-heterocyclic carbenes* **2021**, *5*, 711–725. DOI: *10.1038/s41570-021-00321-1*.

[**18**] Díez-González, S.; Marion, N.; Nolan, S. P. *N-Heterocyclic Carbenes in Late Transition Metal Catalysis* **2009**, *109*, 3612–3676. DOI: *10.1021/cr900074m*.

[**19**] Ghadwal, R. S.; Roesky, H. W.; Granitzka, M.; Stalke, D. *A facile route to functionalized N-heterocyclic carbenes (NHCs) with NHC base-*

stabilized dichlorosilylene **2010**, *132*, 10018–10020. DOI: *10.1021/ja104386q*.

[**20**] Das, T. K.; Biju, A. T. *Progress in Heterocyclic Chemistry*; Progress in Heterocyclic Chemistry; Elsevier, **2020**, 1–82.

[**21**] Mazars, F.; Zaragoza, G.; Delaude, L. *Caffeine and theophylline as sustainable, biosourced NHC ligand precursors for efficient palladium-catalyzed Suzuki–Miyaura cross-coupling reactions* **2022**, *978*, 122489. DOI: *10.1016/j.jorganchem.2022.122489*.

[**22**] Herrmann, W. A. *.; O¨fele, K.; Preysing, D. v.; Schneider, S. K. *Phospha-palladacycles and N-heterocyclic carbene palladium complexes: efficient catalysts for CC-coupling reactions* **2003**, *687*, 229–248.

[**23**] Diez-González, S.; Nolan, S. P. *Palladium-catalyzed reactions using NHC ligands* **2007**, *21*, 47–82.

[**24**] Fürstner, A.; Davies, P. W. *Catalytic Carbophilic Activation: Catalysis by Platinum and Gold π Acids* **2007**, *46*, 3410–3449. DOI: *10.1002/anie.200604335*.

[**25**] Nef, J. U. *Ueber das zweiwerthige Kohlenstoffatom. Die Chemie des Cyans und des Isocyans* **1895**, *287*, 265–359. DOI: *10.1002/jlac.18952870303*.

[**26**] Tschugajeff, L.; Skanawy-Grigorjewa, M.; Posnjak, A. *Über Die Hydrazin-Carbylamin-Komplexe des Platins* **1925**, *148*, 37–42. DOI: *10.1002/zaac.19251480105*.

[**27**] Rouschias, G.; Shaw, B. L. *A revised structure for Chugaev's salt [PtC8H15N6]Cl* **1970**, 183. DOI: *10.1039/C29700000183*.

[**28**] Rouschias, G.; Shaw, B. L. *The chemistry and structure of Chugaev's salt and related compounds containing a cyclic carbene ligand* **1971**, 2097–2104. DOI: *10.1039/J19710002097*.

[**29**] Burke, A., A. L. Balch and J. H. Enemark. *Palladium and Platinum Complexes Resulting from the Addition of Hydrazine to Coordinated Isocyanide* **1970**, *92*, 2555–2557.

[**30**] Butler W. M.; Enemark J. H.; Parks J. E.; Balch A. L. *Chelative addition of hydrazines to coordinated isocyanides. Structure of Chugaev's red salt* **1973**, *12*, 451–457.

[**31**] Stork, J. R., Olmstead, M. M., & Balch, A. L. *Metalation of Xanthine Derivatives and the Formation of Carbene-Substituted Guanine-Containing Complexes.* **2004**, *43*, 7508–7515.

[**32**] Fehlhammer, W. P.; Fritz, M. *Emergence of a CNH and cyano complex based organometallic chemistry* **1993**, *93*, 1243–1280. DOI: *10.1021/cr00019a016*.

[**33**] Skell, P. S.; Sandler, S. R. *Reaction of 1,1-digalocyclopropanes with electrophilic reagents. synthetic route for insertinga carbon atom between the atoms of a double bond* **1958**, *80*, 2024–2025. DOI: *10.1021/ja01541a070*.

[**34**] Fischer, E. O.; Maasböl, A. *On the Existence of a Tungsten Carbonyl Carbene Complex* **1964**, *3*, 580–581. DOI: *10.1002/anie.196405801*.

[**35**] Schönherr, H.-J.; Wanzlick, H.-W. *Chemie nucleophiler Carbene, XVIII1) 1.3.4.5-Tetraphenyl-imidazoliumperchlorat* **1970**, *731*, 176–179. DOI: *10.1002/jlac.19707310121*.

[**36**] Gleiter, R.; Hoffmann, R. *Stabilizing a singlet methylene* **1968**, *90*, 5457–5460. DOI: *10.1021/ja01022a023*.

[**37**] Wanzlick, H. W.; Schönherr, H. J. *Direct Synthesis of a Mercury Salt-Carbene Complex* **1968**, *7*, 141–142.

[**38**] Öfele, K. *Pentacarbonyl(2,3-diphenylcyclopropenyliden)-chrom(0)* **1968**, *80*, 1032–1033.

[**39**] Öfele, K.; Kreiter, C. G. *(1.4-Dimethyl-tetrazolium)-carbonylferrate, Ausgangsprodukte für (1.4-Dimethyl-tetrazolinyliden)- und Bis(methylamino)carben-Komplexe* **1972**, *105*, 529–540. DOI: *10.1002/cber.19721050218*.

[**40**] Igau, A., Grutzmacher, H., Baceiredo, A. & Bertrand, G. *Analogy α,α′-Bis-Carbenoid Triply-Bonded Species: Synthesis of a stable λ3-Phosphacarbene-λ5-Phosphaacetylene* **1988**, *110*, 6463–6466. DOI: *10.1002/chin.198952241*.

[**41**] Arduengo, A. J., III; Harlow, R. L.; Kline, M. *A stable crystalline carbene* **1991**, *113*, 361–363. DOI: *10.1021/ja00001a054*.

[**42**] Schmidt, A.; Wiechmann, S.; Otto, C. F. *Heterocyclic Chemistry in the 21st Century*, 143–172, **2016**; Advances in Heterocyclic Chemistry; Academic Press. DOI: *10.1016/bs.aihch.2016.02.002*.

[**43**] Kuhn, N.; Kratz. T. *Synthesis of Imidazol-2-ylidenes by Reduction of Imidazole-2(3H)-thiones* **1993**, *1993*, 561–562.

[**44**] Guerret, O.; Solé, S.; Gornitzka, H.; Teichert, M.; Trinquier, G.; Bertrand, G. *1,2,4-Triazole-3,5-diylidene: A Building Block for Organometallic Polymer Synthesis* **1997**, *119*, 6668–6669.

[**45**] Lin, J. C. Y.; Huang, R. T. W.; Lee, C. S.; Bhattacharyya, A.; Hwang, W. S.; Lin, I. J. B. *Coinage Metal–N-Heterocyclic Carbene Complexes* **2009**, *109*, 3561–3598. DOI: *10.1021/cr8005153*.

[**46**] Cavallo, L.; Cazin, C. S. L. *N-Heterocyclic Carbenes in Transition Metal Catalysis and Organocatalysis*, 1–22, **2011**; Springer Netherlands: Dordrecht. DOI: *10.1007/978-90-481-2866-2_1*.

[**47**] Arduengo, A. J., III; Dias, H. V. R.; Harlow, R. L.; Kline, M. *Electronic stabilization of nucleophilic carbenes* **1992**, *114*, 5530–5534. DOI: *10.1021/ja00040a007*.

[**48**] Gómez-Suárez, A.; Nelson, D. J.; Nolan, S. P. *Quantifying and understanding the steric properties of N-heterocyclic carbenes* **2017**, *53*, 2650–2660. DOI: *10.1039/C7CC00255F*.

[**49**] Rotella, D. P. *Chapter Four - Heterocycles in drug discovery: Properties and preparation*, *134*, 149–183. DOI: *10.1016/bs.aihch.2020.10.002*.

[**50**] Taniguchi, T. *Advances in chemistry of N-heterocyclic carbene boryl radicals* **2021**, *50*, 8995–9021. DOI: *10.1039/D1CS00385B*.

[**51**] Doddi, A.; Peters, M.; Tamm, M. *N-Heterocyclic Carbene Adducts of Main Group Elements and Their Use as Ligands in Transition Metal Chemistry* **2019**, *119*, 6994–7112. DOI: *10.1021/acs.chemrev.8b00791*.

[**52**] Nesterov, V.; Reiter, D.; Bag, P.; Frisch, P.; Holzner, R.; Porzelt, A.; Inoue, S. *NHCs in Main Group Chemistry* **2018**, *118*, 9678–9842. DOI: *10.1021/acs.chemrev.8b00079*.

[**53**] Kolychev, E. L.; Theuergarten, E.; Tamm, M. *N-heterocyclic carbenes in FLP chemistry* **2013**, *334*, 121–155. DOI: *10.1007/128_2012_379*.

[**54**] Zhao, Q.; Meng, G.; Nolan, S. P.; Szostak, M. *N-Heterocyclic Carbene Complexes in C-H Activation Reactions* **2020**, *120*, 1981–2048. DOI: *10.1021/acs.chemrev.9b00634*.

[**55**] Kuwata, S.; Hahn, F. E. *Complexes Bearing Protic N-Heterocyclic Carbene Ligands* **2018**, *118*, 9642–9677. DOI: *10.1021/acs.chemrev.8b00176*.

[**56**] Bellemin-Laponnaz, S.; Dagorne, S. *Group 1 and 2 and early transition metal complexes bearing N-heterocyclic carbene ligands: coordination chemistry, reactivity, and applications* **2014**, *114*, 8747–8774. DOI: *10.1021/cr500227y*.

[**57**] Schaper, L.; Hock, S.; Herrmann, W. A.; Kuehn, F. *Synthesis and Application of Water-Soluble NHC Transition-Metal Complexes* **2013**, *44.* DOI: *10.1002/CHIN.201314253*.

[**58**] Wang, Z.; Tzouras, N.; Nolan, S. P.; Bi, X. *Silver N-heterocyclic carbenes: emerging powerful catalysts* **2021**, *3*, 674–685. DOI: *10.1016/j.trechm.2021.04.006*.

[**59**] Lazreg, F.; Nahra, F.; Cazin, C. S. L. *Copper–NHC complexes in catalysis* **2015**, *293-294*, 48–79. DOI: *10.1016/j.ccr.2014.12.019*.

[**60**] Velazquez, H. D.; Verpoort, F. *N-heterocyclic carbene transition metal complexes for catalysis in aqueous media* **2012**, *41*, 7032–7060. DOI: *10.1039/C2CS35102A*.

[**61**] Marion, N.; Nolan, S. P. *Well-defined N-heterocyclic carbenes-palladium(II) precatalysts for cross-coupling reactions* **2008**, *41*, 1440–1449. DOI: *10.1021/ar800020y*.

[**62**] Ott, I. *Chapter Four - Metal N-heterocyclic carbene complexes in medicinal chemistry.* **2020**, *75*, 121–148. DOI: *10.1016/bs.adioch.2019.10.008*.

[**63**] Hindi, K. M.; Panzner, M. J.; Tessier, C. A.; Cannon, C. L.; Youngs, W. J. *The medicinal applications of imidazolium carbene-metal complexes* **2009**, *109*, 3859–3884. DOI: *10.1021/cr800500u*.

[**64**] Song, H.; Pietrasiak, E.; Lee, E. *Persistent Radicals Derived from N-Heterocyclic Carbenes for Material Applications* **2022**, *55*, 2213–2223. DOI: *10.1021/acs.accounts.2c00222*.

[**65**] Smith, C. A.; Narouz, M. R.; Lummis, P. A.; Singh, I.; Nazemi, A.; Li, C.-H.; Crudden, C. M. *N-Heterocyclic Carbenes in Materials Chemistry* **2019**, *119*, 4986–5056. DOI: *10.1021/acs.chemrev.8b00514*.

[**66**] Ezugwu, C. I.; Kabir N. A.; Yusubov, M.; Verpoort, F. *Metal–organic frameworks containing N-heterocyclic carbenes and their precursors* **2016**, *307*, 188–210. DOI: *10.1016/j.ccr.2015.06.012*.

[**67**] Mercs, L.; Albrecht, M. *Beyond catalysis: N-heterocyclic carbene complexes as components for medicinal, luminescent, and functional materials applications* **2010**, *39*, 1903–1912. DOI: *10.1039/B902238B*.

[**68**] Fèvre, M.; Pinaud, J.; Gnanou, Y.; Vignolle, J.; Taton, D. *N-Heterocyclic carbenes (NHCs) as organocatalysts and structural components in metal-free polymer synthesis* **2013**, *42*, 2142–2172. DOI: *10.1039/C2CS35383K*.

[**69**] Ryan, S. J.; Candish, L.; Lupton, D. W. *Acyl anion free N-heterocyclic carbene organocatalysis* **2013**, *42*, 4906–4917. DOI: *10.1039/C3CS35522E*.

[**70**] Bugaut, X.; Glorius, F. *Organocatalytic umpolung: N-heterocyclic carbenes and beyond* **2012**, *41*, 3511–3522. DOI: *10.1039/C2CS15333E*.

[**71**] Menon, R. S.; Biju, A. T.; Nair, V. *Recent advances in employing homoenolates generated by N-heterocyclic carbene (NHC) catalysis in carbon–carbon bond-forming reactions* **2015**, *44*, 5040–5052. DOI: *10.1039/C5CS00162E*.

[**72**] Hopkinson, M. N.; Richter, C.; Schedler, M.; Glorius, F. *An overview of N-heterocyclic carbenes* **2014**, *510*, 485–496. DOI: *10.1038/nature13384*.

[**73**] Christmann, M. *N-Heterocyclic Carbenes: A New Concept in Organocatalysis* **2005**, *44*, 2632–2634.

[**74**] Enders, D.; Balensiefer, T. *Organocatalysis: a new era in asymmetric synthesis* **2004**, *37*, 534–541.

[**75**] Grasa, G. A., Singh, R., & Nolan, S. P. *N-heterocyclic carbenes in gold catalysis* **2004**, 971–980.

[**76**] Johnson, J. S. *N-heterocyclic carbenes in catalytic organic synthesis* **2004**, *43*, 1326–1328.

[**77**] Zeitler, K. *An update on NHC–metal catalysed transformations of unsaturated organic substrates* **2005**, *44*, 7506–7510.

[**78**] Costabile, C.; Pragliola, S.; Grisi, F. *C2-Symmetric N-Heterocyclic Carbenes in Asymmetric Transition-Metal Catalysis* **2022**, *14*, 1615. DOI: *10.3390/sym14081615*.

[**79**] Peris, E. *Smart N-Heterocyclic Carbene Ligands in Catalysis* **2018**, *118*, 9988–10031. DOI: *10.1021/acs.chemrev.6b00695*.

[**80**] Berben, L. A.; Bruin, B. de; Heyduk, A. F. *Non-innocent ligands* **2015**, *51*, 1553–1554. DOI: *10.1039/C4CC90480J*.

[**81**] Hindson, K.; Bruin, B. de. *Cooperative & Redox Non-Innocent Ligands in Directing Organometallic Reactivity (Eur. J. Inorg. Chem. 3/2012)* **2012**, *2012*, 340–342. DOI: *10.1002/ejic.201290001*.

[**82**] Annibale, V. T.; Song, D. *Multidentate actor ligands as versatile platforms for small molecule activation and catalysis* **2013**, *3*, 11432–11449. DOI: *10.1039/C3RA40618K*.

[**83**] Zhao, B.; Han, Z.; Ding, K. *The N-H functional group in organometallic catalysis* **2013**, *52*, 4744–4788. DOI: *10.1002/anie.201204921*.

[**84**] van der Vlugt, J. I. *Cooperative Catalysis with First-Row Late Transition Metals* **2012**, *2012*, 363–375. DOI: *10.1002/ejic.201100752*.

[**85**] Blanco, V.; Leigh, D. A.; Marcos, V. *Artificial switchable catalysts* **2015**, *44*, 5341–5370. DOI: *10.1039/C5CS00096C*.

[**86**] Lüning, U. *Switchable Catalysis* **2012**, *51*, 8163–8165. DOI: *10.1002/anie.201204567*.

[**87**] Burrows, A. D. *The design and applications of multifunctional ligands* **2002**, *85*, 199–217. DOI: *10.3184/003685002783238799*.

[**88**] Crabtree, R. H. *Multifunctional ligands in transition metal catalysis* **2011**, *35*, 18–23. DOI: *10.1039/C0NJ00776E*.

[**89**] Benhamou, L.; Chardon, E.; Lavigne, G.; Bellemin-Laponnaz, S.; César, V. *Synthetic Routes to N-Heterocyclic Carbene Precursors* **2011**, *111*, 2705–2733. DOI: *10.1021/cr100328e*.

[**90**] Nelson, D. J.; Nolan, S. P. *Quantifying and understanding the electronic properties of N-heterocyclic carbenes* **2013**, *42*, 6723–6753. DOI: *10.1039/C3CS60146C*.

[**91**] Nelson, D. J.; Nolan, S. P. *N-Heterocyclic Carbenes*, **2014**, 1–24. DOI: *10.1002/9783527671229.ch01*.

[**92**] Clavier, H.; Nolan, S. P. *Percent buried volume for phosphine and N-heterocyclic carbene ligands: steric properties in organometallic chemistry* **2010**, *46*, 841–861. DOI: *10.1039/B922984A*.

[**93**] Glorius, F. *N-Heterocyclic Carbenes in Catalysis—An Introduction* 21; Springer, **2007.** DOI: *10.1007/3418_2006_059.* ISBN-10 3-540-36929-5.

[**94**] Frenking, G.; Solà, M.; Vyboishchikov, S. F. *Chemical bonding in transition metal carbene complexes* **2005**, *690*, 6178–6204. DOI: *10.1016/j.jorganchem.2005.08.054*.

[**95**] Jacobsen, H.; Correa, A.; Costabile, C.; Cavallo, L. *π-Acidity and π-basicity of N-heterocyclic carbene ligands. A computational assessment* **2006**, *691*, 4350–4358. DOI: *10.1016/j.jorganchem.2006.01.026*.

[**96**] Tonner, R.; Heydenrych, G.; Frenking, G. *Bonding Analysis of N-Heterocyclic Carbene Tautomers and Phosphine Ligands in Transition-Metal Complexes: A Theoretical Study* **2007**, *2*, 1555–1567. DOI: *10.1002/asia.200700235*.

[**97**] Jacobsen, H.; Correa, A.; Poater, A.; Costabile, C.; Cavallo, L. *Understanding the M(NHC) (NHC=N-heterocyclic carbene) bond* **2009**, *253*, 687–703. DOI: *10.1016/j.ccr.2008.06.006*.

[**98**] Fröhlich, N.; Pidun, U.; Stahl, M.; Frenking, G. *Carbenes as Pure Donor Ligands: Theoretical Study of Beryllium−Carbene Complexes1* **1997**, *16*, 442–448. DOI: *10.1021/om960752v*.

[**99**] Hu, X.; Tang, Y.; Gantzel, P.; Meyer, K. *Silver Complexes of a Novel Tripodal N-Heterocyclic Carbene Ligand: Evidence for Significant Metal−Carbene π-Interaction* **2003**, *22*, 612–614. DOI: *10.1021/om020935j*.

[**100**] Hu, X.; Castro-Rodriguez, I.; Olsen, K.; Meyer, K. *Group 11 Metal Complexes of N-Heterocyclic Carbene Ligands: Nature of the MetalCarbene Bond* **2004**, *23*, 755–764. DOI: *10.1021/om0341855*.

[**101**] Scott, N. M.; Dorta, R.; Stevens, E. D.; Correa, A.; Cavallo, L.; Nolan, S. P. *Interaction of a Bulky N-Heterocyclic Carbene Ligand with Rh(I) and Ir(I). Double C−H Activation and Isolation of Bare 14-Electron*

Rh(III) and Ir(III) Complexes **2005**, *127*, 3516–3526. DOI: *10.1021/ja043249f*.

[**102**] Garrison, J. C.; Simons, R. S.; Kofron, W. G.; Tessier, C. A.; Youngs, W. J. *Synthesis and structural characterization of a silver complex of a mixed-donor N-heterocyclic carbene linked cyclophane* **2001**, 1780–1781. DOI: *10.1039/B105751K*.

[**103**] Tulloch, A. A. D.; Danopoulos, A. A.; Kleinhenz, S.; Light, M. E.; Hursthouse, M. B.; Eastham, G. *Structural Diversity in Pyridine-N-Functionalized Carbene Copper(I) Complexes* **2001**, *20*, 2027–2031. DOI: *10.1021/om010014t*.

[**104**] Dorta, R.; Stevens, E. D.; Nolan, S. P. *Double C−H Activation in a Rh−NHC Complex Leading to the Isolation of a 14-Electron Rh(III) Complex* **2004**, *126*, 5054–5055. DOI: *10.1021/ja049545+*.

[**105**] Lee, B. C.; Liu, C.-F.; Lin, L. Q. H.; Yap, K. Z.; Song, N.; Ko, C. H. M.; Chan, P. H.; Koh, M. J. *N-Heterocyclic carbenes as privileged ligands for nickel-catalysed alkene functionalisation* **2023**, *52*, 2946–2991. DOI: *10.1039/D2CS00972B*.

[**106**] Heinemann, C.; Thiel, W. *Ab initio study on the stability of diaminocarbenes* **1994**, *217*, 11–16. DOI: *10.1016/0009-2614(93)E1360-S*.

[**107**] Maji, B.; Breugst, M.; Mayr, H. *N-Heterocyclic Carbenes: Organocatalysts with Moderate Nucleophilicity but Extraordinarily High Lewis Basicity* **2011**, *50*, 6915–6919. DOI: *10.1002/anie.201102435*.

[**108**] Arduengo III, A. J.; Krafczyk, R. *Auf der Suche nach Stabilen Carbenen* **1998**, *32*, 6–14. DOI: *10.1002/ciuz.19980320103*.

[**109**] Regitz, M. *Nucleophilic Carbenes: An Incredible Renaissance* **1996**, *35*, 725–728. DOI: *10.1002/anie.199607251*.

[**110**] Alder, R. W.; Blake, M. E.; Chaker, L.; Harvey, J. N.; Paolini, F.; Schütz, J. *When and How Do Diaminocarbenes Dimerize?* **2004**, *43*, 5896–5911. DOI: *10.1002/anie.200400654*.

[**111**] Cartert, E. A.; Goddard III, W. A. *Relation between Singlet-Triplet Gaps and Bond Energies* **1986**, *90*, 998–1001.

[**112**] Graham, D. C.; Cavell, K. J.; Yates, B. F. *Dimerization mechanisms of heterocyclic carbenes* **2005**, *18*, 298–309. DOI: *10.1002/poc.846*.

[**113**] Huynh, H. V. *Electronic Properties of N-Heterocyclic Carbenes and Their Experimental Determination* **2018**, *118*, 9457–9492. DOI: *10.1021/acs.chemrev.8b00067*.

[**114**] Hansch, C.; Leo, A.; Taft, R. W. *A survey of Hammett substituent constants and resonance and field parameters* **1991**, *91*, 165–195. DOI: *10.1021/cr00002a004*.

[**115**] Denk, M. K.; Hezarkhani, A.; Zheng, F.-L. *Steric and Electronic Effects in the Dimerization of Wanzlick Carbenes: The Alkyl Effect* **2007**, *2007*, 3527–3534. DOI: *10.1002/ejic.200700217*.

[**116**] Hillier, A. C.; Sommer, W. J.; Yong, B. S.; Petersen, J. L.; Cavallo, L.; Nolan, S. P. *A Combined Experimental and Theoretical Study Examining the Binding of N-Heterocyclic Carbenes (NHC) to the Cp*RuCl (Cp* = η5-C5Me5) Moiety: Insight into Stereoelectronic Differences between Unsaturated and Saturated NHC Ligands* **2003**, *22*, 4322–4326. DOI: *10.1021/om034016k*.

[**117**] Fantasia, S.; Petersen, J. L.; Jacobsen, H.; Cavallo, L.; Nolan, S. P. *Electronic Properties of N-Heterocyclic Carbene (NHC) Ligands: Synthetic, Structural, and Spectroscopic Studies of (NHC)Platinum(II) Complexes* **2007**, *26*, 5880–5889. DOI: *10.1021/om700857j*.

[**118**] Kelly III, R. A.; Clavier, H.; Giudice, S.; Scott, N. M.; Stevens, E. D.; Bordner, J.; Samardjiev, I.; Hoff, C. D.; Cavallo, L.; Nolan, S. P.

Determination of N-Heterocyclic Carbene (NHC) Steric and Electronic Parameters using the [(NHC)Ir(CO)2Cl] System **2008**, *27*, 202–210. DOI: *10.1021/om701001g*.

[**119**] Leuthäußer, S.; Schwarz, D.; Plenio, H. *Tuning the Electronic Properties of N-Heterocyclic Carbenes* **2007**, *13*, 7195–7203. DOI: *10.1002/chem.200700228*.

[**120**] Gusev, D. G. *Electronic and Steric Parameters of 76 N-Heterocyclic Carbenes in Ni(CO)3(NHC)* **2009**, *28*, 6458–6461. DOI: *10.1021/om900654q*.

[**121**] Iglesias, M.; Beetstra, D. J.; Stasch, A.; Horton, P. N.; Hursthouse, M. B.; Coles, S. J.; Cavell, K. J.; Dervisi, A.; Fallis, I. A. *First Examples of Diazepanylidene Carbenes and Their Late-Transition-Metal Complexes* **2007**, *26*, 4800–4809. DOI: *10.1021/om7004904*.

[**122**] Scarborough, C. C.; Guzei, I. A.; Stahl, S. S. *Synthesis and isolation of a stable, axially-chiral seven-membered N-heterocyclic carbene* **2009**, 2284–2286. DOI: *10.1039/B902460C*.

[**123**] Dröge, T.; Glorius, F. *The Measure of All Rings—N-Heterocyclic Carbenes* **2010**, *49*, 6940–6952. DOI: *10.1002/anie.201001865*.

[**124**] Tolman, C. A. *Steric effects of phosphorus ligands in organometallic chemistry and homogeneous catalysis* **1977**, *77*, 313–348. DOI: *10.1021/cr60307a002*.

[**125**] Huang, J.; Stevens, E. D.; Nolan, S. P.; Petersen, J. L. *Olefin Metathesis-Active Ruthenium Complexes Bearing a Nucleophilic Carbene Ligand* **1999**, *121*, 2674–2678. DOI: *10.1021/ja9831352*.

[**126**] Poater, A.; Cosenza, B.; Correa, A.; Giudice, S.; Ragone, F.; Scarano, V.; Cavallo, L. *SambVca: A Web Application for the Calculation of the Buried Volume of N-Heterocyclic Carbene Ligands* **2009**, *2009*, 1759–1766. DOI: *10.1002/ejic.200801160*.

[**127**] Falivene, L.; Poater, A.; Cavallo, L. *N-Heterocyclic Carbenes*, **2014**, 25–38. DOI: *10.1002/9783527671229.ch02*.

[**128**] Bayat, M.; Sedghi, A.; Ebrahimkhani, L.; Sabounchei, S. J. *N-Heterocyclic carbene or phosphorus ylide: which one forms a stronger bond with group 11 metals? A theoretical study* **2017**, *46*, 207–220. DOI: *10.1039/C6DT03814J*.

[**129**] Cavallo, L.; Correa, A.; Costabile, C.; Jacobsen, H. *Steric and electronic effects in the bonding of N-heterocyclic ligands to transition metals* **2005**, *690*, 5407–5413. DOI: *10.1016/j.jorganchem.2005.07.012*.

[**130**] Dorta, R.; Stevens, E. D.; Hoff, C. D.; Nolan, S. P. *Stable, Three-Coordinate Ni(CO)2(NHC) (NHC = N-Heterocyclic Carbene) Complexes Enabling the Determination of Ni−NHC Bond Energies* **2003**, *125*, 10490–10491. DOI: *10.1021/ja0362151*.

[**131**] Becker, E.; Stingl, V.; Dazinger, G.; Puchberger, M.; Mereiter, K.; Kirchner, K. *Facile Migratory Insertion of a N-Heterocyclic Carbene into a Rutheniumâ˜Carbon Double Bond:â€‰ A New Type of Reaction of a NHC Ligand* **2006**, *128*, 6572–6573. DOI: *10.1021/ja061454k*.

[**132**] Galan, B. R.; Gembicky, M.; Dominiak, P. M.; Keister, J. B.; Diver, S. T. *Carbon Monoxide-Promoted Carbene Insertion into the Aryl Substituent of an N-Heterocyclic Carbene Ligand: Buchner Reaction in a Ruthenium Carbene Complex* **2005**, *127*, 15702–15703. DOI: *10.1021/ja0545618*.

[**133**] Allen, D. P.; Crudden, C. M.; Calhoun, L. A.; Wang, R. *Irreversible cleavage of a carbene–rhodium bond in Rh-N-heterocyclic carbene complexes: implications for catalysis* **2004**, *689*, 3203–3209. DOI: *10.1016/j.jorganchem.2004.07.021*.

[**134**] Danopoulos, A. A.; Tsoureas, N.; Green, J. C.; Hursthouse, M. B. *Migratory insertion in N-heterocyclic carbene complexes of palladium; an experimental and DFT study* **2003**, 756–757. DOI: *10.1039/B212453J*.

[**135**] Jazzar, R. F. R.; Macgregor, S. A.; Mahon, M. F.; Richards, S. P.; Whittlesey, M. K. *C−C and C−H Bond Activation Reactions in N-Heterocyclic Carbene Complexes of Ruthenium* **2002**, *124*, 4944–4945. DOI: *10.1021/ja012475b*.

[**136**] Simms, R. W.; Drewitt, M. J.; Baird, M. C. *Equilibration between a Phosphine−Cobalt Complex and an Analogous Complex Containing an N-Heterocyclic Carbene: The Thermodynamics of a Phosphine−Carbene Exchange Reaction* **2002**, *21*, 2958–2963. DOI: *10.1021/om020110+*.

[**137**] McGuinness, D. S.; Saendig, N.; Yates, B. F.; Cavell, K. J. *Kinetic and Density Functional Studies on Alkyl-Carbene Elimination from PdII Heterocylic Carbene Complexes: A New Type of Reductive Elimination with Clear Implications for Catalysis* **2001**, *123*, 4029–4040. DOI: *10.1021/ja003861q*.

[**138**] Titcomb, L. R.; Caddick, S.; Cloke, F. G. N.; Wilson, D. J.; McKerrecher, D. *Unexpected reactivity of two-coordinate palladium–carbene complexes; synthetic and catalytic implications* **2001**, 1388–1389. DOI: *10.1039/B104297C*.

[**139**] Magill, A. M.; Cavell, K. J.; Yates, B. F. *Basicity of Nucleophilic Carbenes in Aqueous and Nonaqueous SolventsTheoretical Predictions* **2004**, *126*, 8717–8724. DOI: *10.1021/ja038973x*.

[**140**] Konstandaras, N.; Dunn, M. H.; Guerry, M. S.; Barnett, C. D.; Cole, M. L.; Harper, J. B. *The impact of cation structure upon the acidity of triazolium salts in dimethyl sulfoxide* **2020**, *18*, 66–75. DOI: *10.1039/C9OB02258A*.

[**141**] Quinn, P.; Smith, M. S.; Zhu, J.; Hodgson, D. R. W.; O'Donoghue, A. C. *Triazolium Salt Organocatalysis: Mechanistic Evaluation of Unusual Ortho-Substituent Effects on Deprotonation* **2021**, *11*. DOI: *10.3390/catal11091055*.

[**142**] Breslow, R. *On the Mechanism of Thiamine Action. IV.1 Evidence from Studies on Model Systems* **1958**, *80*, 3719–3726. DOI: *10.1021/ja01547a064*.

[**143**] Washabaugh, M. W.; Jencks, W. P. *Thiazolium C(2)-proton exchange: structure-reactivity correlations and the pKa of thiamin C(2)-H revisited* **1988**, *27*, 5044–5053. DOI: *10.1021/bi00414a015*.

[**144**] Bordwell, F. G.; Satish, A. V. *Acidities of C2 hydrogen atoms in thiazolium cations and reactivities of their conjugate bases* **1991**, *113*, 985–990. DOI: *10.1021/ja00003a036*.

[**145**] Alder, R. W.; Allen, P. R.; Williams, S. J. *Stable carbenes as strong bases* **1995**, 1267–1268. DOI: *10.1039/C39950001267*.

[**146**] Kim, Y.-J.; Streitwieser, A. *Basicity of a stable carbene, 1,3-di-tert-butylimidazol-2-ylidene, in THF* **2002**, *124*, 5757–5761. DOI: *10.1021/ja025628j*.

[**147**] Chu, Y.; Deng, H.; Cheng, J.-P. *An Acidity Scale of 1,3-Dialkylimidazolium Salts in Dimethyl Sulfoxide Solution* **2007**, *72*, 7790–7793. DOI: *10.1021/jo070973i*.

[**148**] Feroci, M.; Chiarotto, I.; Inesi, A. *Advances in the Knowledge of N-Heterocyclic Carbenes Properties. The Backing of the Electrochemical Investigation* **2016**, *6.* DOI: *10.3390/catal6110178*.

[**149**] Amyes, T. L.; Diver, S. T.; Richard, J. P.; Rivas, F. M.; Toth, K. *Formation and Stability of N-Heterocyclic Carbenes in Water: The Carbon Acid pKa of Imidazolium Cations in Aqueous Solution* **2004**, *126*, 4366–4374. DOI: *10.1021/ja039890j*.

[**150**] Grishina, A. A.; Polyakova, S. M.; Kunetskiy, R. A.; Císařová, I.; Lyapkalo, I. M. *4,5-Disubstituted N,N′-Di-tert-alkyl Imidazolium Salts: New Synthesis and Structural Features* **2011**, *17*, 96–100. DOI: *10.1002/chem.201002805*.

[**151**] Massey, R. S.; Collett, C. J.; Lindsay, A. G.; Smith, A. D.; O'Donoghue, A. C. *Proton Transfer Reactions of Triazol-3-ylidenes: Kinetic Acidities and Carbon Acid pKa Values for Twenty Triazolium Salts in Aqueous Solution* **2012**, *134*, 20421–20432. DOI: *10.1021/ja308420c*.

[**152**] Dunn, M. H.; Konstandaras, N.; Cole, M. L.; Harper, J. B. *Targeted and Systematic Approach to the Study of pKa Values of Imidazolium Salts in Dimethyl Sulfoxide* **2017**, *82*, 7324–7331. DOI: *10.1021/acs.joc.7b00716*.

[**153**] Matthews, W. S.; Bares, J. E.; Bartmess, J. E.; Bordwell, F. G.; Cornforth, F. J.; Drucker, G. E.; Margolin, Z.; McCallum, R. J.; McCollum, G. J.; Vanier, N. R. *Equilibrium acidities of carbon acids. VI. Establishment of an absolute scale of acidities in dimethyl sulfoxide solution* **1975**, *97*, 7006–7014. DOI: *10.1021/ja00857a010*.

[**154**] Stein, T. H.; Vasiliu, M.; Arduengo, A. J., III; Dixon, D. A. *Lewis Acidity and Basicity: Another Measure of Carbene Reactivity* **2020**, *124*, 6096–6103. DOI: *10.1021/acs.jpca.0c03877*.

[**155**] Silva Moratorio de Moraes, R.; Tereza Miranda Martins, M.; Tavares de Almeida Pinto, G.; Couto Rodrigues, S.; Antunes do Nascimento, P.; Cardoso Cruz, C.; D'Oliveira Góes, K.; Claudia Cunha, A. *An overview on generation and general properties of N-heterocyclic carbenes: Applications of 1,2,4-triazolium carbenes as metal free organocatalysts* **2024**, *17*, 105527. DOI: *10.1016/j.arabjc.2023.105527*.

[**156**] Nesterov, V.; Reiter, D.; Bag, P.; Frisch, P.; Holzner, R.; Porzelt, A.; Inoue, S. *NHCs in Main Group Chemistry* **2018**, *118*, 9678–9842. DOI: *10.1021/acs.chemrev.8b00079*.

[**157**] Kuhn, N.; Al-Sheikh, A. *2,3-Dihydroimidazol-2-ylidenes and their main group element chemistry* **2005**, *249*, 829–857. DOI: *10.1016/j.ccr.2004.10.003*.

[**158**] Nair, V.; Bindu, S.; Sreekumar, V. *N-Heterocyclic Carbenes: Reagents, Not Just Ligands!* **2004**, *43*, 5130–5135. DOI: *10.1002/anie.200301714*.

[**159**] Delaude, L. *Betaine Adducts of N-Heterocyclic Carbenes: Synthesis, Properties, and Reactivity* **2009**, *2009*, 1681–1699. DOI: *10.1002/ejic.200801227*.

[**160**] Delaude, L.; Demonceau, A.; Wouters, J. *Assessing the Potential of Zwitterionic NHC·CS2 Adducts for Probing the Stereoelectronic Parameters of N-Heterocyclic Carbenes* **2009**, *2009*, 1882–1891. DOI: *10.1002/ejic.200801110*.

[**161**] Kirmse, W. *Carbene Complexes of Nonmetals* **2005**, *2005*, 237–260. DOI: *10.1002/ejoc.200400415*.

[**162**] Scattolin, T.; Logvinov, A. A.; Tzouras, N. V.; Cazin, C. S. J.; Nolan, S. P. *Advances in the Synthesis and Applications of N-Heterocyclic Carbene Metal Complexes with a Focus on the Weak Base Route* **2023**, *42*, 2692–2730. DOI: *10.1021/acs.organomet.3c00299*.

[**163**] Jamil, M. S.; Endot, N. A. *Influence of Fluorine Substituents on the Electronic Properties of Selenium-N-Heterocyclic Carbene Compounds* **2020**, *25.* DOI: *10.3390/molecules25215161*.

[**164**] Huynh, H. V.; Han, Y.; Jothibasu, R.; Yang, J. an. *13C NMR Spectroscopic Determination of Ligand Donor Strengths Using N-*

Heterocyclic Carbene Complexes of Palladium(II) **2009**, *28*, 5395–5404. DOI: *10.1021/om900667d*.

[**165**] Back, O.; Henry-Ellinger, M.; Martin, C. D.; Martin, D.; Bertrand, G. *31P NMR Chemical Shifts of Carbene–Phosphinidene Adducts as an Indicator of the π-Accepting Properties of Carbenes* **2013**, *52*, 2939–2943. DOI: *10.1002/anie.201209109*.

[**166**] Verlinden, K.; Buhl, H.; Frank, W.; Ganter, C. *Determining the Ligand Properties of N-Heterocyclic Carbenes from 77Se NMR Parameters* **2015**, *2015*, 2416–2425. DOI: *10.1002/ejic.201500174*.

[**167**] Liske, A.; Verlinden, K.; Buhl, H.; Schaper, K.; Ganter, C. *Determining the π-Acceptor Properties of N-Heterocyclic Carbenes by Measuring the 77Se NMR Chemical Shifts of Their Selenium Adducts* **2013**, *32*, 5269–5272. DOI: *10.1021/om400858y*.

[**168**] Scattolin, T.; Nolan, S. P. *Synthetic Routes to Late Transition Metal–NHC Complexes* **2020**, *2*, 721–736. DOI: *10.1016/j.trechm.2020.06.001*.

[**169**] Martynova, E. A.; Tzouras, N. V.; Pisanò, G.; Cazin, C. S. J.; Nolan, S. P. *The "weak base route" leading to transition metal–N-heterocyclic carbene complexes* **2021**, *57*, 3836–3856. DOI: *10.1039/D0CC08149C*.

[**170**] Chartoire, A.; Claver, C.; Corpet, M.; Krinsky, J.; Mayen, J.; Nelson, D.; Nolan, S. P.; Peñafiel, I.; Woodward, R.; Meadows, R. E. *Recyclable NHC Catalyst for the Development of a Generalized Approach to Continuous Buchwald–Hartwig Reaction and Workup* **2016**, *20*, 551–557. DOI: *10.1021/acs.oprd.5b00349*.

[**171**] Frémont, P. de; Scott, N. M.; Stevens, E. D.; Nolan, S. P. *Synthesis and Structural Characterization of N-Heterocyclic Carbene Gold(I) Complexes* **2005**, *24*, 2411–2418. DOI: *10.1021/om050111c*.

[**172**] Schneider, N.; César, V.; Bellemin-Laponnaz, S.; Gade, L. H. *Synthesis and structural chemistry of oxazolinyl-carbene copper(I) complexes* **2005**, *690*, 5556–5561. DOI: *10.1016/j.jorganchem.2005.06.044*.

[**173**] Mankad, N. P.; Gray, T. G.; Laitar, D. S.; Sadighi, J. P. *Synthesis, Structure, and CO2 Reactivity of a Two-Coordinate (Carbene)copper(I) Methyl Complex* **2004**, *23*, 1191–1193. DOI: *10.1021/om034368r*.

[**174**] Viciu, M. S.; Navarro, O.; Germaneau, R. F.; Kelly, R. A.; Sommer, W.; Marion, N.; Stevens, E. D.; Cavallo, L.; Nolan, S. P. *Synthetic and Structural Studies of (NHC)Pd(allyl)Cl Complexes (NHC = N-heterocyclic carbene)* **2004**, *23*, 1629–1635. DOI: *10.1021/om034319e*.

[**175**] Furst, M. R. L.; Cazin, C. S. J. *Copper N-heterocyclic carbene (NHC) complexes as carbene transfer reagents* **2010**, *46*, 6924–6925. DOI: *10.1039/C0CC02308F*.

[**176**] Lin, I. J.; Vasam, C. S. *Preparation and application of N-heterocyclic carbene complexes of Ag(I)* **2007**, *251*, 642–670. DOI: *10.1016/j.ccr.2006.09.004*.

[**177**] Citadelle, C. A.; Le Nouy, E.; Bisaro, F.; Slawin, A. M. Z.; Cazin, C. S. J. *Simple and versatile synthesis of copper and silver N-heterocyclic carbene complexes in water or organic solvents* **2010**, *39*, 4489–4491. DOI: *10.1039/C0DT00128G*.

[**178**] Wang, H. M. J.; Lin, I. J. B. *Facile Synthesis of Silver(I)−Carbene Complexes. Useful Carbene Transfer Agents* **1998**, *17*, 972–975. DOI: *10.1021/om9709704*.

[**179**] Mokfi, M.; Rust, J.; Lehmann, C. W.; Mohr, F. *Facile N9-Alkylation of Xanthine Derivatives and Their Use as Precursors for N-Heterocyclic Carbene Complexes* **2021**, *26.* DOI: *10.3390/molecules26123705*.

[**180**] Zhu, S.; Liang, R.; Jiang, H. *A direct and practical approach for the synthesis of N-heterocyclic carbene coinage metal complexes* **2012**, *68*, 7949–7955. DOI: *10.1016/j.tet.2012.07.009*.

[**181**] Landers, B.; Navarro, O. *Microwave-Assisted Synthesis of (N-Heterocyclic carbene)MCl Complexes of Group 11 Metals* **2012**, *2012*, 2980–2982. DOI: *10.1002/ejic.201200248*.

[**182**] Dar, M. O.; Mir, R. H.; Mohiuddin, R.; Masoodi, M. H.; Sofi, F. A. *Metal complexes of xanthine and its derivatives: Synthesis and biological activity* **2023**, *246*, 112290. DOI: *10.1016/j.jinorgbio.2023.112290*.

[**183**] Youngs, W. J.; Knapp, A. R.; Wagers, P. O.; Tessier, C. A. *Nanoparticle encapsulated silver carbene complexes and their antimicrobial and anticancer properties: A perspective* **2012**, *41*, 327–336. DOI: *10.1039/C1DT11100K*.

[**184**] Kascatan-Nebioglu, A.; Melaiye, A.; Hindi, K.; Durmus, S.; Panzner, M. J.; Hogue, L. A.; Mallett, R. J.; Hovis, C. E.; Coughenour, M.; Crosby, S. D.; Milsted, A.; Ely, D. L.; Tessier, C. A.; Cannon, C. L.; Youngs, W. J. *Synthesis from Caffeine of a Mixed N-Heterocyclic Carbene−Silver Acetate Complex Active against Resistant Respiratory Pathogens* **2006**, *49*, 6811–6818. DOI: *10.1021/jm060711t*.

[**185**] Kapri, A.; Gupta, N.; Nain, S. *Recent Advances in the Synthesis of Xanthines: A Short Review* **2022**, *2022*, 8239931. DOI: *10.1155/2022/8239931*.

[**186**] Srdjenovic, B.; Djordjevic-Milic, V.; Grujic, N.; Injac, R.; Lepojevic, Z. *Simultaneous HPLC Determination of Caffeine, Theobromine, and Theophylline in Food, Drinks, and Herbal Products* **2008**, *46*, 144–149. DOI: *10.1093/chromsci/46.2.144*.

[**187**] Rosemeyer, H. *The Chemodiversity of Purine as a Constituent of Natural Products* **2004**, *1*, 361–401. DOI: *10.1002/cbdv.200490033*.

[**188**] Daly, J. W. *Caffeine analogs: biomedical impact* **2007**, *64*, 2153–2169. DOI: *10.1007/s00018-007-7051-9*.

[**189**] Legraverend, M.; Grierson, D. S. *The purines: Potent and versatile small molecule inhibitors and modulators of key biological targets* **2006**, *14*, 3987–4006. DOI: *10.1016/j.bmc.2005.12.060*.

[**190**] Welsch, M. E.; Snyder, S. A.; Stockwell, B. R. *Privileged scaffolds for library design and drug discovery* **2010**, *14*, 347–361. DOI: *10.1016/j.cbpa.2010.02.018*.

[**191**] Censi, V.; Caballero, A. B.; Pérez-Hernández, M.; Soto-Cerrato, V.; Korrodi-Gregório, L.; Pérez-Tomás, R.; Dell'Anna, M. M.; Mastrorilli, P.; Gamez, P. *DNA-binding and in vitro cytotoxic activity of platinum(II) complexes of curcumin and caffeine* **2019**, *198*, 110749. DOI: *10.1016/j.jinorgbio.2019.110749*.

[**192**] Ashihara, H.; Mizuno, K.; Yokota, T.; Crozier, A. *Progress in the Chemistry of Organic Natural Products 105*, 1–88, **2017**; Springer International Publishing: Cham. DOI: *10.1007/978-3-319-49712-9_1*.

[**193**] Luo, F.-T.; Lo, H.-K. *Short synthesis of bis-NHC-Pd catalyst derived from caffeine and its applications to Suzuki, Heck, and Sonogashira reactions in aqueous solution* **2011**, *696*, 1262–1265. DOI: *10.1016/j.jorganchem.2010.11.002*.

[**194**] Zhang, J.-J.; Che, C.-M.; Ott, I. *Caffeine derived platinum(II) N-heterocyclic carbene complexes with multiple anti-cancer activities* **2015**, *782*, 37–41. DOI: *10.1016/j.jorganchem.2014.10.041*.

[**195**] Brackemeyer, D.; Hervé, A.; Schulte to Brinke, C.; Jahnke, M. C.; Hahn, F. E. *A Versatile Methodology for the Regioselective C8-*

Metalation of Purine Bases **2014**, *136*, 7841–7844. DOI: *10.1021/ja5030904*.

[**196**] Zhang, J.-J.; Muenzner, J. K.; Abu el Maaty, Mohamed A.; Karge, B.; Schobert, R.; Wölfl, S.; Ott, I. *A multi-target caffeine derived rhodium(i) N-heterocyclic carbene complex: evaluation of the mechanism of action* **2016**, *45*, 13161–13168. DOI: *10.1039/C6DT02025A*.

[**197**] Bertrand, B.; Stefan, L.; Pirrotta, M.; Monchaud, D.; Bodio, E.; Richard, P.; Le Gendre, P.; Warmerdam, E.; Jager, M. H. de; Groothuis, G. M.; Picquet, M.; Casini, A. *Caffeine-Based Gold(I) N-Heterocyclic Carbenes as Possible Anticancer Agents: Synthesis and Biological Properties* **2014**, *53*, 2296–2303. DOI: *10.1021/ic403011h*.

[**198**] Karmis, R. E.; Carrara, S.; Baxter, A. A.; Hogan, C. F.; Hulett, M. D.; Barnard, P. J. *Luminescent iridium(iii) complexes of N-heterocyclic carbene ligands prepared using the 'click reaction'* **2019**, *48*, 9998–10010. DOI: *10.1039/C9DT01362H*.

[**199**] Gusmeroli, M.; Cariello, S.; D'orazio, G.; Bellandi, P.; Sargiotto, C.; Bianchi, D.; Villata, J.; Liguori, R. *Theophylline derivatives with nematocidal activity, their agronomic compositions and relative use.* PCT/IB2020/050685 WO/2020/157668, **Jan 29, 2020**.

[**200**] Tan, T. T. Y.; Hahn, F. E. *Synthesis of Iridium(III) and Rhodium(III) Complexes Bearing C8-Metalated Theophylline Ligands by Directed C–H Activation* **2019**, *38*, 2250–2258. DOI: *10.1021/acs.organomet.9b00184*.

[**201**] Ivanov, É. I.; Kalayanov, G. D.; Yaroshchenko, I. M.; Stepanov, D. E. *New synthesis of caffeine methiodide and its homolog* **1989**, *25*, 1318. DOI: *10.1007/BF00481539*.

[**202**] Oertel, A. M.; Ritleng, V.; Chetcuti, M. J. *N'-Activation of N-Arylimidazoles: Facile Syntheses of N-Alkyl-N'-aryl-imidazolium Iodides from Less Expensive Chloro Substrates* **2009**, *2009*, 1647–1650. DOI: *10.1055/s-0028-1088053*.

[**203**] Ivanov, É. I.; Kalayanov, G. D.; Yaroshchenko, I. M.; Stepanov, D. E. *New synthesis of caffeine methiodide and its homolog* **1989**, *25*, 1318. DOI: *10.1007/BF00481539*.

[**204**] Lundevall, F. J.; Bjørsvik, H.-R. *Lithiation and Alkylation of the Imidazole Backbone* **2023**, *26*, e202201504. DOI: *10.1002/ejoc.202201504*.

[**205**] Schütz, J.; Herrmann, W. A. *Purine-based carbenes at rhodium and iridium* **2004**, *689*, 2995–2999. DOI: *10.1016/j.jorganchem.2004.06.037*.

[**206**] Bredereck, H.; Christmann, O.; Koser, W.; Schellenberg, P.; Nast, R. *Synthesen in der Purinreihe, XV1) Synthesen von Xanthinium- und Guaninium-betainen* **1962**, *95*, 1812–1819. DOI: *10.1002/cber.19620950736*.

[**207**] Hori, M.; Kataoka, T.; Shimizu, H.; Imai, E.; Matsumoto, Y. *Reactions of 8, 9-Dihydroxanthines with Acetylenic Compounds. Formation of Heteropropellanes* **1985**, *33*, 3681–3688. DOI: *10.1248/cpb.33.3681*.

[**208**] Dupont, J. *The Solid, Liquid and Solution Structural Organization of Imidazolium Ionic Liquids* **2004**, *15.* DOI: *10.1590/S0103-50532004000300002*.

[**209**] Guerret, O.; Solé, S.; Gornitzka, H.; Teichert, M.; Trinquier, G.; Bertrand, G. *1,2,4-Triazole-3,5-diylidene: A Building Block for Organometallic Polymer Synthesis* **1997**, *119*, 6668–6669. DOI: *10.1021/ja964191a*.

[**210**] Howells, R. D.; Mc Cown, J. D. *Trifluoromethanesulfonic acid and derivatives* **1977**, *77*, 69–92. DOI: *10.1021/cr60305a005*.

[**211**] Hansen, R. L. *Perfluoroalkanesulfonate Esters as Alkylating Agents* **1965**, *30*, 4322–4324. DOI: *10.1021/jo01023a511*.

[**212**] Holbrey, J. D.; Reichert, W. M.; Swatloski, R. P.; Broker, G. A.; Pitner, W. R.; Seddon, K. R.; Rogers, R. D. *Efficient, halide free synthesis of new, low cost ionic liquids: 1,3-dialkylimidazolium salts containing methyl- and ethyl-sulfate anions* **2002**, *4*, 407–413. DOI: *10.1039/B204469B*.

[**213**] Wasserscheid, P.; Welton, T., Eds. *Ionic Liquids in Synthesis*; Wiley-VCH Verlag GmbH & Co. KGaA, **2002.** ISBN: 9783527312399.

[**214**] Anthony, J. L.; Brennecke, J. F.; Holbrey, J. D.; Maginn, E. J.; Mantz, R. A.; Rogers, R. D.; Trulove, P. C.; Visser, A. E.; Welton, T. *Ionic Liquids in Synthesis*, 41–126, **2002**; Wiley-VCH Verlag GmbH & Co. KGaA. DOI: *10.1002/3527600701.ch3*.

[**215**] Da Gomes Silva, M.; Pereira, M. M. A. *New chiral imidazolium ionic liquids from isomannide* **2011**, *346*, 197–202. DOI: *10.1016/j.carres.2010.11.011*.

[**216**] Kascatan-Nebioglu, A.; Panzner, M. J.; Garrison, J. C.; Tessier, C. A.; Youngs, W. J. *Synthesis and Structural Characterization of N-Heterocyclic Carbene Complexes of Silver(I) and Rhodium(I) from Caffeine* **2004**, *23*, 1928–1931. DOI: *10.1021/om030689r*.

[**217**] Fei, Z.; Zhao, D.; Geldbach, T. J.; Scopelliti, R.; Dyson, P. J. *Brønsted Acidic Ionic Liquids and Their Zwitterions: Synthesis, Characterization and pKa Determination* **2004**, *10*, 4886–4893. DOI: *10.1002/chem.200400145*.

[**218**] Palimkar, S. S.; Siddiqui, S. A.; Daniel, T.; Lahoti, R. J.; Srinivasan, K. V. *Ionic liquid-promoted regiospecific Friedlander annulation: novel*

synthesis of quinolines and fused polycyclic quinolines **2003**, *68*, 9371–9378. DOI: *10.1021/jo035153u*.

[**219**] Hindi, K. M.; Siciliano, T. J.; Durmus, S.; Panzner, M. J.; Medvetz, D. A.; Reddy, D. V.; Hogue, L. A.; Hovis, C. E.; Hilliard, J. K.; Mallet, R. J.; Tessier, C. A.; Cannon, C. L.; Youngs, W. J. *Synthesis, Stability, and Antimicrobial Studies of Electronically Tuned Silver Acetate N-Heterocyclic Carbenes* **2008**, *51*, 1577–1583. DOI: *10.1021/jm0708679*.

[**220**] Khramov, D. M.; Lynch, V.; Bielawski, C. W. *N-Heterocyclic Carbene−Transition Metal Complexes: Spectroscopic and Crystallographic Analyses of \pi-Back-bonding Interactions* **2007**, *26*, 6042–6049.

[**221**] Gao, J.; Liu, J.; Liu, W.; Li, B.; Xin, Y.; Yin, Y.; Gu, J.; Zou, Z. *An efficient and green approach to prepare hydrophilic imidazolium ionic liquids free of halide and its effect on oxygen reduction reaction of Pt/C catalyst* **2012**, *37*, 13167–13177. DOI: *10.1016/j.ijhydene.2012.03.135*.

[**222**] Suarez, P. A. Z.; Einloft, S.; Dullius, J.; Souza R. F.; Dupont, J. *Synthesis and physical-chemical properties of ionic liquids based on 1-n-butyl-3-methylimidazolium cation* **1998**, *95*, 1626–1639. DOI: *10.1051/JCP%3A1998103*.

[**223**] Mohamed, H. A.; Lake, B. R. M.; Laing, T.; Phillips, R. M.; Willans, C. E. *Synthesis and anticancer activity of silver(i)–N-heterocyclic carbene complexes derived from the natural xanthine products caffeine, theophylline and theobromine* **2015**, *44*, 7563–7569. DOI: *10.1039/C4DT03679D*.

[**224**] Duborská, E.; Balíková, K.; Matulová, M.; Zvěřina, O.; Farkas, B.; Littera, P.; Urík, M. *Production of Methyl-Iodide in the Environment* **2021**, *12.* DOI: *10.3389/fmicb.2021.804081*.

[**225**] Mariconda, A.; Iacopetta, D.; Sirignano, M.; Ceramella, J.; D'Amato, A.; Marra, M.; Pellegrino, M.; Sinicropi, M. S.; Aquaro, S.; Longo, P. *Silver and Gold Complexes with NHC-Ligands Derived from Caffeine: Catalytic and Pharmacological Activity* **2024**, *25.* DOI: *10.3390/ijms25052599*.

[**226**] Gibard, C.; Fauché, K.; Guillot, R.; Jouffret, L.; Traïkia, M.; Gautier, A.; Cisnetti, F. *Access to silver-NHC complexes from soluble silver species in aqueous or ethanolic ammonia* **2017**, *840*, 70–74. DOI: *10.1016/j.jorganchem.2017.04.009*.

[**227**] Iglesias, M.; Beetstra, D. J.; Knight, J. C.; Ooi, L.-L.; Stasch, A.; Coles, S.; Male, L.; Hursthouse, M. B.; Cavell, K. J.; Dervisi, A.; Fallis, I. A. *Novel Expanded Ring N-Heterocyclic Carbenes: Free Carbenes, Silver Complexes, And Structures* **2008**, *27*, 3279–3289. DOI: *10.1021/om800179t*.

[**228**] Johnson, N. A.; Southerland, M. R.; Youngs, W. J. *Recent Developments in the Medicinal Applications of Silver-NHC Complexes and Imidazolium Salts* **2017**, *22.* DOI: *10.3390/molecules22081263*.

[**229**] Beig, N.; Goyal, V.; Bansal, R. K. *Application of N-heterocyclic carbene–Cu(I) complexes as catalysts in organic synthesis: a review* **2023**, *19*, 1408–1442. DOI: *10.3762/bjoc.19.102*.

[**230**] Ronga, L.; Varcamonti, M.; Tesauro, D. *Structure-Activity Relationships in NHC-Silver Complexes as Antimicrobial Agents* **2023**, *28.* DOI: *10.3390/molecules28114435*.

[**231**] Kascatan-Nebioglu, A.; Panzner, M. J.; Tessier, C. A.; Cannon, C. L.; Youngs, W. J. *N-Heterocyclic carbene–silver complexes: A new class of antibiotics* **2007**, *251*, 884–895. DOI: *10.1016/j.ccr.2006.08.019*.

[**232**] Gautier, A.; Cisnetti, F. *Advances in metal-carbene complexes as potent anti-cancer agents* **2012**, *4*, 23–32. DOI: *10.1039/c1mt00123j*.

[**233**] Oehninger, L.; Rubbiani, R.; Ott, I. *N-Heterocyclic carbene metal complexes in medicinal chemistry* **2013**, *42*, 3269–3284. DOI: *10.1039/c2dt32617e*.

[**234**] Bernardi, T.; Badel, S.; Mayer, P.; Groelly, J.; Frémont, P. de; Jacques, B.; Braunstein, P.; Teyssot, M.-L.; Gaulier, C.; Cisnetti, F.; Gautier, A.; Roland, S. *High-Throughput Screening of Metal-N-Heterocyclic Carbene Complexes against Biofilm Formation by Pathogenic Bacteria* **2014**, *9*, 1140–1144. DOI: *10.1002/cmdc.201402012*.

[**235**] Wagers, P. O.; Shelton, K. L.; Panzner, M. J.; Tessier, C. A.; Youngs, W. J. *N-Heterocyclic Carbenes*, **2014**, 151–172. DOI: *10.1002/9783527671229.ch06*.

[**236**] Liu, W.; Gust, R. *Update on metal N-heterocyclic carbene complexes as potential anti-tumor metallodrugs* **2016**, *329*, 191–213. DOI: *10.1016/j.ccr.2016.09.004*.

[**237**] Zinner, S. C.; Herrmann, W. A.; Kühn, F. E. *Synthesis and characterization of asymmetric NHC complexes* **2008**, *693*, 1543–1546. DOI: *10.1016/j.jorganchem.2007.10.047*.

[**238**] Zinner, S. C.; Herrmann, W. A.; Kühn, F. E. *A new route to chiral imidazolidine salts and its application in organometallic synthesis* **2008**, *19*, 1532–1535. DOI: *10.1016/j.tetasy.2008.06.006*.

[**239**] Hayes, J. M.; Viciano, M.; Peris, E.; Ujaque, G.; Lledós, A. *Mechanism of Formation of Silver N-Heterocyclic Carbenes Using Silver Oxide: A Theoretical Study* **2007**, *26*, 6170–6183. DOI: *10.1021/om700898d*.

[**240**] Chen, J. C. C.; Lin, I. J. B. *Palladium Complexes Containing a Hemilabile Pyridylcarbene Ligand* **2000**, *19*, 5113–5121. DOI: *10.1021/om000557n*.

[**241**] Catalano, V. J.; Malwitz, M. A.; Etogo, A. O. *Pyridine Substituted N-Heterocyclic Carbene Ligands as Supports for Au(I)–Ag(I) Interactions: Formation of a Chiral Coordination Polymer* **2004**, *43*, 5714–5724. DOI: *10.1021/ic049604k*.

[**242**] Liu, Q.-X.; Yin, L.-N.; Feng, J.-C. *New N-heterocyclic carbene silver(I) and mercury(II) 2-D supramolecular layers by the π–π stacking interactions* **2007**, *692*, 3655–3663. DOI: *10.1016/j.jorganchem.2007.05.005*.

[**243**] Liu, Q.-X.; Yin, L.-N.; Wu, X.-M.; Feng, J.-C.; Guo, J.-H.; Song, H.-B. *New N-heterocyclic carbene mercury(II) and silver(I) complexes* **2008**, *27*, 87–94. DOI: *10.1016/j.poly.2007.08.046*.

[**244**] Kühl, O.; Saravanakumar, S.; Ullah, F.; Kindermann, M. K.; Jones, P. G.; Köckerling, M.; Heinicke, J. *Anellated N-heterocyclic carbenes: 1,3-Dineopentyl-benzimidazol-2-ylidene, structural aspects of C-protonated precursor salts and an AgCl complex* **2008**, *27*, 2825–2832. DOI: *10.1016/j.poly.2008.06.006*.

[**245**] Moore, L. R.; Cooks, S. M.; Anderson, M. S.; Schanz, H.; Griffin, S. T.; Rogers, R. D.; Kirk, M. C.; Shaughnessy, K. H. *Synthesis and Characterization of Water-Soluble Silver and Palladium Imidazol-2-ylidene Complexes with Noncoordinating Anionic Substituents* **2006**, *25*, 5151–5158. DOI: *10.1021/om060552b*.

[**246**] Magill, A. M.; Cavell, K. J.; Yates, B. F. *Basicity of Nucleophilic Carbenes in Aqueous and Nonaqueous SolventsTheoretical Predictions* **2004**, *126*, 8717–8724. DOI: *10.1021/ja038973x*.

[**247**] Newman, C. P.; Clarkson, G. J.; Rourke, J. P. *Silver(I) N-heterocyclic carbene halide complexes: A new bonding motif* **2007**, *692*, 4962–4968. DOI: *10.1016/j.jorganchem.2007.07.041*.

[**248**] Frémont, P. de; Scott, N. M.; Stevens, E. D.; Ramnial, T.; Lightbody, O. C.; Macdonald, C. L. B.; Clyburne, J. A. C.; Abernethy, C. D.; Nolan, S. P. *Synthesis of Well-Defined N-Heterocyclic Carbene Silver(I) Complexes* **2005**, *24*, 6301–6309. DOI: *10.1021/om050735i*.

[**249**] Lee, C. K.; Vasam, C. S.; Huang, T. W.; Wang, H. M. J.; Yang, R. Y.; Lee, C. S.; Lin, I. J. B. *Silver(I) N-Heterocyclic Carbenes with Long N-Alkyl Chains* **2006**, *25*, 3768–3775. DOI: *10.1021/om060198h*.

[**250**] Tulloch, A. A. D.; Danopoulos, A. A.; Winston, S.; Kleinhenz, S.; Eastham, G. *N-Functionalised heterocyclic carbene complexes of silver* **2000**, 4499–4506. DOI: *10.1039/B007504N*.

[**251**] Guerret, O.; Solé, S.; Gornitzka, H.; Teichert, M.; Trinquier, G.; Bertrand, G. *1,2,4-Triazolium-5-ylidene and 1,2,4-triazol-3,5-diylidene as new ligands for transition metals* **2000**, *600*, 112–117. DOI: *10.1016/S0022-328X(00)00037-1*.

[**252**] Caytan, E.; Roland, S. *Structure of Silver–N-Heterocyclic Carbenes in Solution: Evidence of Equilibration in DMSO at Very Different Time Scales by 1H NMR Experiments* **2014**, *33*, 2115–2118. DOI: *10.1021/om401124y*.

[**253**] Knapp, A. R.; Panzner, M. J.; Medvetz, D. A.; Wright, B. D.; Tessier, C. A.; Youngs, W. J. *Synthesis and antimicrobial studies of silver N-heterocyclic carbene complexes bearing a methyl benzoate substituent* **2010**, *364*, 125–131. DOI: *10.1016/j.ica.2010.08.008*.

[**254**] Nielsen, D. J.; Cavell, K. J.; Skelton, B. W.; White, A. H. *A pyridine bridged dicarbene ligand and its silver(I) and palladium(II)*

complexes: synthesis, structures, and catalytic applications **2002**, *327*, 116–125. DOI: *10.1016/S0020-1693(01)00677-6*.

[**255**] Ogba, O. M.; Warner, N. C.; O'Leary, D. J.; Grubbs, R. H. *Recent advances in ruthenium-based olefin metathesis* **2018**, *47*, 4510–4544. DOI: *10.1039/C8CS00027A*.

[**256**] Falivene, L.; Credendino, R.; Poater, A.; Petta, A.; Serra, L.; Oliva, R.; Scarano, V.; Cavallo, L. *SambVca 2. A Web Tool for Analyzing Catalytic Pockets with Topographic Steric Maps* **2016**, *35*, 2286–2293. DOI: *10.1021/acs.organomet.6b00371*.

[**257**] Lee, K. M.; Lee, C. K.; Lin, I. J. B. *A Facile Synthesis of Unusual Liquid-Crystalline Gold(I) Dicarbene Compounds* **1997**, *36*, 1850–1852. DOI: *10.1002/anie.199718501*.

[**258**] Oehninger, L.; Spreckelmeyer, S.; Holenya, P.; Meier, S. M.; Can, S.; Alborzinia, H.; Schur, J.; Keppler, B. K.; Wölfl, S.; Ott, I. *Rhodium(I) N-Heterocyclic Carbene Bioorganometallics as in Vitro Antiproliferative Agents with Distinct Effects on Cellular Signaling* **2015**, *58*, 9591–9600. DOI: *10.1021/acs.jmedchem.5b01159*.

[**259**] Ghosh, A. K.; Catalano, V. J. *Synthesis and Characterization of a Series of New Luminescent NHC-Coordinated AuI–AgI Tetra- and Polymetallic Complexes Containing Benzoate-Bridged Ag2 Dimers* **2009**, *2009*, 1832–1843. DOI: *10.1002/ejic.200801208*.

[**260**] Landers, B.; Navarro, O. *Microwave-Assisted Synthesis of (N-Heterocyclic carbene)MCl Complexes of Group 11 Metals* **2012**, *2012*, 2980–2982. DOI: *10.1002/ejic.201200248*.

[**261**] Collado, A.; Gómez-Suárez, A.; Martin, A. R.; Slawin, A. M. Z.; Nolan, S. P. *Straightforward synthesis of [Au(NHC)X] (NHC = N-heterocyclic carbene, X = Cl, Br, I) complexes* **2013**, *49*, 5541–5543. DOI: *10.1039/C3CC43076F*.

[**262**] Visbal, R.; Laguna, A.; Gimeno, M. C. *Simple and efficient synthesis of [MCl(NHC)] (M = Au, Ag) complexes* **2013**, *49*, 5642–5644. DOI: *10.1039/C3CC42919A*.

[**263**] Fillat, M. F.; Gimeno, M. C.; Laguna, A.; Latorre, E.; Ortego, L.; Villacampa, M. D. *Synthesis, Structure and Bactericide Activity of (Aminophosphane)gold(I) Thiolate Complexes* **2011**, *2011*, 1487–1495. DOI: *10.1002/ejic.201001195*.

[**264**] Chass, G. A.; O'Brien, C. J.; Hadei, N.; Kantchev, E. A. B.; Mu, W.-H.; Fang, D.-C.; Hopkinson, A. C.; Csizmadia, I. G.; Organ, M. G. *Density Functional Theory Investigation of the Alkyl–Alkyl Negishi Cross-Coupling Reaction Catalyzed by N-Heterocyclic Carbene (NHC)–Pd Complexes* **2009**, *15*, 4281–4288. DOI: *10.1002/chem.200900042*.

[**265**] Organ, M. G.; Çalimsiz, S.; Sayah, M.; Hoi, K. H.; Lough, A. J. *Pd-PEPPSI-IPent: An Active, Sterically Demanding Cross-Coupling Catalyst and Its Application in the Synthesis of Tetra-Ortho-Substituted Biaryls* **2009**, *121*, 2419–2423. DOI: *10.1002/ange.200805661*.

[**266**] O'Brien, C. J.; Kantchev, E. A. B.; Valente, C.; Hadei, N.; Chass, G. A.; Lough, A.; Hopkinson, A. C.; Organ, M. G. *Easily Prepared Air- and Moisture-Stable Pd–NHC (NHC=N-Heterocyclic Carbene) Complexes: A Reliable, User-Friendly, Highly Active Palladium Precatalyst for the Suzuki–Miyaura Reaction* **2006**, *12*, 4743–4748. DOI: *10.1002/chem.200600251*.

[**267**] Kantchev, E.; O'Brien, C. J.; Organ, M. G. *Pd-N-heterocyclic carbene (NHC) catalysts for cross-coupling reactions* **2006**, *39*, 97–111.

[**268**] Luo, F.-T.; Lo, H.-K. *Short synthesis of bis-NHC-Pd catalyst derived from caffeine and its applications to Suzuki, Heck, and Sonogashira reactions in aqueous solution* **2011**, *696*, 1262–1265. DOI: *10.1016/j.jorganchem.2010.11.002*.

[**269**] Krossing, I.; Raabe, I. *Noncoordinating Anions—Fact or Fiction? A Survey of Likely Candidates* **2004**, *43*, 2066–2090. DOI: *10.1002/anie.200300620*.

[**270**] Martin, R. *Practical hardness scales for metal ion complexes* **2002**, *339*, 27–33. DOI: *10.1016/S0020-1693(02)00922-2*.

[**271**] Li, F. F.; Ma, J. F.; Song, S. Y.; Yang, J.; Jia, H. Q.; Hu, N. H. *Syntheses, Structures, and Characterizations of Four New Silver(I) Sulfonate Coordination Polymers with Neutral Ligands* **2006**, *6*, 209–215. DOI: *10.1021/cg050293d*.

[**272**] Yuan, D.; Huynh, H. V. *Sulfur-functionalized N-heterocyclic carbene complexes of Pd(II): syntheses, structures and catalytic activities* **2012**, *17*, 2491–2517. DOI: *10.3390/molecules17032491*.

[**273**] Kishore, R.; Das, S. K. *Synthesis, structural characterization and properties of new N-heterocyclic carbene Ag(I) complexes* **2013**, *1053*, 38–47. DOI: *10.1016/j.molstruc.2013.08.051*.

[**274**] Dash, C.; Shaikh, M. M.; Butcher, R. J.; Ghosh, P. *Highly Convenient Regioselective Intermolecular Hydroamination of Alkynes Yielding Ketimines Catalyzed by Gold(I) Complexes of 1,2,4-triazole Based N-heterocyclic Carbenes* **2010**, *49*, 4972–4983. DOI: *10.1021/ic100087d*.

[**275**] Ray, S.; Mohan, R.; Singh, J. K.; Samantaray, M. K.; Shaikh, M. M.; Panda, D.; Ghosh, P. *Anticancer and Antimicrobial Metallopharmaceutical Agents Based on Palladium, Gold, and Silver N-Heterocyclic Carbene Complexes* **2007**, *129*, 15042–15053. DOI: *10.1021/ja075889z*.

[**276**] Yiğit, B.; Işık, Y.; Barut Celepci, D.; Evren, E.; Yiğit, M.; Gürbüz, N.; Özdemir, İ. *Ruthenium(II) complexes bearing N-heterocyclic carbene ligands with wingtip groups and their catalytic activity in the*

transfer hydrogenation of ketones **2020**, *499*, 119199. DOI: *10.1016/j.ica.2019.119199*.

[**277**] Paas, M.; Wibbeling, B.; Fröhlich, R.; Hahn, F. E. *Silver and Rhodium Complexes of Stable, Monomeric Imidazolidin-2-ylidenes: Synthesis, Reactivity and Decomposition Pathway* **2006**, *2006*, 158–162. DOI: *10.1002/ejic.200500777*.

This dissertation investigates the design, synthesis, and coordination behavior of N-heterocyclic carbene ligands derived from theophylline. Special emphasis is placed on developing synthetic pathways toward metal–NHC complexes, particularly silver- and gold-based systems, due to their structural uniqueness and emerging relevance in anticancer research. The work enhances the understanding of biomolecule-inspired ligand frameworks within coordination chemistry.

Inorganic Chemistry *University of Wuppertal* *2025*

Bergische Universität Wuppertal *2025*